Image Cover Sheet

CLASSIFICATION	SYSTEM NUMBER 505377
UNCLASSIFIED	

TITLE

AEROBALLISTIC RANGE TESTS OF THE BASIC FINNER REFERENCE PROJECTILE AT
SUPERSONIC VELOCITIES

System Number:

Patron Number:

Requester:

Notes:

		Form Approved OMB No. 0704-0188

Report Documentation Page

1. REPORT DATE **AUG 1997**	2. REPORT TYPE	3. DATES COVERED

4. TITLE AND SUBTITLE **Aeroballistic Range Tests of the Basic Finner Reference Projectile at Supersonic Velocities**	5a. CONTRACT NUMBER
	5b. GRANT NUMBER
	5c. PROGRAM ELEMENT NUMBER
6. AUTHOR(S)	5d. PROJECT NUMBER
	5e. TASK NUMBER
	5f. WORK UNIT NUMBER
7. PERFORMING ORGANIZATION NAME(S) AND ADDRESS(ES) **Defence R&D Canada - Valcartier,2459 Pie-XI Blvd North,Quebec (Quebec) G3J 1X5 Canada, ,**	8. PERFORMING ORGANIZATION REPORT NUMBER
9. SPONSORING/MONITORING AGENCY NAME(S) AND ADDRESS(ES)	10. SPONSOR/MONITOR'S ACRONYM(S)
	11. SPONSOR/MONITOR'S REPORT NUMBER(S)

12. DISTRIBUTION/AVAILABILITY STATEMENT
Approved for public release; distribution unlimited.

13. SUPPLEMENTARY NOTES

14. ABSTRACT
Free-flight tests were conducted in the Defence Research Establishment V alcartier (DREV) Aero ballistic Range on the Basic Finner reference projectile from transonic to high supersonic velocities. The projectile consisted of four rectangular fins on a cone-cylinder body with a total length-to-diameter ratio of 10.0. Fin cants of 0?, 2? and 4? were imposed. The Mach number range tested was between 1.0 and 4.5. All the main aerodynamic coefficients and stability derivatives were well determined using linear theory, six-degree-of-freedom single- and multiple-fit reductions techniques. The results were also compared with results from other aeroballistic ranges. The fins on the models fired at Mach 4.5 ablated during flight. A dynamic stability analysis showed a Magnus instability at certain Mach numbers and spin rates.

15. SUBJECT TERMS

16. SECURITY CLASSIFICATION OF:			17. LIMITATION OF ABSTRACT	18. NUMBER OF PAGES **152**	19a. NAME OF RESPONSIBLE PERSON
a. REPORT **unclassified**	b. ABSTRACT **unclassified**	c. THIS PAGE **unclassified**			

Standard Form 298 (Rev. 8-98)
Prescribed by ANSI Std Z39-18

DEFENCE RESEARCH ESTABLISHMENT
CENTRE DE RECHERCHES POUR LA DÉFENSE
VALCARTIER, QUÉBEC

DREV - TM - 9703

Unlimited Distribution/Distribution illimitée

AEROBALLISTIC RANGE TESTS OF THE
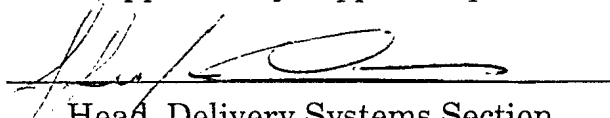BASIC FINNER REFERENCE PROJECTILE
AT SUPERSONIC VELOCITIES

by

A. D. Dupuis and W. Hathaway*

August/août 1997

* Arrow Tech Associates

Approved by / approuvé par

Head, Delivery Systems Section
Chef, Section systèmes de lancement

30 July 97

Date

ABSTRACT

Free-flight tests were conducted in the Defence Research Establishment Valcartier (DREV) Aeroballistic Range on the Basic Finner reference projectile from transonic to high supersonic velocities. The projectile consisted of four rectangular fins on a cone-cylinder body with a total length-to-diameter ratio of 10.0. Fin cants of 0°, 2° and 4° were imposed. The Mach number range tested was between 1.0 and 4.5. All the main aerodynamic coefficients and stability derivatives were well determined using linear theory, six-degree-of-freedom single- and multiple-fit reductions techniques. The results were also compared with results from other aeroballistic ranges. The fins on the models fired at Mach 4.5 ablated during flight. A dynamic stability analysis showed a Magnus instability at certain Mach numbers and spin rates.

RÉSUMÉ

Des essais en vol libre ont été effectués dans le corridor aérobalistique du Centre de recherches pour la défense Valcartier (CRDV) avec le projectile de référence Basic Finner à des vitesses transsoniques et supersoniques. Le projectile était muni de quatre ailettes rectangulaires sur un corps cone-cylindre avec un allongement de 10. L'inclinaison des ailettes par rapport au corps principal était de 0°, 2° et 4°. La gamme de nombres de Mach se situait entre 1.0 et 4.5. Tous les coefficients aérodynamiques principaux et les dérivés de stabilité ont été très bien déterminés avec les méthodologies de réduction des données linéaires et six degrés de liberté par les options de réduction simple et multiple. Les résultats sont aussi comparés à des résultats d'autres corridors aérobalistiques. Les ailettes sur les modèles tirés à Mach 4.5 ont subi une ablation. Une analyse de stabilité dynamique a démontré une instabilité Magnus à certains nombres de Mach et taux de roulis.

TABLE OF CONTENTS

EXECUTIVE SUMMARY

The DREV Aeroballistic Range is a unique facility where projectile trajectories are accurately determined and converted to aerodynamic coefficients and stability derivatives. Even though the DREV Aeroballistic range has been fully operational since 1990, other priorities (small caliber Range Limited Training Ammunition, 105-mm Spinning Tubular Projectiles and several international obligations) prevented firing a reference projectile configuration to evaluate the accuracy of the determined coefficients. It was therefore deemed necessary to fire the Basic Finner reference projectile in the DREV Aeroballistic range. The opportunity was also taken to increase the aerodynamic data base to higher supersonic Mach numbers which was lacking with the previous tests. This increase in the data base will allow empirical and analytical prediction tools to be adjusted with reliable and absolute data at the higher Mach numbers.

The Basic Finner configuration was used for many years as a reference projectile and it was tested extensively in other aeroballistic ranges and in wind tunnels. The model consists of a 20° nose cone on a cylindrical body with four rectangular fins. The l/d of the model was 10.0. The nominal diameter of the projectiles was 30 mm. Fin cants of 0°, 2° and 4° were imposed to produce a desired roll motion. The highest Mach numbers tested at the other aeroballistic ranges was Mach 3 and the data analysis used at the time consisted only of linear theory.

All of the main aerodynamic coefficients (C_{x0}, $C_{N\alpha}$, $C_{M\alpha}$, C_{Mq}, $C_{np\alpha}$, C_{lp}, $C_{l\delta}\delta$) were very well determined over a Mach number range of 1.05 to 4.5. Some nonlinear behaviors in the axial force and in the static pitch moment were also determined. The aerodynamic coefficients determined from these tests are in excellent agreement with published data.

A dynamic stability analysis explained a growth in angle of attack that was observed on some shots as the projectile flew downrange. This was attributed to a Magnus dynamic instability on the precession mode. A stability diagram showing the onset of instability as a function of spin rate (or cant angle) and Mach number was also determined. Some aeroheating aspects were observed on the projectiles fired at the highest muzzle velocity of approximately 1520 m/s.

The results show that the DREV Aeroballistic Range is a unique and excellent tool to obtain the dynamics of a projectile in flight and the absolute values for the aerodynamic coefficients. Other facilities, such as wind tunnels or predictive tools, such as computational fluid dynamics, are useful for relative comparisons but cannot provide absolute values with a high degree of reliability and are quite limited in the acquisition of dynamic stability derivatives.

NOMENCLATURE

Variable	Computer Output	Description
A		Cross sectional area of projectile (m^2)
d		Diameter of projectile (mm)
C_D	CD	Total drag coefficient
C_{D0}	CD0	Drag force coefficient at zero angle of attack
$C_{D_{\bar{\delta}2}}$	CDSQ	Yaw drag coefficient derivative
c. g.	CG	Center of gravity (m)
C_{lp}		Roll damping moment coefficient
$C_{l\delta}$		Roll moment coefficient due to fin cant
$C_{l\gamma}$	Clg	Induced roll moment coefficient
C_{np}	Cnp	Magnus moment coefficient
$C_{n\gamma}$	Cng	Induced yaw moment coefficient
C_{nsm}	Cnsm	Side moment coefficient
C_N	CN	Normal force coefficient
$C_{N_\delta}\delta_A$	CNda	Trim force coefficient component
$C_{N_\delta}\delta_B$	CNdB	Trim force coefficient component
C_M	Cm	Static pitch moment coefficient
C_{Mq}	Cmq	Pitch damping moment coefficient
$C_{M_\delta}\delta_A$	Cmda	Trim moment coefficient component
$C_{M_\delta}\delta_B$	CmdB	Trim moment coefficient component
$C_{m\gamma}$	Cmg	Induced pitching moment coefficient
C_{x0}	CX	Axial force coefficient at zero angle of attack
C_{Yp}	CYp	Magnus moment coefficient
$C_{Y\gamma}$	CYg	Induced normal force coefficient
$C_{Z\gamma}$	CZg	Induced normal force coefficient
I_x, I_y	-	Axial and transverse moments of inertia (kg m^2)
l	-	Length of projectile (m)
l/d	-	Length-to-diameter ratio
m	-	Mass of projectile (kg)

M	Mach	Mach number
p	-	Spin rate (rad/s or deg/m)
Re_l	-	Reynolds number based on length of projectile
s_g	-	Gyroscopic stability factor
u, v, w	-	Projectile component velocities (m/s)
V	-	Total projectile velocity (m/s)
X, Y, Z	-	Projectile coordinates (m)
t	-	Time of flight (s)
$\overline{\alpha}$	a	Total angle of attack (deg)
$\overline{\alpha}_{max}$	AMAX	Maximum angle of attack (deg)
λ_N, λ_P	LN, LP	Nutation and precession damping (1/m)
θ, ψ, ϕ	–	Projectile orientation (deg)
δ	-	Fin cant angle (rad or deg)
$\overline{\delta}^2$	DBSQ	Mean squared yaw (deg^2)
ε	-	Sine of the total angle of attack, $\sin \overline{\alpha} = \dfrac{v^2 + w^2}{V^2}$
ρ	-	Air density (kg/m^3)
6DOF	-	Six degree of freedom

Subscripts

$\overline{\alpha}_i$	ai (i)	Derivative with respect to ε_i
M	M	Variation with Mach number

Examples

$C_{M\overline{\alpha}}$	Cma	Pitching moment coefficient slope
$C_{M\overline{\alpha}3}$	Cma3	Pitching moment coefficient w.r.t. ε^3
$C_{Mq\overline{\alpha}2}$	Cmq2	Pitch damping coefficient w.r.t. ε^2

1.0 INTRODUCTION

This memorandum presents free-flight data that have been reduced to aerodynamic coefficients from tests on the Basic Finner reference projectile. The model consisted of four rectangular fins on a cone-cylinder body with a l/d of 10. These tests and data analysis were carried out in the Defence Research Establishment Valcartier (DREV) Aeroballistic Range. Twenty six models were fired in the Mach number range of 1.05 to 4.5.

The Basic Finner configuration was used for many years as a reference projectile and it was tested extensively in other aeroballistic ranges and in wind tunnels. The highest Mach numbers tested at the other aeroballistic ranges was Mach 3. The data analysis used at the time consisted of linear theory where the motion had to be decoupled in time-distance for drag, swerve for normal force, pitch and yaw for aerodynamic yaw moments and roll for the roll damping and roll producing moment coefficients.

It was therefore deemed necessary to fire some Basic Finner projectile in the DREV Aeroballistic Range to compare the accuracy of the determined aerodynamic coefficient and stability derivatives with published data. Even though the DREV Aeroballistic Range has been fully operational since 1990, other priorities prevented firing this projectile configuration until recently. The opportunity was also taken to increase the aerodynamic data base to higher supersonic Mach numbers which was lacking with the previous tests. This increase in the data base will allow empirical and analytical prediction tools to be adjusted with reliable and absolute data at the higher Mach numbers. Also, computational fluid dynamic studies could also use the data to validate their predictions.

The data analyses used in the DREV tests consisted of the linear theory and the six-degree-of-freedom Maximum Likelihood Function methods. The latter method was not utilized in the analysis of the published data. The motion is not decoupled in the six degree-of-freedom (6DOF) analysis. The 6DOF data reduction system can also simultaneously fit multiple data sets (up to five) to

a common set of aerodynamics. Using this multiple-fit approach, a more complete range of angle of attack and roll orientation combinations is available for analysis than would be available from a single flight. This increases the accuracy of the determined aerodynamics over the entire range of angle of attack and roll orientations. Using this reduction technique would also verify the previously published data, especially the dynamic stability derivatives which are difficult to obtain in the best of circumstances.

All of the main aerodynamic coefficients (C_{x0}, $C_{N\alpha}$, $C_{M\alpha}$, C_{Mq}, C_{np_α}, C_{l_p}, $C_{l_\delta}\delta$) were determined in linear theory and in both the 6DOF single- and multiple-fit data reduction techniques. Some nonlinear aerodynamic coefficients were also determined as well as some Mach number dependence on the main coefficients with the multiple-fit reductions. These aerodynamic coefficients are also compared with the previously published data.

A dynamic stability analysis was also accomplished to explain the flight behavior of several shots. Motion plots, comparing the theoretical trajectories with the experimental ones, are included for all test shots as well as photographs of typical shock structures at the various velocity regimes. Some ablation due to aerodynamic heating was also observed.

This work was performed at DREV from March 1995 to December 1995 under Work Unit 2ea14, Flight Mechanics of Munitions.

2.0 FACILITY DESCRIPTION

The Defence Research Establishment Valcartier (DREV) Aeroballistic Range (Refs. 1 and 2) is an insulated steel-clad concrete structure used to study the exterior ballistics of various free-flight configurations. The range complex consists of a gun bay, control room and the instrumented range (Fig. 1a). A massive blast wall is located in front of the building to stop sabot pieces and minimize vibrations transmitted to the range structure and instrumentation. Projectiles of caliber ranging from 5.56 to 155 mm, including

tracer types, may be launched. Large-caliber models have been fired up to Mach 7.

The 230-metre instrumented length of the range has a 6.1-m square cross section with a possibility of 54 instrumented sites along the range (Fig. 1b). For these tests all of the stations were operational. These sites house fully instrumented orthogonal shadowgraph stations that yield photographs of the shadow of the projectile as it flies down the range. The maximum shadowgraph window, an imaginary circle within which a projectile will cast a shadow on both reflective screens, is 1.6 m in diameter. There are also four Schlieren stations (three operational for these tests) at the beginning of the range that yield high quality flow photographs. The range is also air conditioned to maintain a constant relative humidity of approximately 45%. The nominal operational conditions of the range are 20° C at standard atmospheric conditions. The spark source and reference point locations that were used were deduced from a standard survey. A dynamic calibration was conducted in the downrange coordinate only.

3.0 MODELS AND TEST CONDITIONS

3.1 Model Configuration

The Basic Finner reference model consists of a 20° nose cone on a cylindrical body with four rectangular fins, as shown in Fig. 2. The configuration was based on Refs. 3, 4 and 5. The l/d of the model was 10.0. The fin dimensions were 1 cal x 1 cal and conical in shape with a thickness of 0.08 cal at the base of the fin. The leading edges of the fins were very sharp with a radius 0.004 cal. The meplat of the nose was also at a radius of a 0.004 cal. The nominal diameter of the tested projectiles was 30 mm.

The models were ballasted to obtain a center of gravity at approximately 5.5 calibers from the nose of the projectiles to assure static

stability at all tested Mach numbers. The ogive of the model was made of a high-density alloy and the fins and the cylindrical portion of the projectile were made of steel. The nominal physical properties of the models tested are given in Table I and the physical properties of each test projectile are listed in Table II.

The fins were deliberately canted to produce roll motion. Nominal fin cants of 0.0°, 2.0° and 4.0° were applied. All the fins were canted at the same nominal cant angle on one model to produce a clockwise roll motion when the projectile is viewed from the rear. The fin cant of each individual fin were measured and the average fin cant angles for each model are given in Table III. Figure 3a shows the tested projectile at the three nominal fin cant angles.

The models (A01-A04, A11-A14, A21-A24), were specifically designed to be fired at the lower velocities and were made of stress-proofed steel with a 100 000 psi yield. All the other projectiles were made with AISI 4340 Heat Treated to a ROC "C" 40-42 hardness so that they could withstand the highly expected launch accelerations at the higher velocities.

The models were modified by adding roll pins to measure the projectile's roll orientation in the Aeroballistic Range (Fig. 3b). Two roll pins are shown in the figure but the smaller one was clipped off for the tests to simplify the film reading.

3.2 Sabot Design

The sabot for the model (Fig. 3b) consisted of a two-piece petal type made of aluminum and was designed to be fired from a 110-mm smooth bore powdered gun. It had four projectile centering screws at the front of the sabot. The saw cut lengths on each side were adjusted to obtain adequate petal separation for the expected velocities. Teflon riders were situated at the front and the rear of the sabot to protect the gun tube from erosion due to friction. A sabot base pad seal was also used to prevent gas leakage pass the sabot body. The projectile rested on a two piece steel pad (not shown) situated at the base

of the sabot to transmit the launch loads to aluminum sabot. The complete drawings of the sabot design are given in Appendix A. The mass of the combined sabot-projectile was approximately 3.6 kg.

All the models were fired from a 110-mm smooth bore gun and worked well at the velocities tested which ranged from 340 to 1511 m/s. Typical model-sabot separations at 6.1 m from the muzzle are shown in Fig. 4 at muzzle velocities of approximately 380 and 1511 m/s. As can be observed, the petals separated cleanly from the projectile and all the sabot pieces were stopped by the massive sabot trap located in front of the instrumented range.

3.3 Test Conditions and Particularities

Twenty-six (26) projectiles were fired in this aeroballistic range program. As part of the experimental design, it was planned to fire, at one nominal Mach number, projectiles with the three fin cant nominal angles. This was done so as to be able to use the full capability of the multiple fit option in the data reduction software in obtaining the aerodynamic coefficients. Also, the whole Mach number range between 1.0 to 4.5 was to be covered.

Due to the expected high launch loads at the higher velocities, two propellant types were utilized. The NQM 044 propellant was used to fire the projectile- sabot at the lower velocities ranging between 380 and 1159 m/s and NQM 047 was used for the higher velocities.

The propellant type, the charge mass, the muzzle velocities and which model was fired at a particular velocity are given in Table IV. The model number with the appropriate nominal fin cant angle are also provided. The number between parentheses below the model number is the mid-range Mach number for that particular shot and an average was taken to obtain the reference Mach numbers necessary for the data reduction process and to select the shot groupings for the multiple data reductions. The muzzle velocity indicated is the average for the number of projectiles fired at that charge. The

associated propellant charge mass is also given. The fins of Shot A14 ablated during in flight and no films could be analyzed. There were also indications that Models A01 and A11 had slight fin ablation (see Section 5.2). The propellant charged was slightly reduced for Shot A23 due to this.

The measured physical properties of each test projectile are given in Table II and the projectiles which had roll data are also indicated. The roll pins of Shots A01 and A23 could not be read on the films. The range conditions for each test projectile at time of firing are given in Table V. The Reynolds number, based on the length of the projectile, ranged between 7.00×10^6 and 30.0×10^6 for the Mach number range of 1.0 to 4.5, respectively.

Typical shadowgraph photographs showing the flow structure around the projectile at various Mach numbers are shown in Figs. 5 to 7. The supersonic flow structures at Mach 4.5 and 3.0 are shown in Figs. 5 and 6 respectively. The boundary layer growth along the projectiles is clearly seen. The transonic flow structure on projectile A10 is shown on three photographs (Fig. 7) as the projectile flew downrange. The velocity and Mach number given on each caption were deduced from the six-degree-of-freedom data reduction techniques. It can be noticed that as the projectile decelerates, the bow shock becomes more normal and the fin shock gets further away from the fins.

The numbering scheme to refer to the shots is as follows. The shot numbers are identified by two letters followed by 8 digits, as for example DA95030111. The "D" implies that the biases from a dynamic calibration were taken into account for this shot. Other numbers (950301) indicates the date (year, month and date) that the projectile was fired in the range. The last two digits correspond to the shot number. For the example given above, the shot number corresponds to the eleventh shot that was fired in the range on March 1st, 1995.

4.0 FREE-FLIGHT DATA REDUCTION

Extraction of the aerodynamic coefficients and stability derivatives is the primary goal in analyzing the trajectories measured in the DREV Aeroballistic Range. This is done by means of the Ballistic Range Data Analysis System (BARDAS, Ref. 6), shown in Fig. 8. This program, BARDAS, incorporates a standard linear theory and a six-degree-of-freedom (6DOF) numerical integration technique. The 6DOF routine incorporates the Maximum Likelihood Method (MLM) to match the theoretical trajectory with the experimentally measured trajectory. The MLM is an iterative procedure that adjusts the aerodynamic coefficients to maximize a likelihood function. The application of this likelihood function eliminates the inherent assumption, in least-square theory, that the magnitude of the measurement noise must be consistent between parameters (irrespective of units). In general, the aerodynamic coefficients are nonlinear functions of angle of attack, Mach number and roll angle.

BARDAS represents a complete ballistic-range data reduction system capable of analyzing both symmetric and asymmetric models. The essential steps of the data reduction system are (1) to assemble the dynamic data (time, position, angles), model measured physical properties and atmospheric conditions, (2) to perform linear theory analysis, and (3) to perform 6DOF analysis.

These three steps have been integrated into BARDAS to provide the test scientist with a convenient and efficient means of interaction. At each step in the analysis, permanent records for each shot are maintained so that subsequent analyses with data modification are much faster.

The 6DOF data reduction system can also simultaneously fit multiple data sets (up to five) to a common set of aerodynamics. Using this multiple-fit approach, a more complete range of angle of attack and roll orientation combinations is available for analysis than would be available from a single

flight. This increases the accuracy of the determined aerodynamics over the entire range of angle of attack and roll orientations.

The aerodynamic data presented in this document were obtained using the linear theory analysis, the fixed-plane 6DOF analysis (MLMFXPL) with both single- and multiple-fit data correlation techniques after a dynamic calibration, as discussed below. The equations of motion have been derived in a fixed-plane coordinate system, with Coriolis effects included. The formal derivation of the fixed-plane model is given in Ref. 7.

All the results presented here were deduced after the dynamic calibration biases were accounted for in the X-direction. The details of the dynamic calibration for the DREV Aeroballistic Range are given in Ref. 8 and the methodology is explained in Ref. 9.

5.0 FREE-FLIGHT RESULTS AND DISCUSSIONS

The aerodynamic coefficients and stability derivatives that were reduced from the free-flight trajectories measured in the Aeroballistic Range are presented in both tabular and plotted form for both the linear theory analysis and 6DOF reductions. All of the determined aerodynamic coefficients are given at the mid-range measured Mach number.

5.1 Linear Theory Results

The linear theory results are presented in Tables VI and VII. The probable errors of fit from the decoupled motion (downrange, swerve, angular and roll) of the linear theory analysis are given in Table V. The maximum angle of attack observed ranged between 0.7° and 9.0°.

The linear theory parameters deduced from the decoupled motion are given in Table VI. All the shots, except for three (DA13, DA22 and DA23) were

dynamically stable, as observed by the negative precession and nutation damping modes. The linear theory parameters indicate the precession arm does not damp (positive value) for these three shots. These will be further investigated in the six-degree-of-freedom analyses.

The aerodynamic coefficients deduced from the linear theory parameters are presented in Table VII. The methodology to obtain the aerodynamic coefficients from the linear theory parameters is explained in Ref. 6. The main aerodynamic coefficients (C_{D0}, $C_{N\alpha}$, $C_{M\alpha}$) are consistent and the probable errors of fit of the motion (Table V) are quite acceptable. All the models were statically stable, as shown by the negative slope of the pitch moment coefficient. There is some dispersion in C_{Mq} and C_{np_α} mainly due to the low angles of attack on some shots. The linear analysis does not fit for a roll moment due to a fin cant ($C_{l_\delta}\delta$), and therefore, the roll damping coefficient (C_{l_p}) in the linear theory results are irrelevant (Table VII). These coefficients and any nonlinearities are best modeled and reduced with the 6DOF reduction technique of the next section.

5.2 Six-Degree-of-Freedom Results

The determined aerodynamic coefficients, their respective probable errors, and the probable errors between the theoretical and experimental trajectories for the axial, angular and roll motions are given in Table VIII and Table IX for the single-fit and multiple-fit data reduction techniques, respectively. The moment reference center for the pitch and Magnus moment coefficients was at 55% of the length from the nose of the projectile (5.50 cal). All the results are given at the mid-range Mach number for the single-fit data reductions and at the average mid-range Mach numbers for the multiple-fit data reductions.

A coefficient that appears with a value and a (*) between parentheses directly below, indicates that this coefficient was held constant and one that has a (-) between parentheses indicates that this coefficient was solved for and

that the probable error for this coefficient was higher than 100%, that is, it does not influence the fit and is considered undetermined. Those with numbers between parentheses represent the probable error for that particular coefficient.

The multiple-fit groups were chosen by Mach numbers, as mentioned previously (Table IV). Eight groups of multiple-fit data reductions were conducted. Whenever possible, individual shots with all three fin cant angles were included in the multiple fits. Two shots (DA22 and DA01) were not included in the multiple-fit data reduction process. The first one since it is believed that $C_{l_\delta}\delta$ and C_{l_p} are at the transonic trend extreme and the second shot (DA01) is believed to be flying in a resonance condition. Unique C_{X0} were solved for the multiple-shot groups at Mach number of 1.832, 2.375, 2.718 and 3.147 since the probable error of fits improved considerably when doing so.

As seen from the Tables VIII and IX, all of the main aerodynamic coefficients (C_{X0}, $C_{N\alpha}$, $C_{M\alpha}$, C_{Mq}, C_{np_α}, C_{l_p}, $C_{l_\delta}\delta$) were very well determined as indicated by the low probable errors of fits on the coefficients. The aerodynamic trims were solved for all the shots that had low spin rates (no fin cant). The nonlinear axial force coefficient ($C_{x_{\alpha^2}}$) was well determined in the multiple-fit data reductions. The cubic pitch moment coefficient term ($C_{M_{\alpha^3}}$) was also determined with both the single- and multiple-fit data reduction techniques at the higher Mach numbers where high angles of attacks were achieved. The variation of the $C_{M\alpha}$ and C_{X0} with Mach number changes rapidly in the transonic region as noticed by the determined coefficients ($C_{M\alpha M}$ and C_{X0M}) in the multiple-fit data reductions. These last two coefficients were also solved for in the single-fit reductions (results not in Table) and were consistent with the multiple-fit results.

An attempt to solve for a pure side moment with no influence of spin (C_{nsm}) in lieu of the Magnus moment (C_{np_α}) was conducted and in all the cases a better fit was obtained when C_{np_α} was solved for.

The probable errors of the single and multiple fits are of the order of 0.7 mm in the downrange coordinate, 0.4 mm in the swerve motion, 0.08° in pitch and yaw and of the order of 1.5° in roll. These fits are considered excellent and are consistent with other tests conducted in the DREV Aeroballistic Range. The 6DOF probable errors of fits are smaller than the linear theory ones because of the better mathematical modeling of the motion, such as the inclusion of aerodynamic trims, angle of attack dependent terms and variation with Mach number.

The fins of Shot DA14 fired at an approximate velocity of 1520 m/s ablated during flight. The shadowgraphs showed a continuous light streak on them, which is consistent with observed burning fins on other projectiles fired in the DREV Aeroballistic Range (Ref. 10) where fins ablated. Due to this, no aerodynamic data could be obtained for this shot. The fins of the Basic Finner models were made of steel and were rectangular in shape with a very sharp leading edge. The fin ablation is believed to be caused by the same process as the one observed in Ref. 10. That is, the prime area of heating occurs on the fin leading edge, where the interaction between the fin bow shock, which separates the boundary layer, and the separation shock generated at the leading edge of the viscous interaction, gives rise to a supersonic jet, which impinges on the fin. It is there that the effect of ablation is most apparent, and this interaction causes the re-entrant profile on the fin leading edge.

Two other shots (DA01 and DA11) fired at the same approximate velocity showed some indication that some form of ablation occurred. This was noticed by traces of carbon deposits around the fin cutout imprints on the cardboard target at the end of range indicating that some fin ablation occurred. These two shots were fired at the same propellant charge as shot DA14. This seems to indicate that Shot DA14's muzzle velocity was just a bit higher than the other two and that it was enough to initiate the ablation process.

5.3 Comparison of 6DOF Single- and Multiple-Fit Results

A comparison of the reduced aerodynamic coefficients from the 6DOF data reductions techniques with the single- and multiple-fits results are given in Figs. 9 to 16. The single-fit data points are shown as crosses, while the multiple-fit data reduction results are given as a solid circles.

Appendix B presents, for every test shot, the total angle-of-attack history with the observed angular motion and the theoretical determined one with the reduced aerodynamic coefficients. When a multiple-fit data reduction was conducted, these are given in priority, and if not available, the single-fit ones are presented. The experimental data points (open circles) and the calculated trajectory (continuous line) from the determined coefficients are compared. This allows a verification that the reduced aerodynamic coefficients do fit the experimental trajectory satisfactorily. For every shot, the total angle of attack, the angular motion plots and the spin rate in deg/m are given as a function of the downrange coordinate as well as the motion in the pitch-yaw plane. On the spin plots, the nutation pitch frequency is also given.

The axial force coefficient at zero angle of attack (C_{X0}) as a function of Mach number is shown in Fig. 9. The agreement is excellent between the single fit and the multiple fits. There is a bit of scatter in the single-fit results. The single-fit reductions for this coefficient are plotted in Fig. 10 versus Mach number and with the nominal fin cant angle indicated. This was conducted to investigate any influence of spin on the axial force coefficient and no specific trends can be inferred from Fig. 10 that would indicate such an effect.

$C_{N\alpha}$, the normal coefficient slope, versus Mach number is displayed in Fig. 11. There is some scatter in the single fit results due to some low angle-of-attack cases. One single point, Shot DA01, at Mach 4.45 seems to be above the trend at the higher supersonic Mach number. The spin history of this shot indicates (Appendix B) that it went through resonance. The probable error in the angular motion for this shot is 0.15° and well above the others. Also, as mentioned previously, some indication of fin ablation was also noticed on this

shot which might influence some coefficients. The transonic peak point at approximately Mach 1.25 seems to have been missed at this trial.

The variation of the pitching moment coefficient slope, $C_{M\alpha}$, with Mach number is shown in Fig. 12. The scatter in the results was very small. The transonic peak point was also not obtained. The change in $C_{M\alpha}$ with Mach number in the transonic region is quite high. $C_{M_{\alpha^3}}$ was well determined at Mach numbers above 3.5 (Table IX).

The determined pitch damping coefficient, C_{Mq}, as a function of Mach number is presented in Fig. 13. The scatter is higher than for the other coefficients but the main trend can be observed. The multiple-fit data point at Mach 2.4 does not follow the main trend. The single-fit data point (DA27) at -400 was well determined and the angular motion (Appendix B) shows a possible Magnus instability.

The Magnus moment coefficient slope, C_{np_α}, is given in Fig. 14. The coefficient was well determined and the agreement between the single and multiple fits is very good. At Mach 1.8 the coefficient is approximately -35 and decreases gradually to -9 as the Mach number increases to Mach 4.5. The magnitude changes very rapidly in the transonic region (1.05 < M < 1.7) to peak at approximately -330 at Mach 1.3 and then falls rapidly to zero just over Mach 1. The multiple fit at 1.05 did not detect any C_{np_α} at all.

C_{l_p}, the roll damping coefficient, is demonstrated versus Mach number in Fig. 15. As with the other cases, it is well determined and the agreement is very good. The transonic peak for this coefficient seems to have been found at roughly Mach 1.4 on Shot DA22.

The data reduction process solves for a total roll moment coefficient due to fin cant $C_{l_\delta}\delta$. This coefficient produces the required moment to impose a roll motion or desired spin rate on the projectile. It is solved individually when conducting multiple fits since it is unique for a particular projectile or fin cant.

The coefficient that is usually published is C_{l_δ} and in this case, per radian. To achieve this, the fin cant angles must be measured with accuracy and this was done (Table III). Only the shots with some cant angles can be used in this process. The combined values $C_{l_\delta}\delta$ and the computed C_{l_δ} based on the average measured fin cants are given in Table X for each individual shot number and these are based on the single fit data reductions. The trend of C_{l_δ} with Mach number is offered in Fig. 16.

6.0 COMPARISON OF DREV RESULTS WITH PUBLISHED DATA

As the Basic Finner served as a reference or a calibration projectile for many years, there is sufficient data to compare the DREV results with. This projectile was extensively tested in other aeroballistic ranges (Ref. 3 - 5) mostly from Mach 1.0 to 3.0. The data reduction process utilized in these reports was based only on the linear theory analysis. Ref. 3 was utilized to compare the main aerodynamic coefficients of C_{x0}, $C_{N\alpha}$, $C_{M\alpha}$, C_{Mq} and Ref. 4 for C_{l_p} and C_{l_δ}. The Magnus moment coefficient slope, C_{np_α}, was not compared since the data of Ref. 3 was very erratic and there was high scatter.

The aerodynamic coefficients of those two reports were transformed to the terminology and convention used in this memorandum. The moment coefficients were transferred to the center of gravity of the projectiles fired in the DREV Aeroballistic Range.

The results from the DREV Aeroballistic Range with the multiple-data reduction technique are compared with the published data of Refs. 3 and 4 in Fig. 17. The agreement is excellent. Some of the scatter in the results of the published data might be inferred from the limitations of the linear theory analysis and the magnitude of the angles of attack.

7.0 DYNAMIC STABILITY ANALYSIS

Several shots showed a large increase in angular growth while some shots were initially damping and increased in angular growth as the projectile flew downrange. Shot DA13 at Mach 1.25 and DA22 at Mach 1.38 show (Annex B) an increase in angle of attack as the projectile flies downrange. The initial angle of attacks for both shots were approximately 2° and DA13 grew to 3° while DA22 to 10° at 250 m. The other shot at the same approximate Mach number, DA09, showed regular damping trend in angle of attack. The last shot had no fin cant, while DA13 and DA22 had fin cants of 2° and 4°, respectively, producing different spin rates as seen in Appendix B. The magnitude of the Magnus coefficient slope in this Mach number region is also very high as shown in Fig. 14. The combined high magnitude of C_{np_α} and the high spin rate achieved seems to indicate a Magnus instability. The approximate steady spin rates of the 2° and 4° fins cants (Appendix B) are approximately 65 deg/m and 125 deg/m, respectively.

Shot numbers DA26, DA27, DA28 and DA29 show the initial angle of attack damping and then increasing slightly as the projectile flew down range (Appendix B). All of these shots have a 4° fin cant and the spin rate increases rapidly as the projectile flies down the range. The Mach number range of these shots is between 1.8 and 2.7 and the magnitude of the Magnus moment coefficient slope lies between -100 and -25 in this Mach number range.

To obtain a better understanding of this, a dynamic stability analysis was conducted. The angular motion can best be explained with the linear theory analysis formulation (Ref. 6). The pitch and yaw motions are modeled by a damped sinusoidal function. The yaw damping factors of the nutation and precession arms are given, respectively, by (Ref. 11):

$$\lambda_N = \frac{\rho A}{4 m} \left[-C_{N\alpha} \left(1 - \frac{1}{\sigma} \right) + \frac{k_2^{-2}}{2} \left(1 + \frac{1}{\sigma} \right) C_{Mq} + \frac{k_1^{-2}}{\sigma} C_{np_\alpha} \right] \qquad [1]$$

and

$$\lambda_P = \frac{\rho A}{4\,m} \left[-C_{N\alpha}\left(1 + \frac{1}{\sigma}\right) + \frac{k_2^{-2}}{2}\left(1 - \frac{1}{\sigma}\right)C_{Mq} - \frac{k_1^{-2}}{\sigma}\,C_{np\alpha} \right] \qquad [2]$$

where:

$$k_1^{-2} = \frac{m\,d^2}{I_x} \qquad [3]$$

$$k_2^{-2} = \frac{m\,d^2}{I_y} \qquad [4]$$

$$\sigma = \sqrt{1 - \frac{1}{s_g}} \qquad [5]$$

where s_g is given by

$$s_g = \frac{2\,I_x^2\,p^2}{\pi\,I_y\,\rho\,C_{M\alpha}\,V^2\,d^3} \qquad [6]$$

The above formulation is usually utilized for a spin stabilized projectile but it also holds for finned projectiles with adequate spin rates. In this case the gyroscopic stability factor is negative, since $C_{M\alpha}$ is negative.

The criterion for a projectile to be dynamically stable is that the fast and slow arm damping factors be negative. By inspection of the two damping terms above, equation [1] and [2], a high negative Magnus moment coefficient slope, $C_{np\alpha}$, combined with a high spin rate can only render the precession arm unstable, i.e. greater than zero.

A computer algorithm was written to calculate the precession damping term as a function of spin rate for different Mach numbers. The aerodynamic coefficients determined from the aeroballistic range using the multiple-fit data

reduction technique (Table IX), the nominal physical properties of the test projectile as well as typical atmospheric conditions at time of firing were utilized.

The results of the calculations are given in Fig. 18 on two different scales. The precession damping term, λ_p, is given as a function of the spin rate in deg/m for various Mach numbers. If $\lambda_p > 0.0$, the projectile is dynamically unstable and the angle of attack will increase as the projectile flies downrange. The range of spin rate induced by the 0°, 2° and 4° fin cants lies between 0 deg/m and 135° deg/m (Appendix B).

The first observation is that at Mach 1.29 the precession arm goes positive at a spin rate of approximately 30°/m. The two shots that were fired at this approximate Mach number, as explained previously, had a spin rate higher than 30°/m and showed an angular growth, especially for the 4° cant model. Therefore, it can be concluded that a Magnus dynamic instability will occur in the transonic regime for projectiles with high fin cants.

For all the other Mach numbers that were calculated, the precession arm becomes positive, i.e. unstable, in the range of spin rate that lies between 120 deg/m and 160 deg/m. Since the steady spin rates obtained for the 4° cant models are approximately 125 deg/m and some went even as high as 135 deg/m, the possibilities of a Magnus instability to occur are rather high. No doubt that it is at the limit. A higher fin cant angle would definitely have caused a dynamic instability at all Mach numbers. This also explains why some 4° cant models showed some angular growth while others did not.

8.0 CONCLUSIONS

The aerodynamic characteristics of the Basic Finner projectile were determined from free-flight tests in the DREV Aeroballistic Range with the full complement of stations. The Mach number ranged between Mach 1.05 and 4.5. The rectangular fins of the projectiles were canted at nominal angles of $0°$, $2°$ and $4°$ producing spin rates in the range of 0 deg/m, 65 deg/m and 125 deg/m, respectively. All of the main aerodynamic coefficients (C_{X0}, $C_{N\alpha}$, $C_{M\alpha}$, C_{Mq}, $C_{np\alpha}$, C_{l_p}, $C_{l_\delta}\delta$) were very well determined. This was confirmed by the probable errors of the reduced coefficients and the low probable errors of fits between the experimental and theoretical trajectories of the linear theory analyses and 6DOF reduction techniques. Some nonlinear behaviors in the axial force and in the static pitch moment were also determined from multiple fits.

There was very good agreement between the single and multiple fits with probable errors of fits of approximately 0.7 mm in the downrange coordinate, 0.4 mm in the swerve motion, $0.08°$ in pitch and yaw and of the order of $1.5°$ in roll. Detailed flow photographs showing the shock structure and boundary layer growth in the range of Mach numbers tested are also given.

The aerodynamic coefficients determined from these tests were also compared with published data from other free-flight aeroballistic ranges. The agreement is excellent and the data base was extended to Mach 4.5 with these tests. The Magnus moment coefficient slope obtained from the DREV Aeroballistic Range tests can be considered better determined that the published data.

A dynamic stability analysis explained a growth in angle of attack that was observed on some shots as the projectile flew downrange. This was attributed to a Magnus dynamic instability on the precession mode. A stability diagram showing the onset of instability as a function of spin rate (or çant angle) and Mach number was also determined. It was shown that for transonic Mach numbers and for spin rates greater than 30 deg/m, the projectile would

be dynamically unstable. At Mach numbers greater than 1.8, the projectile would be dynamically unstable if the spin rates are greater than approximately 120 deg/m.

Some aeroheating aspects were detected on the projectiles fired at the highest muzzle velocity of approximately 1520 m/s. This was observed on previous tests in the DREV Aeroballistic Range and is believed to be caused by the same phenomenon. That is, the prime area of heating occurs on the fin leading edge, where the interaction between the fin bow shock, which separates the boundary layer, and the separation shock generated at the leading edge of the viscous interaction, gives rise to a supersonic jet, which impinges on the fin.

9.0 ACKNOWLEDGMENTS

The authors would like to thank Mr. M. Normand, who designed the sabot, for launching the models and assisted in all the trials and Mr. C. Julien and Mme L. Audet for the operation of the range and their many required adjustments on the Schlieren system during the Aeroballistic Range trials. Also, the perseverance of Mme. S. Lafond, of SNC-IT, in the developing, loading and reading the films with such thoroughness is greatly appreciated and is shown in the quality of the reduced coefficients. We are also greatful to the trials team for these tests for their devotion in making these tests a success.

10.0 <u>REFERENCES</u>

1. Drouin, G., Dupuis, A. and Côté, F., "Instrumentation Development and Data Analysis for the DREV Aeroballistic Range", DREV M-2800/87, March 1987, UNCLASSIFIED

2. Dupuis, A. and Drouin, G., "The DREV Aeroballistic Range and Data Analysis System", AIAA Paper No. 88-2017, AIAA 15th Aerodynamic Testing Conference, San Diego, California, 18-20 May, 1988.

3. MacAllister, L. C., "The Aerodynamic Properties of a Simple Non Rolling Finned Cone-Cylinder Configuration Between Mach Numbers 1.0 and 2.5", BRL Report No. 934, May 1955

4. Nicolaides, J. D. and Bolz, R. E., "On the Pure Rolling Motion of Winged and/or Finned Missiles in Varying Supersonic Flight", BRL Report No. 799, March 1952

5. Nicolaides, J. D. and MacAllister, L. C., "A Review of Aeroballistic Range Research on a Winged and/or Finned Missiles", Ballistic Technical Note No. 5, Bureau of Ordnance, Department of the Navy, Oct. 1954

6. "Ballistic Range Data Analysis System (BARDAS)", Arrow Tech Associates Inc., DREV Contract No. W7701-0-1227, March 1992.

7. Hathaway, W. H. and Whyte, R., "Aeroballistic Research Facility Free-Flight Data Analysis using the Maximum Likelihood function", AFATL-TR-79-98, December 1979, UNCLASSIFIED

8. Dupuis, A. D. and Hathaway, W. H., "Aerodynamic Characteristic of a Finned Projectile at Supersonic and Hypersonic Speeds from Free-Flight Tests, DREV R-9404, October 1994, UNCLASSIFIED

9. Whyte, R. and Hathaway, W., "Dynamic Calibration of Spark Aeroballistic Ranges", 44th Aeroballistic Range Association Meeting, 13-17 September, 1993, Munich.

10. Dupuis, A. D., Edwards, J. and Normand, M., "Aerodynamic Characteristic and Aeroheating Aspects of Two Hypersonic Configurations From Free-Flight Tests", DREV - R - 9428, October 1995, UNCLASSIFIED

11. "Projectile Design Analysis System (PRODAS)", Arrow Tech Associates Inc., DREV Contract No. W7701-0-1227, March 1992.

TABLE I
Nominal physical properties of model

d	(mm)	30.00
m	(kg)	1.58
I_x	(kg-cm^2)	1.92
I_y	(kg-cm^2)	97.85
l	(cm)	30.00
CG	(cm from nose)	16.50

TABLE II

Physical properties of test projectiles

Shot Number	Projectile Diameter (mm)	Mass (kg)	Axial Inertia (kg-m2)	Inertia Y (kg-m2)	Inertia Z (kg-m2)	Inertia XY (kg-m2)	Length (mm)	CG (mm)	CG (cal from nose)	Roll (pins)
DA95022010	29.969	1.58	0.192E-03	0.981E-02	0.981E-02	0.000E+00	300.072	164.902	5.502	YES
DA95022219	29.974	1.58	0.192E-03	0.979E-02	0.979E-02	0.000E+00	300.025	165.179	5.511	YES
DA95022230	29.969	1.58	0.192E-03	0.980E-02	0.980E-02	0.000E+00	299.898	165.058	5.508	YES
DA95030613	29.746	1.58	0.192E-03	0.979E-02	0.979E-02	0.000E+00	299.542	164.835	5.541	YES
DA95022009	29.969	1.58	0.191E-03	0.979E-02	0.979E-02	0.000E+00	300.050	165.007	5.506	YES
DA95030622	29.972	1.59	0.193E-03	0.982E-02	0.982E-02	0.000E+00	300.076	165.246	5.513	YES
DA95021318	29.969	1.58	0.192E-03	0.979E-02	0.979E-02	0.000E+00	300.025	165.215	5.513	YES
DA95021529	29.972	1.58	0.193E-03	0.982E-02	0.982E-02	0.000E+00	299.898	164.944	5.503	YES
DA95021308	29.972	1.58	0.192E-03	0.977E-02	0.977E-02	0.000E+00	300.072	165.139	5.510	YES
DA95021328	29.959	1.58	0.192E-03	0.980E-02	0.980E-02	0.000E+00	300.025	165.173	5.513	YES
DA95020907	29.972	1.58	0.191E-03	0.974E-02	0.974E-02	0.000E+00	300.050	165.210	5.512	YES
DA95021317	29.966	1.58	0.191E-03	0.978E-02	0.978E-02	0.000E+00	299.364	164.378	5.485	YES
DA95020927	29.959	1.58	0.192E-03	0.982E-02	0.982E-02	0.000E+00	300.076	165.048	5.509	YES
DA95020906	29.969	1.58	0.191E-03	0.978E-02	0.978E-02	0.000E+00	300.072	165.013	5.506	YES
DA95020916	29.974	1.58	0.192E-03	0.980E-02	0.980E-02	0.000E+00	299.720	164.723	5.496	YES
DA95030603	29.972	1.59	0.193E-03	0.984E-02	0.984E-02	0.000E+00	300.127	165.094	5.508	YES
DA95022205	29.969	1.58	0.191E-03	0.977E-02	0.977E-02	0.000E+00	300.072	165.148	5.511	YES
DA95022215	29.972	1.58	0.192E-03	0.978E-02	0.978E-02	0.000E+00	299.974	165.229	5.513	YES
DA95022726	29.969	1.58	0.192E-03	0.979E-02	0.979E-02	0.000E+00	300.025	165.083	5.508	YES
DA95022702	29.972	1.58	0.192E-03	0.979E-02	0.979E-02	0.000E+00	299.619	164.740	5.496	YES
DA95030121	29.972	1.59	0.193E-03	0.984E-02	0.984E-02	0.000E+00	299.492	164.520	5.489	YES
DA95022712	29.974	1.59	0.193E-03	0.982E-02	0.982E-02	0.000E+00	299.847	164.964	5.504	YES
DA95031523	29.979	1.59	0.193E-03	0.982E-02	0.982E-02	0.000E+00	300.050	165.243	5.512	NO
DA95030101	29.972	1.59	0.193E-03	0.981E-02	0.981E-02	0.000E+00	299.593	164.689	5.495	NO
DA95030111	29.979	1.59	0.193E-03	0.984E-02	0.984E-02	0.000E+00	300.050	165.208	5.511	YES

TABLE III
Measured average fin cant angles

| MODEL | Fin cant angle | |
NUMBER	(deg)	(rad)
A01	0.000792	0.000014
A02	0.001000	0.000017
A03	0.000458	0.000008
A05	0.000417	0.000007
A06	0.000708	0.000012
A07	0.000708	0.000012
A08	0.000667	0.000012
A09	0.000833	0.000015
A10	0.000458	0.000008
A11	2.000542	0.034916
A12	2.000292	0.034912
A13	2.000625	0.034918
A15	2.000000	0.034907
A16	2.000208	0.034910
A17	2.000667	0.034918
A18	2.000042	0.034907
A19	2.000417	0.034914
A21	4.000500	0.069822
A22	4.000417	0.069821
A23	4.000375	0.069820
A26	4.000042	0.069814
A27	4.000208	0.069817
A28	4.000083	0.069815
A29	4.000042	0.069814
A30	4.000125	0.069815

TABLE IV
Summary of launch conditions

a) Propellant NQM 044

Mid Range Mach Ref #	$\overline{V}_{muz}$ (m/s)	Propellant Charge Mass (kg)	Nominal fin cant angle (deg)		
			0	2	4
3.1	1159	4.536	-	A15 (3.31)	A26 (3.34)
3.1	1035	4.082	A05,A03 (2.97, 2.97)	-	-
2.7	947	3.630	A06 (2.74)	A16 (2.75)	A27 (2.67)
2.4	830	3.176	A07 (2.37)	A17 (2.42)	A28 (2.35)
1.8	643	2.268	A08 (1.85)	A18 (1.80)	A29 (1.85)
1.3	466	1.814	A09 (1.33)	A13 (1.26)	A22 (1.38)
1.1	380	1.360	A10 (1.05)	A19 (1.06)	A30 (1.12)

b) Propellant NQM 047

Mid Range Mach Ref #	$\overline{V}_{muz}$ (m/s)	Propellant Charge Mass (kg)	Nominal fin cant angle (deg)		
			0	2	4
4.4	1511	6.260, 5.896[23]	A01 (4.42)	A11, A14* (4.47, -)	A23 (4.13)
3.75	1298	5.444	A02 (3.68)	A12 (3.78)	A21 (3.74)

* Fins ablated during flight - no films

TABLE V

Range conditions

Shot Number	No. of Stations	Observed Distance (m)	Air Density (kg/m3)	Speed of Sound (m/sec)	Reynolds Number (length)		X (m)	Probable Error Swerve (m)	Angle (deg)	Roll (deg)
DA95022010	48	180.0	1.17143	344.00	0.699E+07		0.0006	0.0011	0.070	0.41
DA95022219	48	180.0	1.17792	343.68	0.704E+07		0.0006	0.0004	0.082	0.36
DA95022230	49	190.0	1.17643	343.88	0.742E+07		0.0006	0.0004	0.059	18.30
DA95030613	52	210.0	1.17949	343.96	0.836E+07		0.0009	0.0004	0.084	0.90
DA95022009	51	200.0	1.17998	343.59	0.889E+07		0.0006	0.0006	0.086	0.48
DA95030622	51	210.0	1.17952	344.00	0.920E+07		0.0008	0.0004	0.113	3.01
DA95021318	51	210.0	1.17301	343.74	0.119E+08		0.0007	0.0003	0.058	0.52
DA95021529	50	210.0	1.19148	343.68	0.124E+08		0.0007	0.0003	0.114	0.85
DA95021308	51	210.0	1.17472	343.74	0.123E+08		0.0007	0.0012	0.080	1.62
DA95021328	51	210.0	1.17718	343.59	0.156E+08		0.0008	0.0004	0.071	0.84
DA95020907	50	210.0	1.15631	343.73	0.155E+08		0.0006	0.0011	0.094	0.30
DA95021317	50	210.0	1.17843	343.41	0.161E+08		0.0007	0.0003	0.074	14.84
DA95020927	51	210.0	1.15687	343.78	0.174E+08		0.0009	0.0006	0.107	0.68
DA95020906	45	180.0	1.16084	343.66	0.180E+08		0.0007	0.0005	0.086	0.57
DA95020916	42	187.5	1.15931	343.83	0.180E+08		0.0008	0.0004	0.073	0.55
DA95030603	52	210.0	1.18152	343.83	0.198E+08		0.0007	0.0007	0.076	0.55
DA95022205	53	210.0	1.17484	343.85	0.197E+08		0.0007	0.0019	0.094	6.19
DA95022215	50	210.0	1.17395	343.91	0.220E+08		0.0007	0.0003	0.070	0.95
DA95022726	52	210.0	1.20303	343.52	0.227E+08		0.0007	0.0013	0.085	20.14
DA95022702	51	210.0	1.19975	343.64	0.250E+08		0.0007	0.0019	0.076	4.88
DA95030121	52	210.0	1.18519	343.60	0.251E+08		0.0008	0.0009	0.202	16.36
DA95022712	50	210.0	1.19728	343.52	0.256E+08		0.0006	0.0004	0.082	2.70
DA95031523	52	210.0	1.18066	343.83	0.276E+08		0.0006	0.0005	0.101	0.00
DA95030101	36	150.0	1.18209	343.88	0.296E+08		0.0008	0.0006	0.132	0.00
DA95030111	51	210.0	1.18122	343.80	0.299E+08		0.0009	0.0007	0.111	8.16

TABLE VI

Linear theory parameters

Shot Number	Mach Number	DBSQ (deg**2)	Nutation Vector [K10] (deg)	Precession Vector [K20] (deg)	Nutation Damping [L1] (1/m)	Precession Damping [L2] (1/m)	Nutation Frequency [W10] (deg/m)	Precession Frequency [W20] (deg/m)	Nutation Change [WD1] (deg/m2)	Precession Change [WD2] (deg/m2)
DA95022010	1.056	0.4	0.79	0.64	-0.00544	-0.00572	14.541	-14.473	0.00000	0.00000
DA95022219	1.057	2.1	1.86	1.09	-0.00504	-0.00646	15.116	-14.372	0.00000	0.00000
DA95022230	1.116	0.1	0.38	0.38	-0.00570	-0.00494	15.845	-14.398	0.00000	0.00000
DA95030613	1.254	2.4	0.98	0.91	-0.01631	0.00413	14.970	-14.198	0.00000	0.00000
DA95022009	1.332	0.7	1.10	0.91	-0.00556	-0.00806	14.410	-14.307	0.00000	0.00000
DA95030622	1.380	17.9	0.16	0.89	-0.00734	0.01110	13.712	-12.797	0.00000	0.00000
DA95021318	1.799	0.5	0.80	0.72	-0.00713	-0.00273	11.431	-10.375	0.00000	0.00000
DA95021529	1.846	0.6	0.81	0.66	-0.00855	-0.00039	11.736	-9.716	0.00000	0.00000
DA95021308	1.850	0.9	1.06	0.97	-0.00478	-0.00508	10.638	-10.626	0.00000	0.00000
DA95021328	2.348	0.3	0.75	0.47	-0.00785	-0.00121	9.866	-7.922	0.00000	0.00000
DA95020907	2.364	0.4	0.78	0.62	-0.00465	-0.00465	8.820	-8.853	0.00000	0.00000
DA95021317	2.413	2.0	1.21	1.50	-0.00542	-0.00246	9.195	-8.224	0.00000	0.00000
DA95020927	2.663	3.4	1.57	1.77	-0.00708	-0.00096	8.991	-7.137	0.00000	0.00000
DA95020906	2.741	1.9	1.29	1.30	-0.00294	-0.00394	7.798	-7.861	0.00000	0.00000
DA95020916	2.749	0.1	0.26	0.07	-0.00200	-0.00200	8.392	-7.118	0.00000	0.00000
DA95030603	2.969	0.1	0.35	0.28	-0.00437	-0.00385	7.482	-7.414	0.00000	0.00000
DA95022205	2.970	1.6	1.21	1.23	-0.00362	-0.00330	7.495	-7.511	0.00000	0.00000
DA95022215	3.312	2.8	1.41	1.71	-0.00494	-0.00205	7.314	-6.451	0.00000	0.00000
DA95022726	3.337	0.4	0.44	0.66	-0.00428	-0.00175	7.755	-6.068	0.00000	0.00000
DA95022702	3.681	8.0	2.50	2.77	-0.00261	-0.00324	6.559	-6.556	0.00000	0.00000
DA95030121	3.741	17.0	4.06	3.56	-0.00560	-0.00082	7.473	-5.736	0.00000	0.00000
DA95022712	3.774	4.7	1.98	1.98	-0.00472	-0.00142	6.782	-5.881	0.00000	0.00000
DA95031523	4.127	2.6	1.40	1.33	-0.00533	0.00004	6.787	-5.073	0.00000	0.00000
DA95030101	4.422	45.3	5.42	6.28	-0.00420	-0.00225	6.105	-6.060	0.00000	0.00000
DA95030111	4.471	16.3	3.53	3.81	-0.00349	-0.00203	6.213	-5.392	0.00000	0.00000

TABLE VII

Linear theory aerodynamic coefficients

Shot Number	Mach Number	DBSQ	CD	CD0	CDSQ	CNa	Cma	Cmq	Cnpa	Roll Fit Clp	Frequency Fit Clp
DA95022010	1.056	0.4	0.871	0.868	23.141	16.391	-50.786	-319.4	63.737	13.746	0.000
DA95022219	1.057	2.1	0.882	0.866	25.140	18.390	-52.022	-333.3	29.490	-9.058	0.000
DA95022230	1.116	0.1	0.854	0.853	29.087	22.337	-54.772	-289.2	-8.039	3.416	0.000
DA95030613	1.254	2.4	0.775	0.756	25.862	18.522	-51.982	-416.1	-407.288	-24.739	0.000
DA95022009	1.332	0.7	0.705	0.701	18.762	11.422	-49.282	-475.1	356.002	32.327	0.000
DA95030622	1.380	17.9	0.746	0.625	22.321	15.371	-42.073	418.7	-282.505	-35.438	0.000
DA95021318	1.799	0.5	0.596	0.593	17.859	12.039	-28.524	-331.7	-45.396	-25.377	0.000
DA95021529	1.846	0.6	0.599	0.596	16.643	10.823	-27.076	-277.2	-43.383	-16.379	0.000
DA95021308	1.850	0.9	0.571	0.565	22.083	16.263	-27.085	-330.3	269.034	21.394	0.000
DA95021328	2.348	0.3	0.500	0.498	15.208	10.181	-18.764	-338.2	-29.411	-9.269	0.000
DA95020907	2.364	0.4	0.479	0.478	12.456	7.532	-18.945	-360.2	3.039	4.491	0.000
DA95021317	2.413	2.0	0.480	0.471	14.794	9.870	-18.096	-278.8	-25.793	2.773	0.000
DA95020927	2.663	3.4	0.455	0.441	13.344	8.804	-15.710	-307.3	-26.194	-7.198	0.000
DA95020906	2.741	1.9	0.406	0.398	13.231	8.691	-14.888	-242.1	-126.322	-2.481	0.000
DA95020916	2.749	0.1	0.451	0.451	6.497	1.957	-14.543	-89.7	-0.333	2.405	0.000
DA95030603	2.969	0.1	0.385	0.385	15.758	11.638	-13.310	-319.3	-56.540	11.999	0.000
DA95022205	2.970	1.6	0.381	0.376	11.063	6.942	-13.489	-250.8	150.009	32.950	0.000
DA95022215	3.312	2.8	0.358	0.348	12.228	8.300	-11.331	-263.6	-22.203	-10.020	0.000
DA95022726	3.337	0.4	0.376	0.375	12.628	8.700	-11.036	-205.7	-9.448	3.513	0.000
DA95022702	3.681	8.0	0.333	0.304	11.842	8.170	-10.106	-209.0	1139.350	-57.738	0.000
DA95030121	3.741	17.0	0.359	0.297	11.881	8.209	-10.256	-244.4	-17.207	3.656	0.000
DA95022712	3.774	4.7	0.321	0.305	11.302	7.694	-9.419	-228.2	-22.274	-15.795	0.000
DA95031523	4.127	2.6	0.291	0.283	10.897	7.482	-8.243	-195.3	-18.088	0.000	0.000
DA95030101	4.422	45.3	0.408	0.243	11.941	8.721	-8.845	-261.0	-267.211	0.000	0.000
DA95030111	4.471	16.3	0.303	0.249	10.856	7.701	-8.034	-214.1	-9.275	4.057	0.000

TABLE VIII

Six-degree-of freedom aerodynamic coefficients - Single fit

Shot Number	Mach Number	DBSQ ABARM	CX CX2	CNa CNa3	CYpa Cnpa	Cma Cma3	Cmq Cmq2	CZga3 Cmga3	CYga3 Cnga3	Clga2 Cnsm	Clp Cld	CNda CNdB	Cmda CmdB	X(m) Y-Z(m)	Angle(deg) Roll(deg)
DA95022010	1.056	0.4	0.868	18.73	0.00	-50.489	-332.0	0.0	0.0	0.00	-18.200	0.000	0.021	0.0005	0.072
			(0.%)	(7.%)	(*)	(0.%)	(11.%)	(*)	(*)	(*)	(*)	(*)	(4.%)		
		1.3	6.500	0.00	0.00	0.00	0.0	0.0	0.0	0.00	-0.001	0.000	0.011	0.0003	0.431
			(*)	(*)	(*)	(*)	(*)	(*)	(*)	(*)	(2.%)	(*)	(4.%)		
DA95022219	1.058	2.0	0.868	18.02	0.00	-51.605	-349.6	0.0	0.0	0.00	-18.240	0.000	0.000	0.0005	0.080
			(0.%)	(3.%)	(*)	(0.%)	(7.%)	(*)	(*)	(*)	(0.%)	(*)	(*)		
		2.7	6.500	0.00	0.92	0.00	0.0	0.0	0.0	0.00	0.288	0.000	0.000	0.0003	0.692
			(*)	(*)	(-)	(*)	(*)	(*)	(*)	(*)	(0.%)	(*)	(*)		
DA95022230	1.116	0.1	0.854	18.50	0.00	-54.595	-320.0	0.0	0.0	0.00	-18.145	0.000	0.000	0.0007	0.058
			(0.%)	(*)	(*)	(0.%)	(*)	(*)	(*)	(*)	(0.%)	(*)	(*)		
		0.7	6.500	0.00	-25.00	0.00	0.0	0.0	0.0	0.00	0.562	0.000	0.000	0.0003	2.106
			(*)	(*)	(35.%)	(*)	(*)	(*)	(*)	(*)	(0.%)	(*)	(*)		
DA95030613	1.254	2.3	0.760	18.81	0.00	-52.604	-386.0	0.0	0.0	0.00	-23.564	0.000	0.000	0.0008	0.088
			(0.%)	(5.%)	(*)	(0.%)	(14.%)	(*)	(*)	(*)	(0.%)	(*)	(*)		
		2.2	6.500	0.00	-307.56	0.00	0.0	0.0	0.0	0.00	0.340	0.000	0.000	0.0004	1.881
			(*)	(*)	(5.%)	(*)	(*)	(*)	(*)	(*)	(0.%)	(*)	(*)		
DA95022009	1.332	0.8	0.701	16.29	0.00	-49.917	-505.5	0.0	0.0	0.00	-24.000	0.000	0.003	0.0007	0.082
			(0.%)	(7.%)	(*)	(0.%)	(6.%)	(*)	(*)	(*)	(*)	(*)	(15.%)		
		2.0	6.500	0.00	-320.00	0.00	0.0	0.0	0.0	0.00	-0.011	0.000	-0.023	0.0003	1.005
			(*)	(*)	(*)	(*)	(*)	(*)	(*)	(*)	(0.%)	(*)	(4.%)		
DA95030622	1.377	15.8	0.708	16.37	0.00	-45.883	-500.0	0.0	0.0	0.00	-28.986	0.000	0.000	0.0013	0.087
			(0.%)	(3.%)	(*)	(0.%)	(*)	(*)	(*)	(*)	(1.%)	(*)	(*)		
		8.9	6.500	0.00	-223.25	0.00	0.0	0.0	0.0	0.00	0.925	0.000	0.000	0.0004	3.541
			(*)	(*)	(0.%)	(*)	(*)	(*)	(*)	(*)	(0.%)	(*)	(*)		
DA95021318	1.799	0.6	0.594	11.29	0.00	-28.977	-385.8	0.0	0.0	0.00	-22.935	0.000	0.000	0.0008	0.056
			(0.%)	(7.%)	(*)	(0.%)	(6.%)	(*)	(*)	(*)	(0.%)	(*)	(*)		
		1.6	4.300	0.00	-41.14	0.00	0.0	0.0	0.0	0.00	0.401	0.000	0.000	0.0003	0.827
			(*)	(*)	(11.%)	(*)	(*)	(*)	(*)	(*)	(0.%)	(*)	(*)		

Shot Number	Mach Number	DBSQ / ABARM	CX / CX2	CNa / CNa3	CYpa / Cnpa	Cma / Cma3	Cmq / Cmq2	CZga3 / Cmga3	CYga3 / Cnga3	Clga2 / Cnsm	Clp / Cld	CNda / CNdB	Cmda / CmdB	|	Probable Error X(m) / Y-Z(m)	Angle(deg) / Roll(deg)
DA95021529	1.846	0.6	0.598	11.80	0.00	-27.450	-370.0	0.0	0.0	0.00	-22.188	0.000	0.000	|	0.0011	0.105
			(0.%)	(*)	(*)	(0.%)	(*)	(*)	(*)	(*)	(0.%)	(*)	(*)	|		
		1.5	4.300	0.00	-34.53	0.00	0.0	0.0	0.0	0.00	0.760	0.000	0.000	|	0.0003	0.912
			(*)	(*)	(10.%)	(*)	(*)	(*)	(*)	(*)	(0.%)	(*)	(*)	|		
DA95021308	1.850	1.0	0.567	11.80	0.00	-27.511	-416.3	0.0	0.0	0.00	-22.400	0.000	0.004	|	0.0007	0.072
			(0.%)	(*)	(*)	(0.%)	(5.%)	(*)	(*)	(*)	(*)	(*)	(4.%)	|		
		2.0	4.300	0.00	-36.00	0.00	0.0	0.0	0.0	0.00	-0.001	0.000	-0.012	|	0.0004	1.468
			(*)	(*)	(*)	(*)	(*)	(*)	(*)	(*)	(8.%)	(*)	(1.%)	|		
DA95021328	2.348	0.4	0.500	10.37	0.00	-19.738	-294.8	0.0	0.0	0.00	-18.315	0.000	0.000	|	0.0010	0.072
			(0.%)	(10.%)	(*)	(0.%)	(11.%)	(*)	(*)	(*)	(0.%)	(*)	(*)	|		
		1.1	3.300	0.00	-21.90	0.00	0.0	0.0	0.0	0.00	0.622	0.000	0.000	|	0.0004	2.667
			(*)	(*)	(13.%)	(*)	(*)	(*)	(*)	(*)	(0.%)	(*)	(*)	|		
DA95020907	2.364	0.5	0.478	10.17	0.00	-19.021	-330.0	0.0	0.0	0.00	-18.300	0.000	-0.007	|	0.0007	0.067
			(0.%)	(6.%)	(*)	(0.%)	(*)	(*)	(*)	(*)	(*)	(*)	(3.%)	|		
		1.4	3.300	0.00	-24.00	0.00	0.0	0.0	0.0	0.00	0.000	0.000	0.018	|	0.0002	0.301
			(*)	(*)	(*)	(*)	(*)	(*)	(*)	(*)	(2.%)	(*)	(2.%)	|		
DA95021317	2.414	2.1	0.473	9.92	0.00	-18.120	-298.6	0.0	0.0	0.00	-18.273	0.000	0.000	|	0.0007	0.071
			(0.%)	(3.%)	(*)	(0.%)	(5.%)	(*)	(*)	(*)	(1.%)	(*)	(*)	|		
		2.6	3.300	0.00	-23.94	0.00	0.0	0.0	0.0	0.00	0.311	0.000	0.000	|	0.0003	5.420
			(*)	(*)	(10.%)	(*)	(*)	(*)	(*)	(*)	(1.%)	(*)	(*)	|		
DA95020927	2.663	3.7	0.446	8.95	0.00	-15.964	-397.9	0.0	0.0	0.00	-16.736	0.000	0.000	|	0.0012	0.070
			(0.%)	(4.%)	(*)	(0.%)	(3.%)	(*)	(*)	(*)	(0.%)	(*)	(*)	|		
		3.4	2.900	0.00	-25.84	0.00	0.0	0.0	0.0	0.00	0.566	0.000	0.000	|	0.0006	1.691
			(*)	(*)	(4.%)	(*)	(*)	(*)	(*)	(*)	(0.%)	(*)	(*)	|		
DA95020906	2.741	2.1	0.400	8.92	0.00	-14.877	-254.3	0.0	0.0	0.00	-16.700	0.000	0.016	|	0.0008	0.073
			(0.%)	(3.%)	(*)	(0.%)	(6.%)	(*)	(*)	(*)	(*)	(*)	(2.%)	|		
		2.5	2.900	0.00	-23.00	0.00	0.0	0.0	0.0	0.00	-0.001	0.000	-0.007	|	0.0003	0.640
			(*)	(*)	(*)	(*)	(*)	(*)	(*)	(*)	(2.%)	(*)	(3.%)	|		

Shot Number	Mach Number	DBSQ ABARM	CX CX2	CNa CNa3	CYpa Cnpa	Cma Cma3	Cmq Cmq2	CZga3 Cmga3	CYga3 Cnga3	Clga2 Cnsm	Clp Cld	CNda CNdB	Cmda CmdB	Probable Error X(m) Y-Z(m)	Angle(deg) Roll(deg)
DA95020916	2.749	0.0	0.452	9.00	0.00	-15.373	-300.0	0.0	0.0	0.00	-15.991	0.000	0.000	0.0009	0.072
			(0.%)	(*)	(*)	(2.%)	(*)	(*)	(*)	(*)	(0.%)	(*)	(*)		
		0.3	2.900	0.00	-23.00	0.00	0.0	0.0	0.0	0.00	0.269	0.000	0.000	0.0004	1.902
			(*)	(*)	(*)	(*)	(*)	(*)	(*)	(*)	(0.%)	(*)	(*)		
DA95030603	2.969	0.1	0.385	8.00	0.00	-13.900	-250.0	0.0	0.0	0.00	-13.300	0.000	-0.003	0.0006	0.073
			(0.%)	(*)	(*)	(1.%)	(*)	(*)	(*)	(*)	(*)	(*)	(4.%)		
		0.6	2.500	0.00	-20.00	0.00	0.0	0.0	0.0	0.00	-0.002	0.000	0.004	0.0004	0.454
			(*)	(*)	(*)	(*)	(*)	(*)	(*)	(*)	(1.%)	(*)	(3.%)		
DA95022205	2.970	1.7	0.376	8.72	0.00	-13.535	-275.4	0.0	0.0	0.00	-13.300	0.000	0.013	0.0007	0.063
			(0.%)	(3.%)	(*)	(0.%)	(5.%)	(*)	(*)	(*)	(*)	(*)	(1.%)		
		2.3	2.500	0.00	-20.00	0.00	0.0	0.0	0.0	0.00	0.002	0.000	-0.016	0.0002	1.522
			(*)	(*)	(*)	(*)	(*)	(*)	(*)	(*)	(2.%)	(*)	(1.%)		
DA95022215	3.312	3.0	0.350	8.41	0.00	-11.485	-231.9	0.0	0.0	0.00	-13.886	0.000	0.000	0.0007	0.056
			(0.%)	(2.%)	(*)	(0.%)	(4.%)	(*)	(*)	(*)	(0.%)	(*)	(*)		
		2.9	2.500	0.00	-16.61	0.00	0.0	0.0	0.0	0.00	0.234	0.000	0.000	0.0003	1.309
			(*)	(*)	(7.%)	(*)	(*)	(*)	(*)	(*)	(0.%)	(*)	(*)		
DA95022726	3.338	0.4	0.376	8.19	0.00	-11.233	-250.0	0.0	0.0	0.00	-13.398	0.000	0.000	0.0009	0.057
			(0.%)	(6.%)	(*)	(0.%)	(*)	(*)	(*)	(*)	(0.%)	(*)	(*)		
		1.0	2.500	0.00	-20.00	0.00	0.0	0.0	0.0	0.00	0.462	0.000	0.000	0.0003	1.910
			(*)	(*)	(*)	(*)	(*)	(*)	(*)	(*)	(0.%)	(*)	(*)		
DA95022702	3.682	8.5	0.310	8.13	0.00	-10.169	-210.7	0.0	0.0	0.00	-13.000	-0.007	0.018	0.0006	0.073
			(0.%)	(1.%)	(*)	(0.%)	(3.%)	(*)	(*)	(*)	(*)	(19.%)	(10.%)		
		4.9	2.000	0.00	-14.00	0.00	0.0	0.0	0.0	0.00	-0.001	0.002	0.003	0.0004	1.895
			(*)	(*)	(*)	(*)	(*)	(*)	(*)	(*)	(6.%)	(83.%)	(61.%)		
DA95030121	3.745	17.6	0.309	8.45	0.00	-9.457	-277.1	0.0	0.0	0.00	-13.415	0.000	0.000	0.0007	0.079
			(0.%)	(1.%)	(*)	(0.%)	(2.%)	(*)	(*)	(*)	(0.%)	(*)	(*)		
		7.3	2.000	0.00	-14.31	-95.15	0.0	0.0	0.0	0.00	0.449	0.000	0.000	0.0003	2.543
			(*)	(*)	(2.%)	(4.%)	(*)	(*)	(*)	(*)	(0.%)	(*)	(*)		

Shot Number	Mach Number	DBSQ ABARM	CX CX2	CNa CNa3	CYpa Cnpa	Cma Cma3	Cmq Cmq2	CZga3 Cmga3	CYga3 Cnga3	Clga2 Cnsm	Clp Cld	CNda CNdB	Cmda CmdB		Probable Error X(m) Y-Z(m)	Angle(deg) Roll(deg)
DA95022712	3.775	5.0	0.308	7.92	0.00	-9.275	-204.7	0.0	0.0	0.00	-12.546	0.000	0.000		0.0007	0.056
			(0.%)	(1.%)	(*)	(0.%)	(3.%)	(*)	(*)	(*)	(1.%)	(*)	(*)			
		3.7	2.000	0.00	-18.70	-90.00	0.0	0.0	0.0	0.00	0.214	0.000	0.000		0.0003	2.652
			(*)	(*)	(4.%)	(*)	(*)	(*)	(*)	(*)	(0.%)	(*)	(*)			
DA95031523	4.127	2.7	0.285	7.65	0.00	-8.432	-152.4	0.0	0.0	0.00	-12.000	0.000	0.000		0.0009	0.073
			(0.%)	(2.%)	(*)	(0.%)	(7.%)	(*)	(*)	(*)	(*)	(*)	(*)			
		2.5	2.000	0.00	-16.27	0.00	0.0	0.0	0.0	0.00	0.399	0.000	0.000		0.0003	0.000
			(*)	(*)	(4.%)	(*)	(*)	(*)	(*)	(*)	(1.%)	(*)	(*)			
DA95030101	4.425	46.6	0.268	8.97	0.00	-7.950	-155.4	0.0	0.0	0.00	-12.000	0.000	-0.038		0.0006	0.148
			(4.%)	(1.%)	(*)	(0.%)	(6.%)	(*)	(*)	(*)	(*)	(*)	(7.%)			
		11.2	1.766	0.00	-13.00	-50.00	0.0	0.0	0.0	0.00	0.029	0.000	0.012		0.0006	0.000
			(50.%)	(*)	(*)	(*)	(*)	(*)	(*)	(*)	(4.%)	(*)	(65.%)			
DA95030111	4.473	17.7	0.257	7.76	0.00	-7.342	-247.2	0.0	0.0	0.00	-11.718	0.000	0.000		0.0007	0.083
			(0.%)	(1.%)	(*)	(0.%)	(2.%)	(*)	(*)	(*)	(1.%)	(*)	(*)			
		7.0	2.000	0.00	-9.66	-93.13	0.0	0.0	0.0	0.00	0.205	0.000	0.000		0.0004	5.225
			(*)	(*)	(5.%)	(4.%)	(*)	(*)	(*)	(*)	(1.%)	(*)	(*)			

TABLE IX

Six-degree-of freedom aerodynamic coefficients - Multiple fits

Shot Numbers	Mach Number	DBSQ ABARM	CX CX2 CX4	CNa CNa3 CNa5	CYpa Cnpa Cnpa3	Cma Cma3 Cma5	Cmq Cmq2 Cmq4	CZga3 Cmga3 Cmga	CYga3 Cnga3 Cnga5	Clga2 CXga2 Clp	CXM CmaM CnsM	Probable Error X(m) Y-Z(m)	Angle(deg) Roll(deg)
DA95022230 DA95022010	1.077	0.9	0.863	18.47	0.00	-52.648	-322.4	0.0	0.0	0.00	-0.24	0.0006	0.072
			(0.%)	(2.%)	(*)	(0.%)	(5.%)	(*)	(*)	(*)	(3.%)		
DA95022219		2.7	6.500	0.00	0.00	0.000	0.0	0.0	0.0	0.00	-65.20	0.0003	1.307
			(*)	(*)	(*)	(*)	(*)	(*)	(*)	(*)	(6.%)		
			0.000	0.00	0.00	0.000	0.0	0.0	0.0	-18.16	0.00		
			(*)	(*)	(*)	(*)	(*)	(*)	(*)	(0.%)	(*)		
DA95022009 DA95030613	1.293	1.5	0.731	18.27	0.00	-50.968	-487.4	0.0	0.0	0.00	-0.75	0.0009	0.090
			(0.%)	(3.%)	(*)	(0.%)	(6.%)	(*)	(*)	(*)	(1.%)		
		2.1	6.500	0.00	-321.97	0.000	0.0	0.0	0.0	0.00	40.85	0.0004	1.506
			(*)	(*)	(3.%)	(*)	(*)	(*)	(*)	(*)	(4.%)		
			0.000	0.00	0.00	0.000	0.0	0.0	0.0	-23.57	0.00		
			(*)	(*)	(*)	(*)	(*)	(*)	(*)	(0.%)	(*)		
DA95021318 DA95021529	1.832	0.7	0.585	11.78	0.00	-27.976	-377.7	0.0	0.0	0.00	-0.29	0.0009	0.079
			(*)	(4.%)	(*)	(0.%)	(4.%)	(*)	(*)	(*)	(*)		
DA95021308		2.0	4.300	0.00	-35.61	0.000	0.0	0.0	0.0	0.00	29.48	0.0003	1.484
			(*)	(*)	(7.%)	(*)	(*)	(*)	(*)	(*)	(7.%)		
			0.000	0.00	0.00	0.000	0.0	0.0	0.0	-22.35	0.00		
			(*)	(*)	(*)	(*)	(*)	(*)	(*)	(0.%)	(*)		
DA95021328 DA95020907	2.375	1.0	0.484	10.52	0.00	-18.904	-306.5	0.0	0.0	0.00	-0.16	0.0008	0.069
			(*)	(2.%)	(*)	(0.%)	(4.%)	(*)	(*)	(*)	(*)		
DA95021317		2.6	3.300	0.00	-24.33	0.000	0.0	0.0	0.0	0.00	19.24	0.0003	3.464
			.(*)	(*)	(7.%)	(*)	(*)	(*)	(*)	(*)	(5.%)		
			0.000	0.00	0.00	0.000	0.0	0.0	0.0	-18.31	0.00		
			(*)	(*)	(*)	(*)	(*)	(*)	(*)	(0.%)	(*)		
DA95020916 DA95020906	2.718	1.9	0.435	9.01	0.00	-15.199	-335.5	0.0	0.0	0.00	-0.15	0.0010	0.071
			(*)	(2.%)	(*)	(0.%)	(3.%)	(*)	(*)	(*)	(*)		
DA95020927		3.3	2.900	0.00	-22.68	0.000	0.0	0.0	0.0	0.00	13.77	0.0004	1.798
			(*)	(*)	(4.%)	(*)	(*)	(*)	(*)	(*)	(3.%)		
			0.000	0.00	0.00	0.000	0.0	0.0	0.0	-16.65	0.00		
			(*)	(*)	(*)	(*)	(*)	(*)	(*)	(0.%)	(*)		

Shot Numbers		Mach Number	DBSQ ABARM	CX CX2 CX4	CNa CNa3 CNa5	CYpa Cnpa Cnpa3	Cma Cma3 Cma5	Cmq Cmq2 Cmq4	CZga3 Cmga3 Cmga	CYga3 Cnga3 Cnga5	Clga2 CXga2 Clp	CXM CmaM CnsM	Probable Error X(m) Y-Z(m)	Angle(deg) Roll(deg)
DA95030603	DA95022726	3.147	1.3	0.373	8.69	0.00	-12.456	-260.1	0.0	0.0	0.00	-0.04	0.0007	0.063
				(*)	(1.%)	(*)	(0.%)	(3.%)	(*)	(*)	(*)	(*)		
DA95022205	DA95022215		2.9	2.500	0.00	-19.58	0.000	0.0	0.0	0.0	0.00	5.92	0.0003	1.582
				(*)	(*)	(5.%)	(*)	(*)	(*)	(*)	(*)	(1.%)		
				0.000	0.00	0.00	0.000	0.0	0.0	0.0	-13.50	0.00		
				(*)	(*)	(*)	(*)	(*)	(*)	(*)	(0.%)	(*)		
DA95022702	DA95022712	3.734	10.1	0.309	8.32	0.00	-9.533	-239.8	0.0	0.0	0.00	-0.02	0.0007	0.072
				(0.%)	(1.%)	(*)	(0.%)	(1.%)	(*)	(*)	(*)	(33.%)		
DA95030121			7.2	2.129	0.00	-13.92	-90.425	0.0	0.0	0.0	0.00	5.48	0.0004	2.841
				(9.%)	(*)	(2.%)	(2.%)	(*)	(*)	(*)	(*)	(2.%)		
				0.000	0.00	0.00	0.000	0.0	0.0	0.0	-13.18	0.00		
				(*)	(*)	(*)	(*)	(*)	(*)	(*)	(0.%)	(*)		
DA95031523	DA95030111	4.300	10.2	0.271	7.74	0.00	-7.853	-247.0	0.0	0.0	0.00	-0.08	0.0008	0.088
				(0.%)	(1.%)	(*)	(0.%)	(2.%)	(*)	(*)	(*)	(3.%)		
			7.0	2.000	0.00	-13.72	-93.319	0.0	0.0	0.0	0.00	2.94	0.0004	3.658
				(*)	(*)	(3.%)	(4.%)	(*)	(*)	(*)	(*)	(3.%)		
				0.000	0.00	0.00	0.000	0.0	0.0	0.0	-11.71	0.00		
				(*)	(*)	(*)	(*)	(*)	(*)	(*)	(1.%)	(*)		

TABLE X

Roll moment coefficient due to fin cant

Model Number	Fin cant (δ) (rad)	$C_{l_\delta}\delta$	C_{l_δ} (/rad)
DA11	0.03492	0.20480	5.87
DA12	0.03491	0.21440	6.14
DA13	0.03492	0.34032	9.75
DA15	0.03491	0.23350	6.70
DA16	0.03491	0.26900	7.71
DA17	0.03492	0.31094	8.91
DA18	0.03491	0.40053	11.47
DA19	0.03491	0.28781	8.24
DA21	0.06982	0.44952	6.44
DA22	0.06982	0.92464	13.24
DA23	0.06982	0.39934	5.72
DA26	0.06981	0.46234	6.62
DA27	0.06982	0.56609	8.11
DA28	0.06982	0.62231	8.91
DA29	0.06981	0.75968	10.88
DA30	0.06982	0.56184	8.05

DREV aeroballistic range
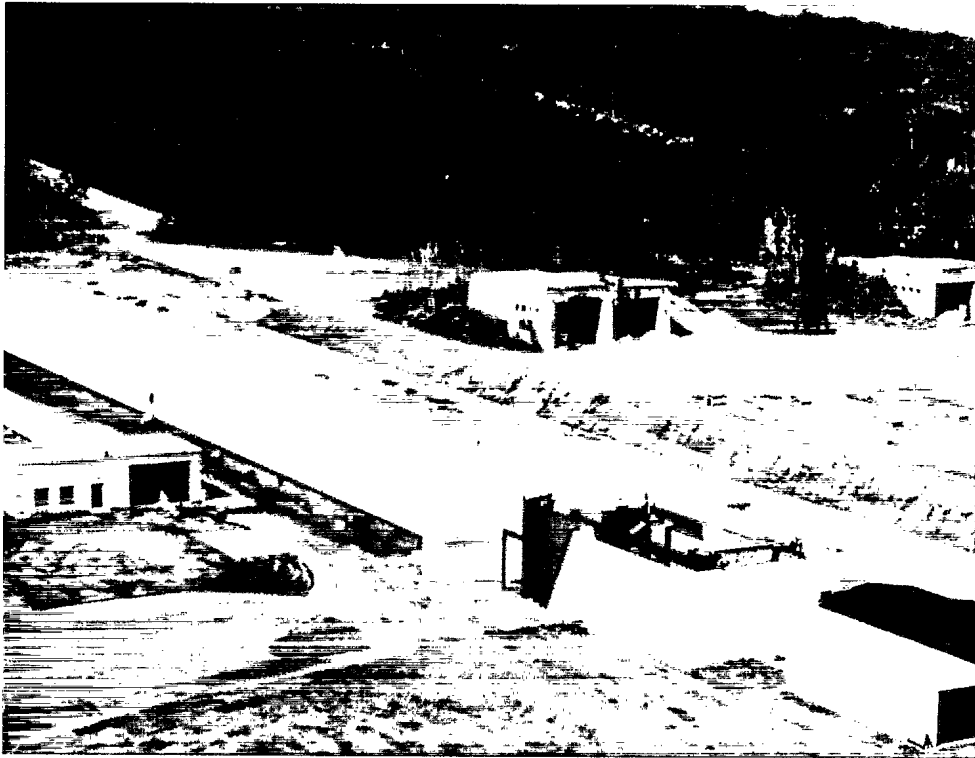
Fig. 1a) Photograph of aeroballistic range complex
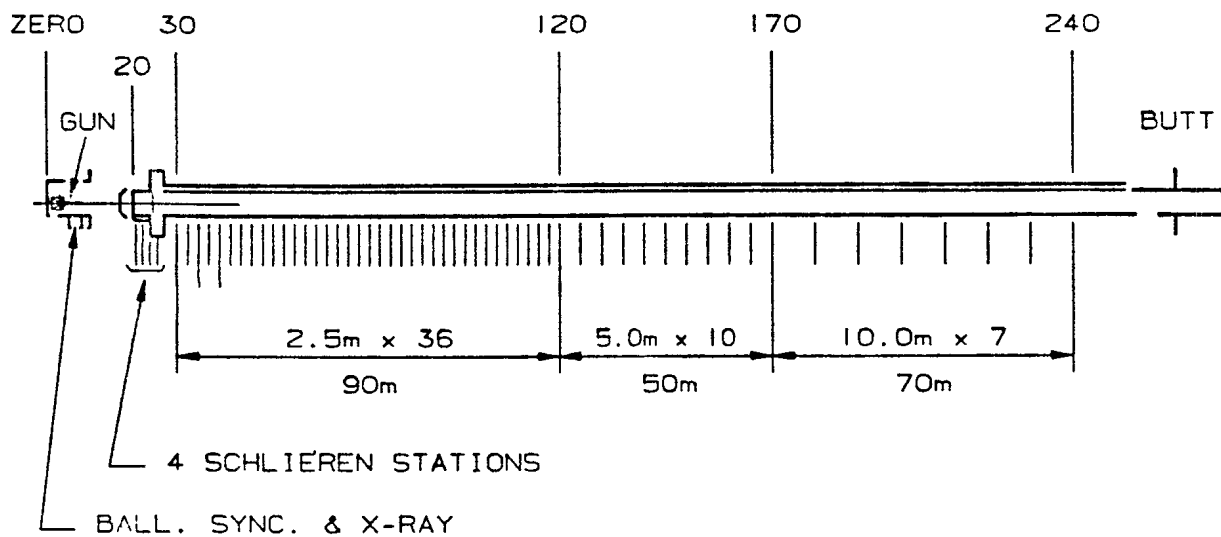
Fig. 1b) Photographic station spacing
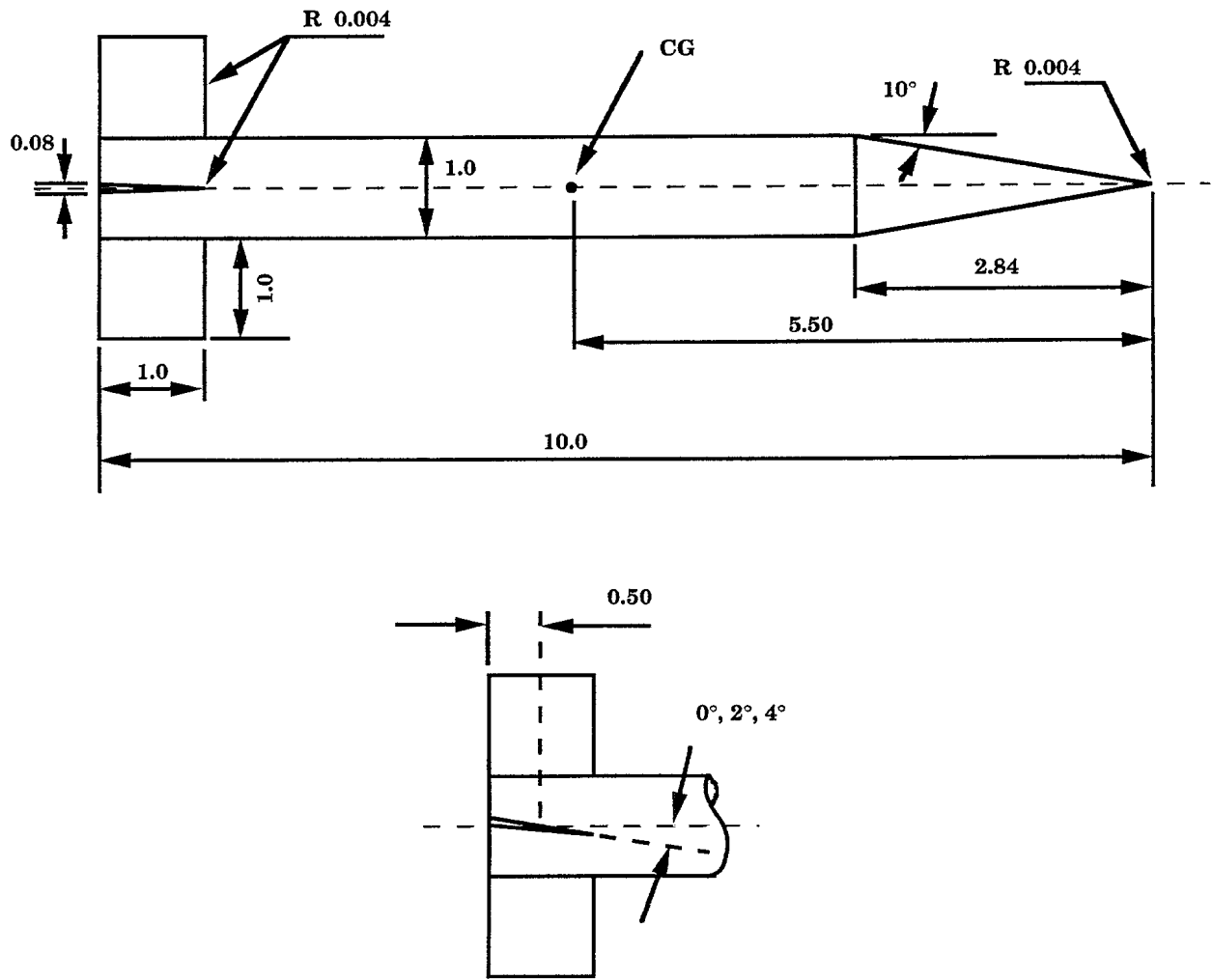
FIGURE 2 - MODEL configuration (Dimensions in calibres 1 cal = 30.0 mm)

Photographs of model and sabot package
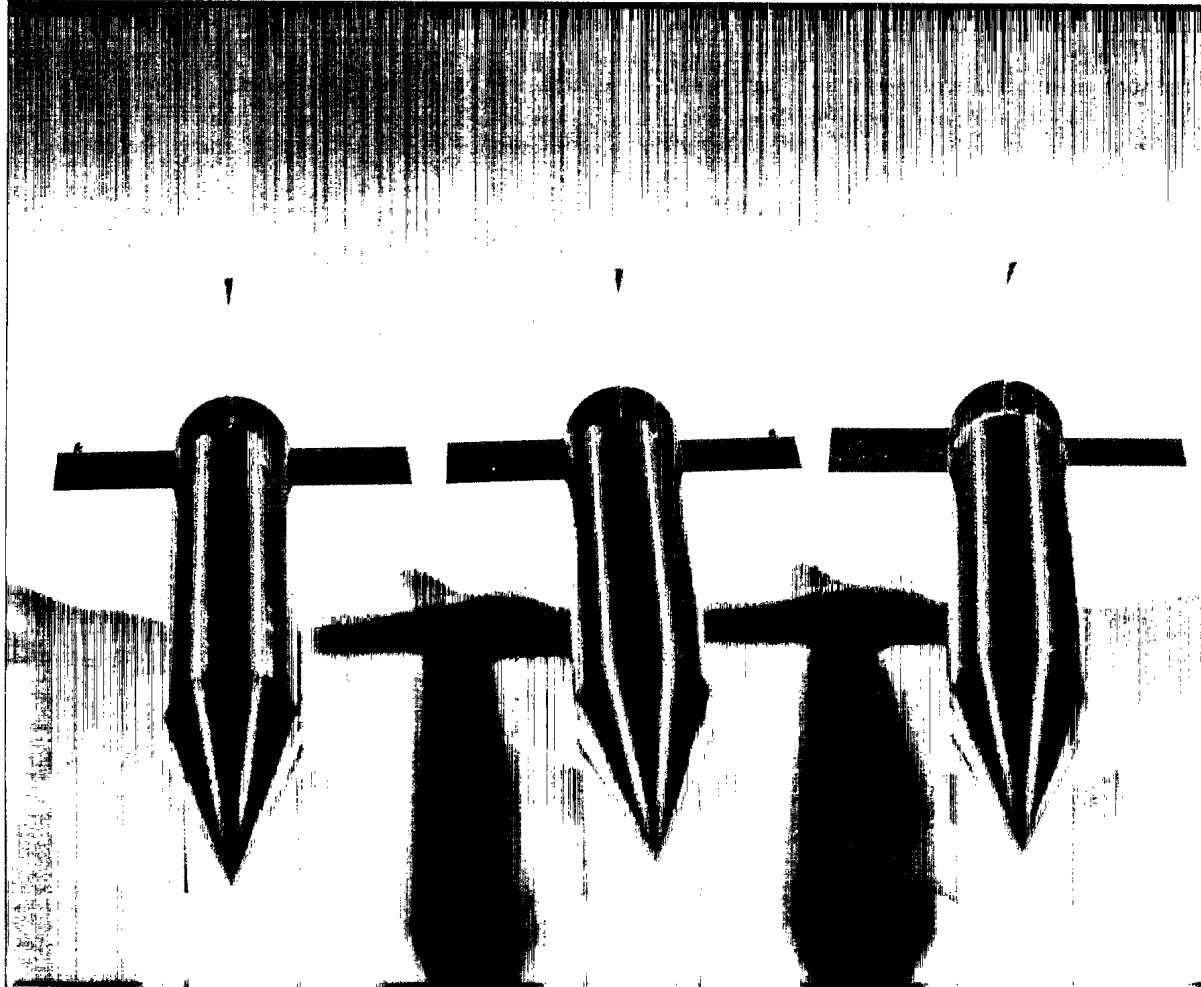
FIGURE 3 - a) Tested projectiles showing fin cants
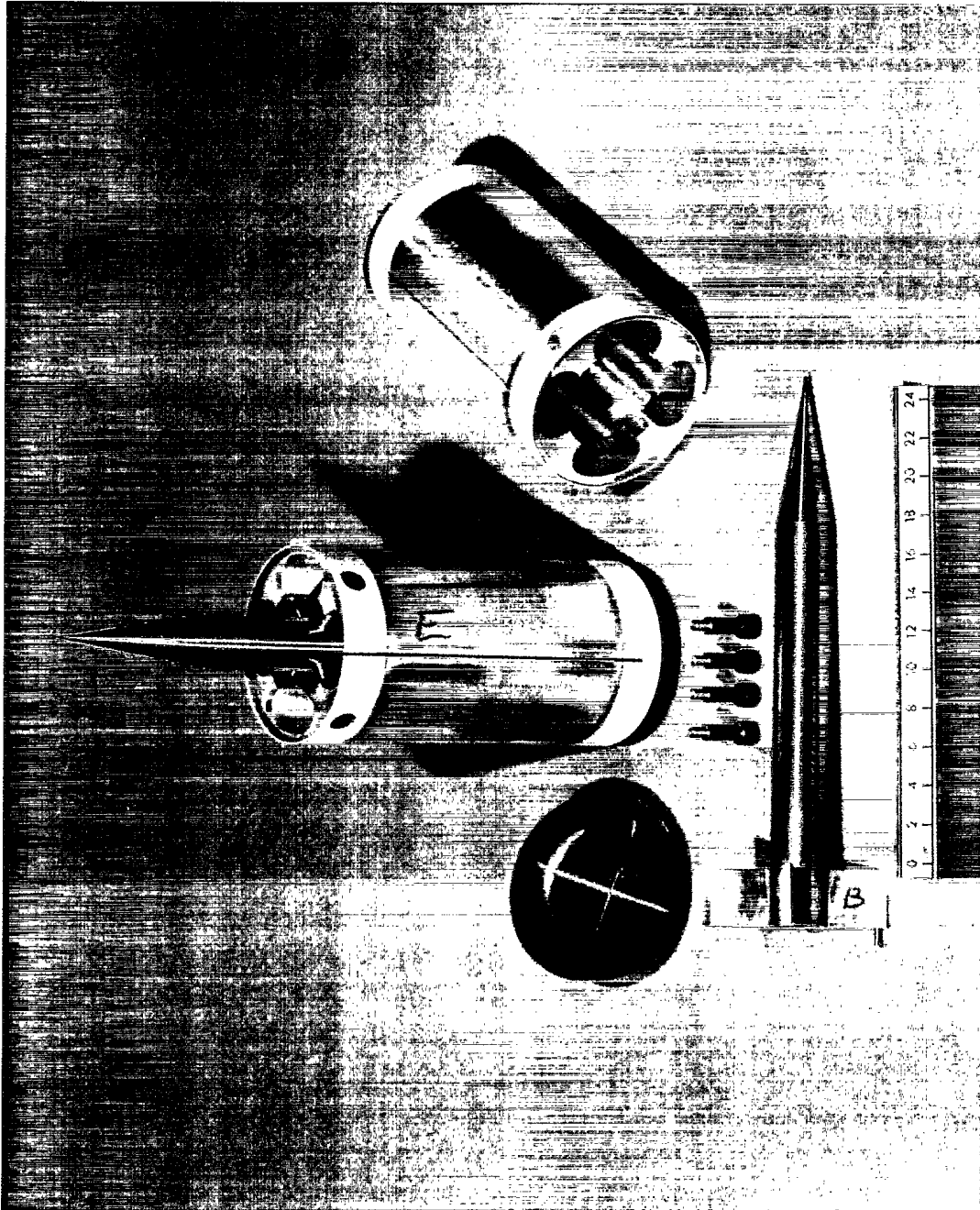
b) Model - sabot package

Typical model - sabot separation

FIGURE 4 - a) Model A30, V_{muz} = 380 m/s
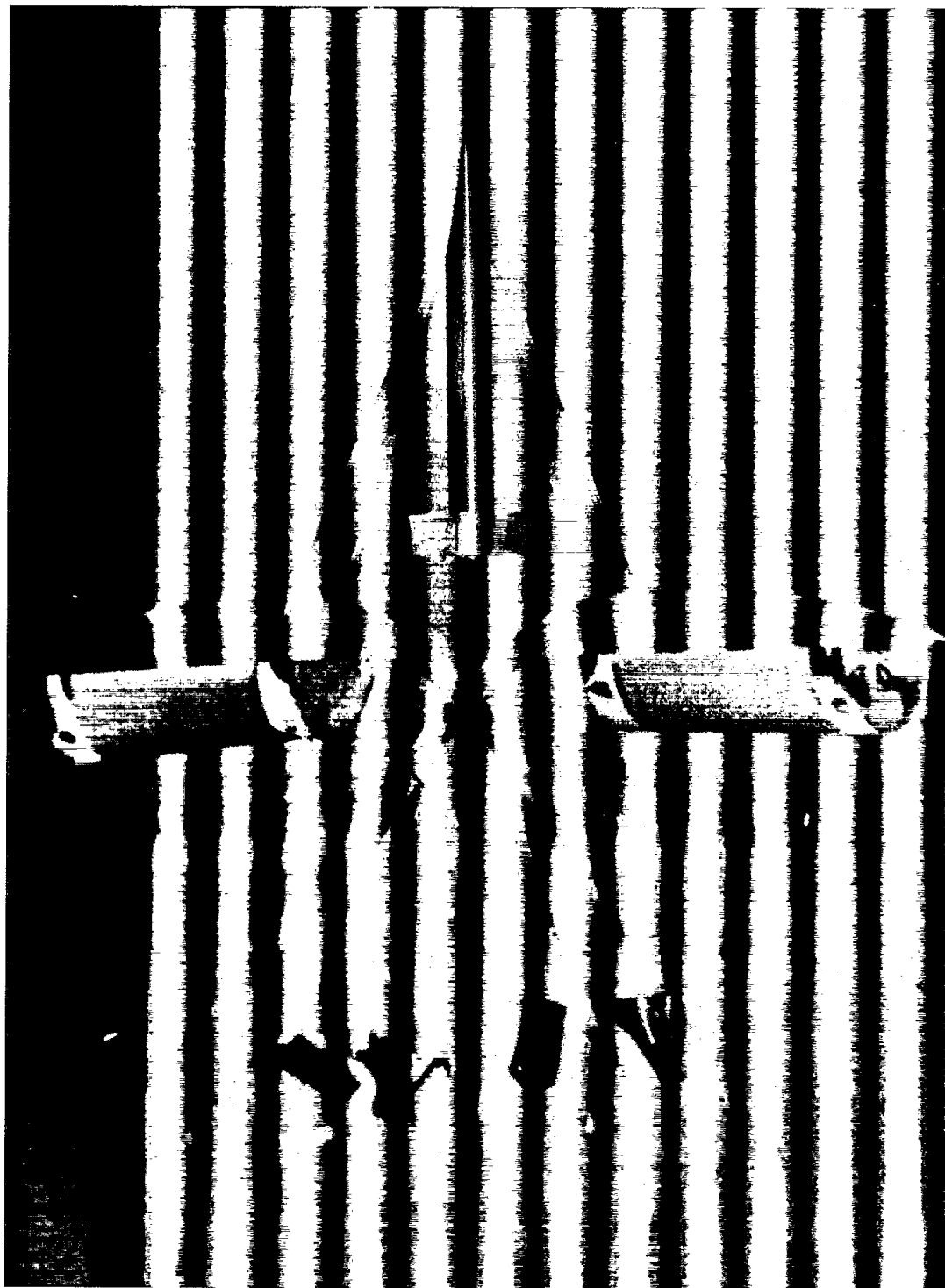
b) Model A23, V_{muz} = 1159 m/s
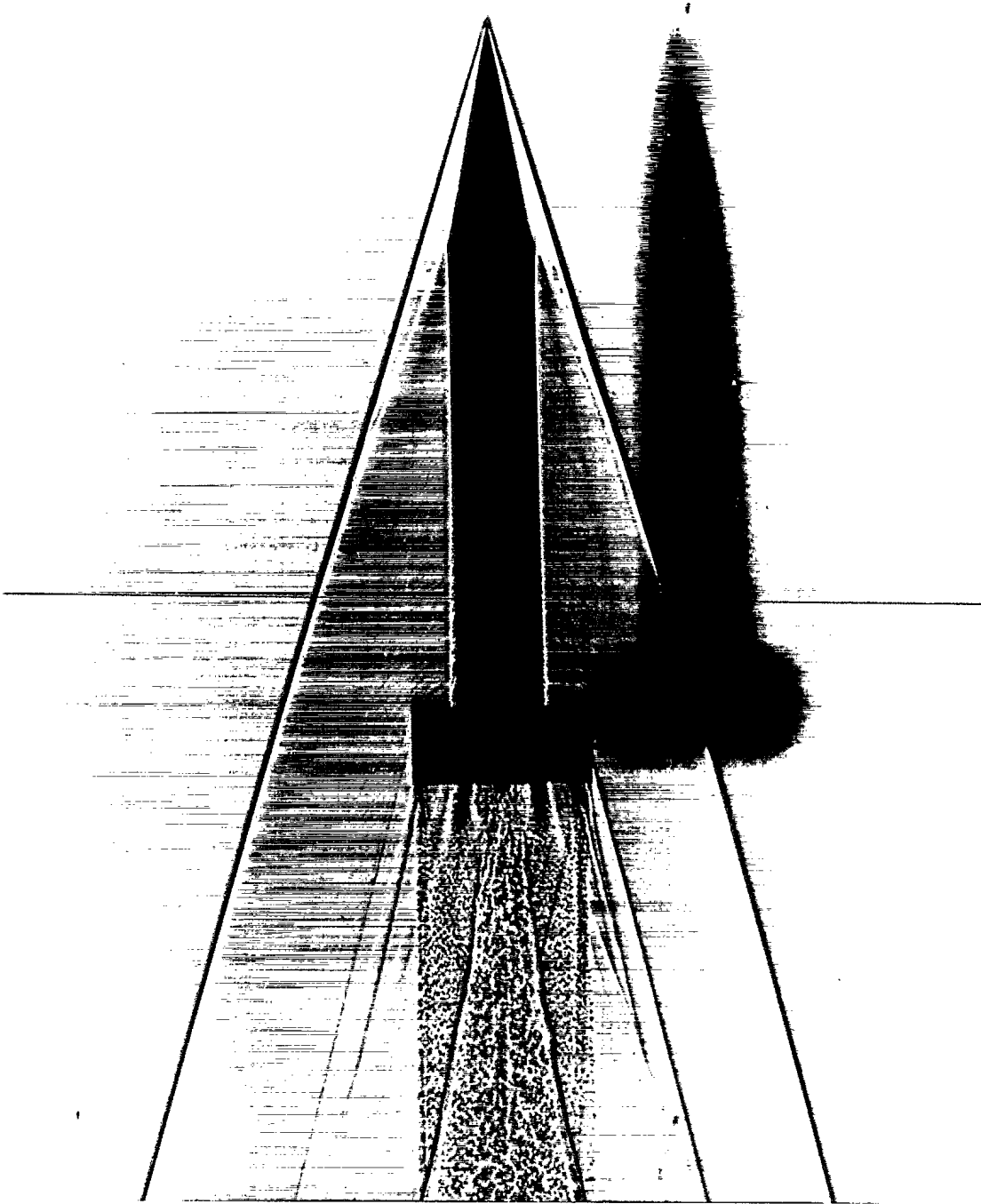
FIGURE 5 - Shadowgraph photograph of Shot A11, Mach = 4.5
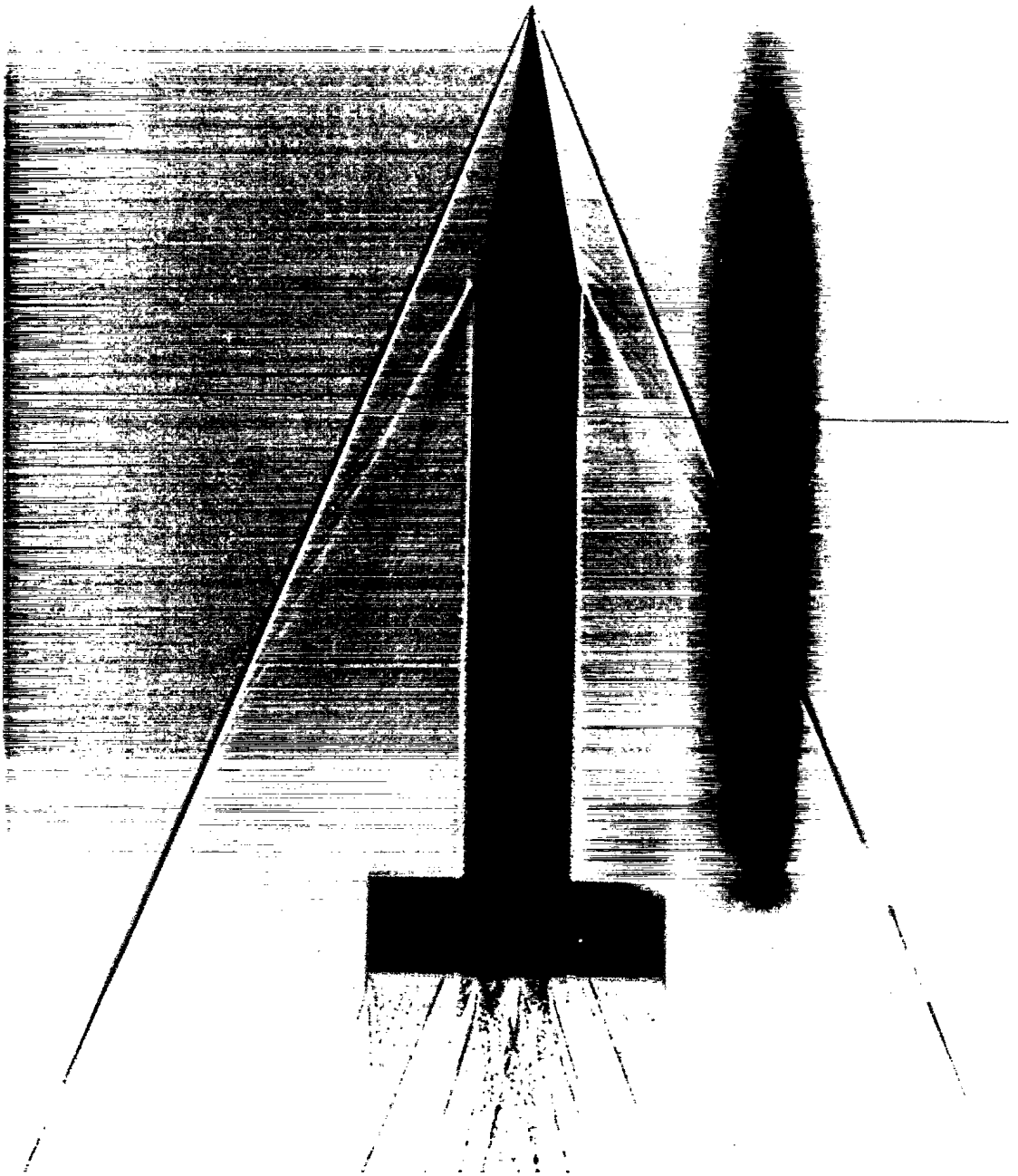
FIGURE 6 - Shadowgraph photograph of Shot A05, Mach = 3.0

Shadowgraph photographs of Shot A10
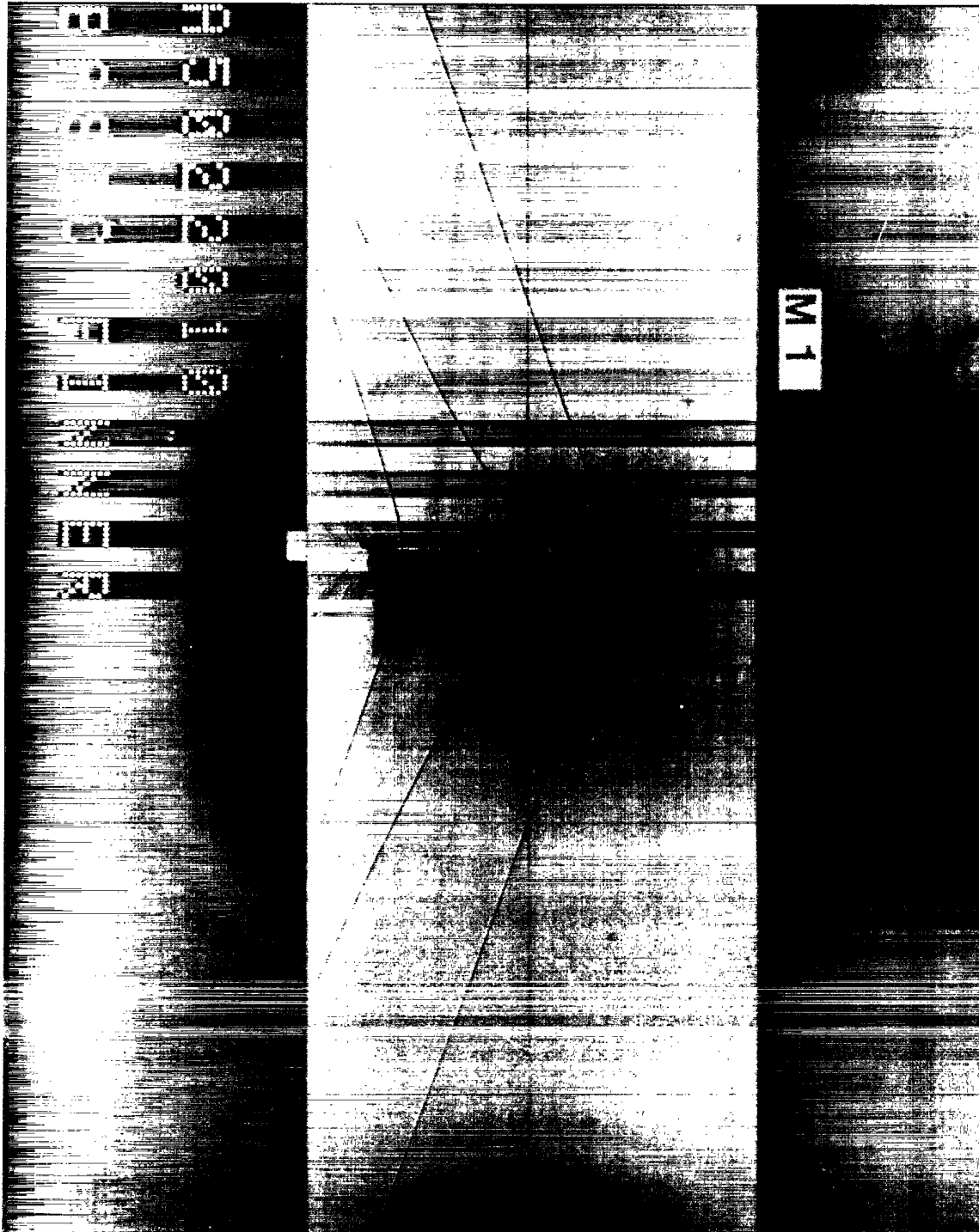
FIGURE 7 - a) V = 370.7 m/s, Mach = 1.078
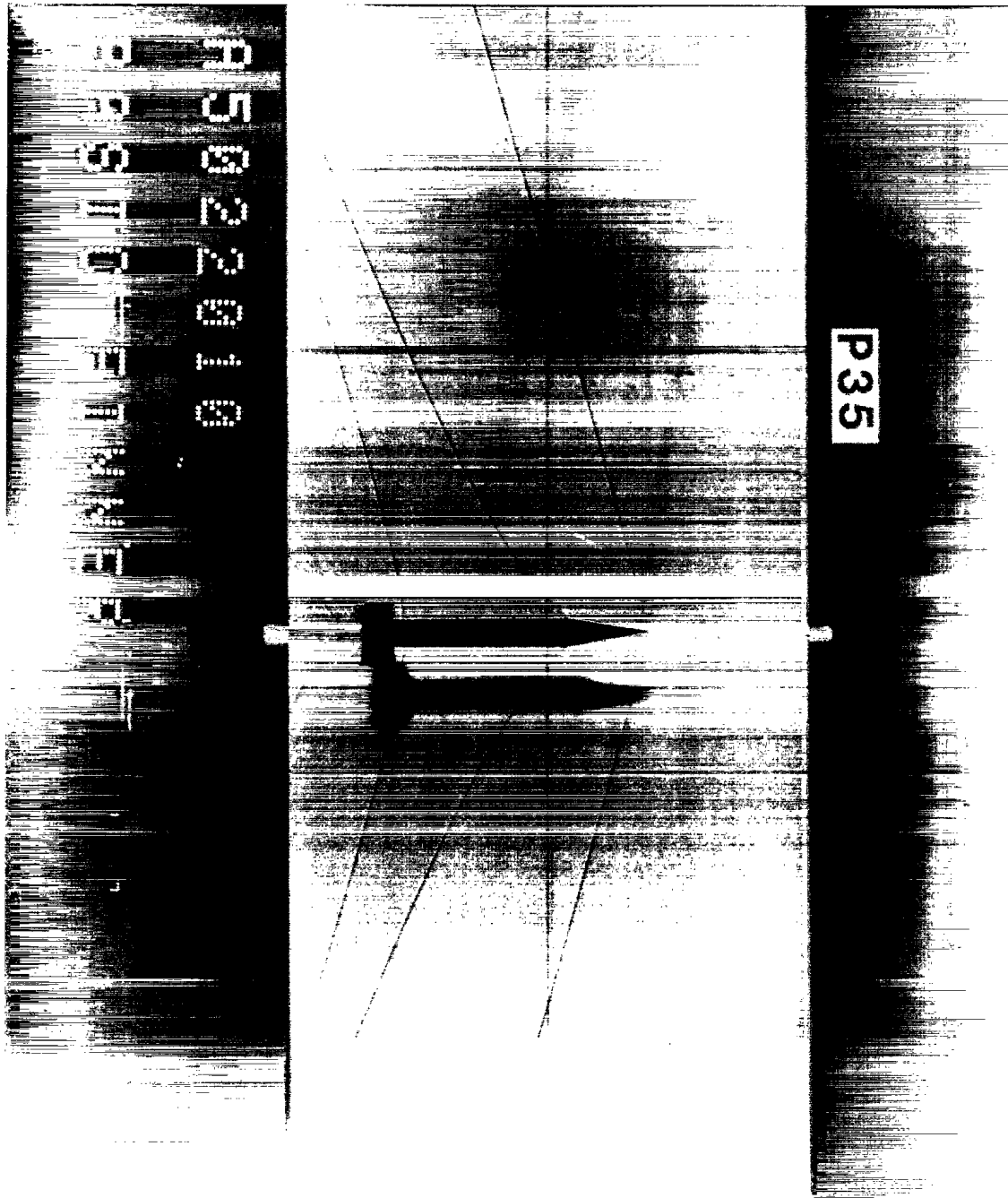
FIGURE 7 - b) V = 363.7 m/s, Mach = 1.057
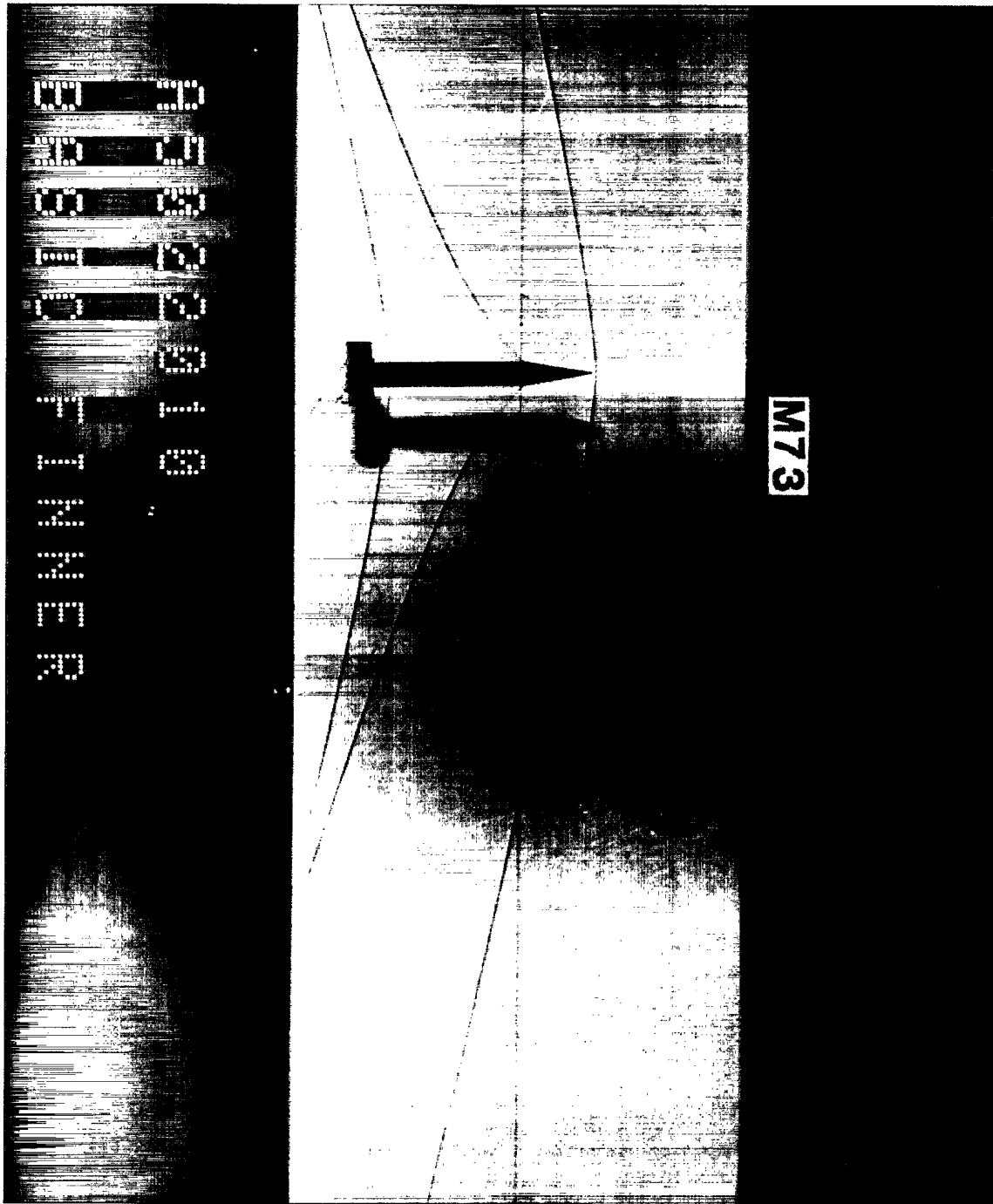
FIGURE 7 - c) V = 355.9 m/s, Mach = 1.035
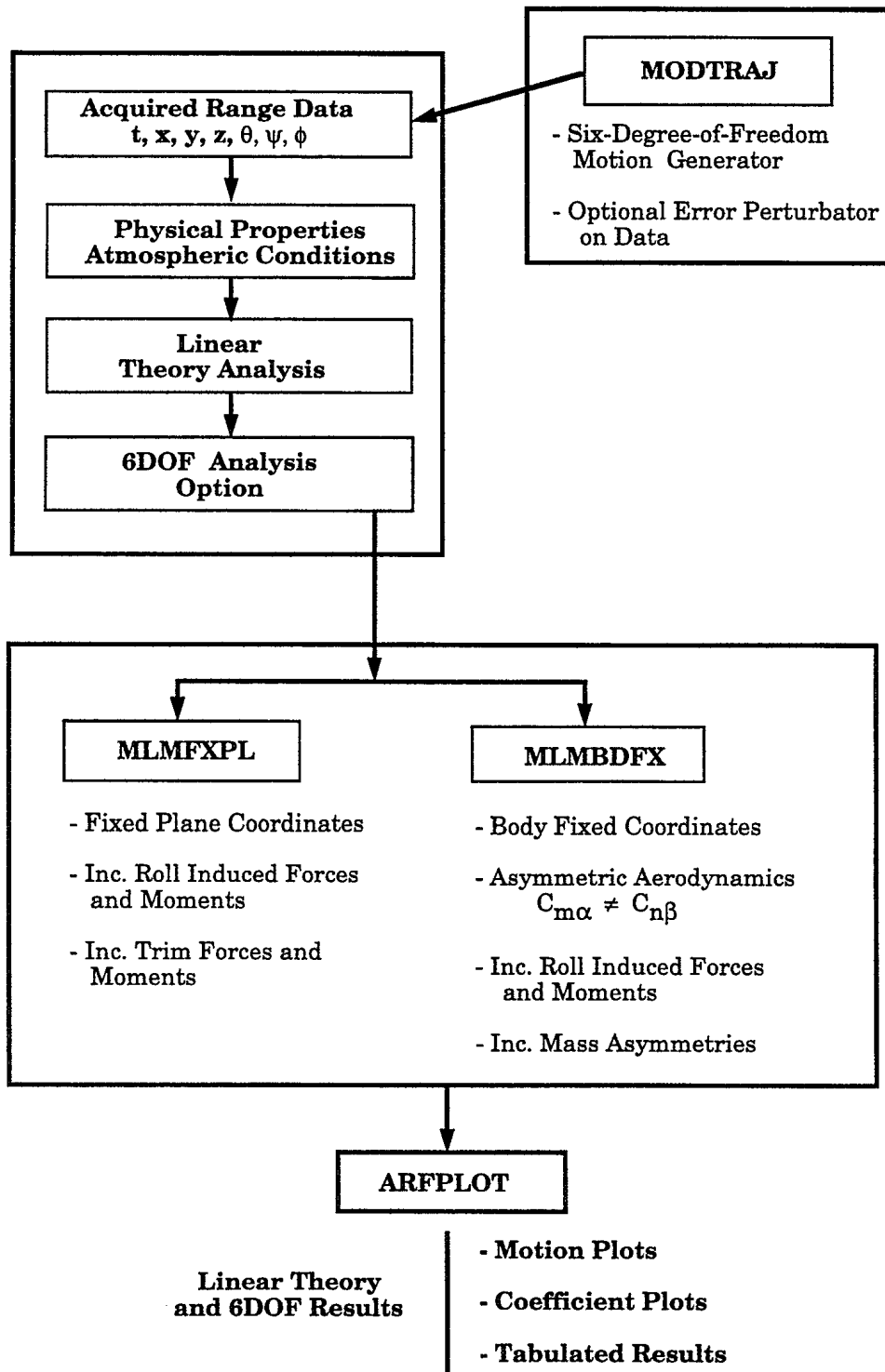
FIGURE 8 - DREV Aeroballistic Range Data Analysis System (BARDAS)
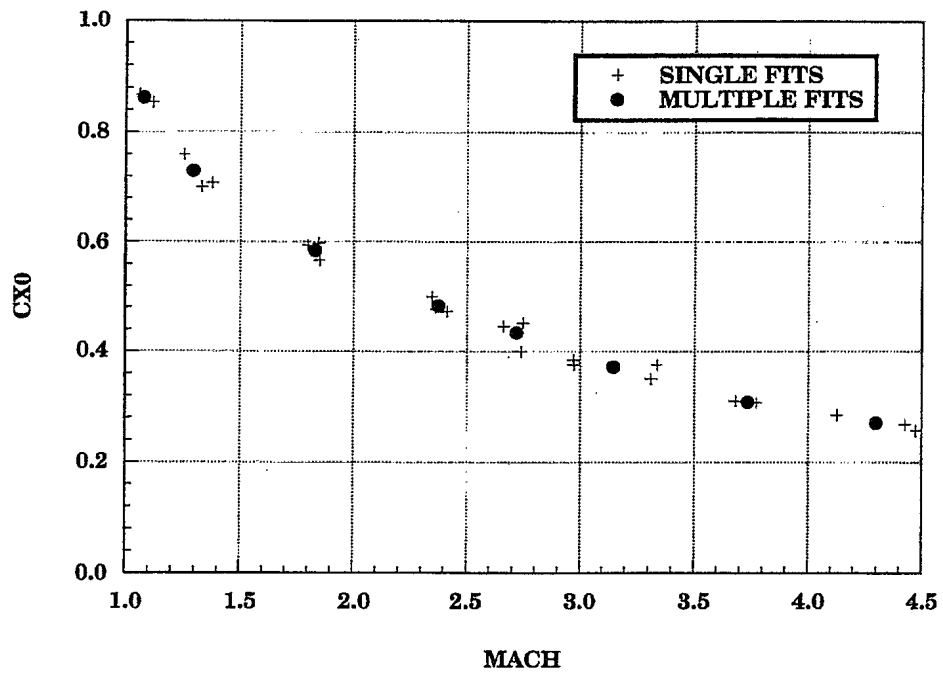
FIGURE 9 - Axial force coefficient versus Mach Number
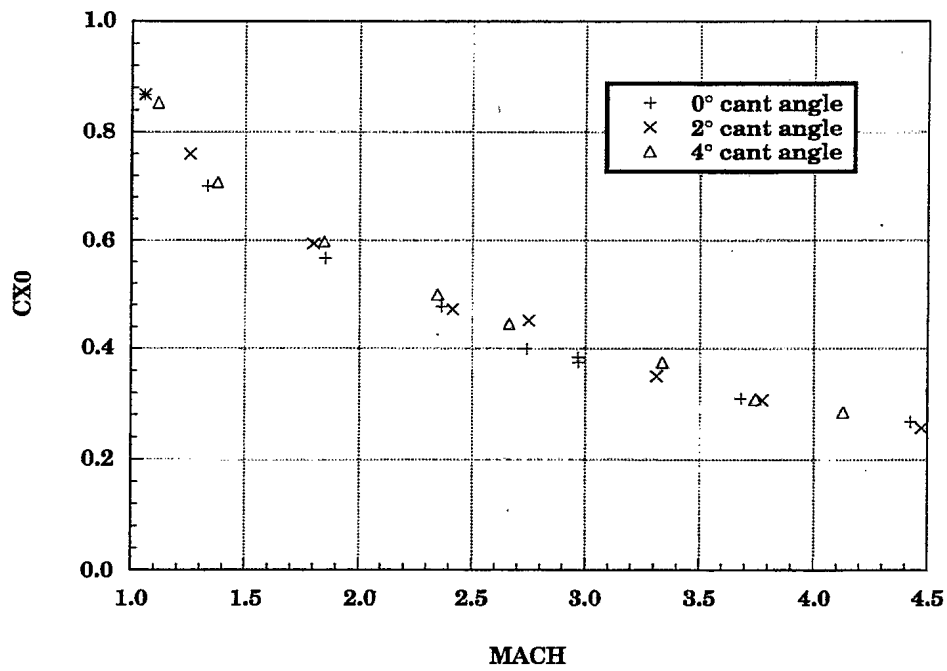
FIGURE 10 - Effect of spin rate on axial force coefficient
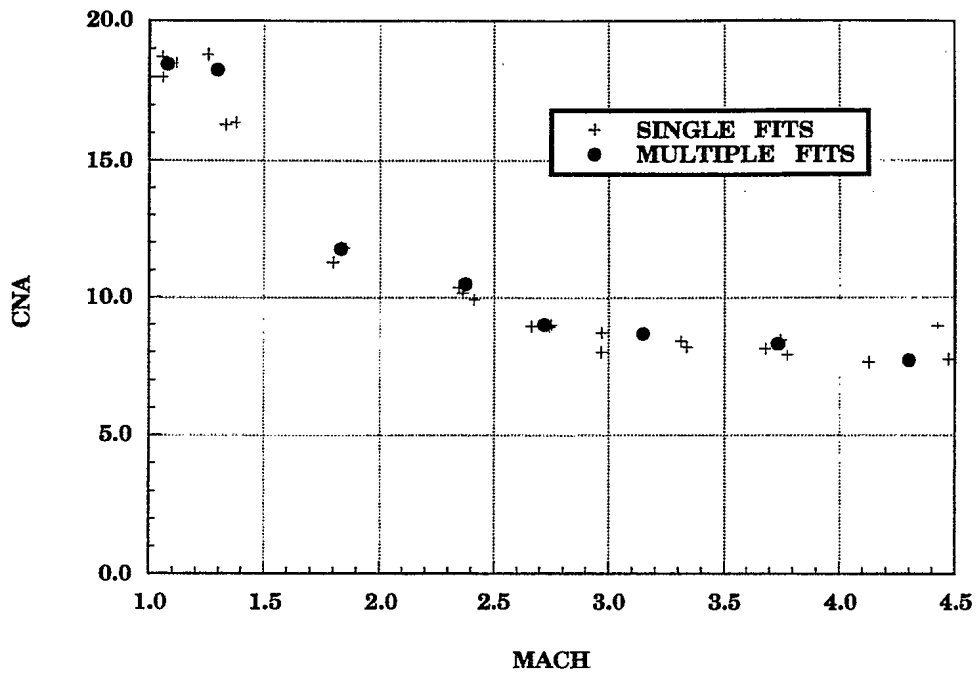
FIGURE 11 - Normal force coefficient slope versus Mach number
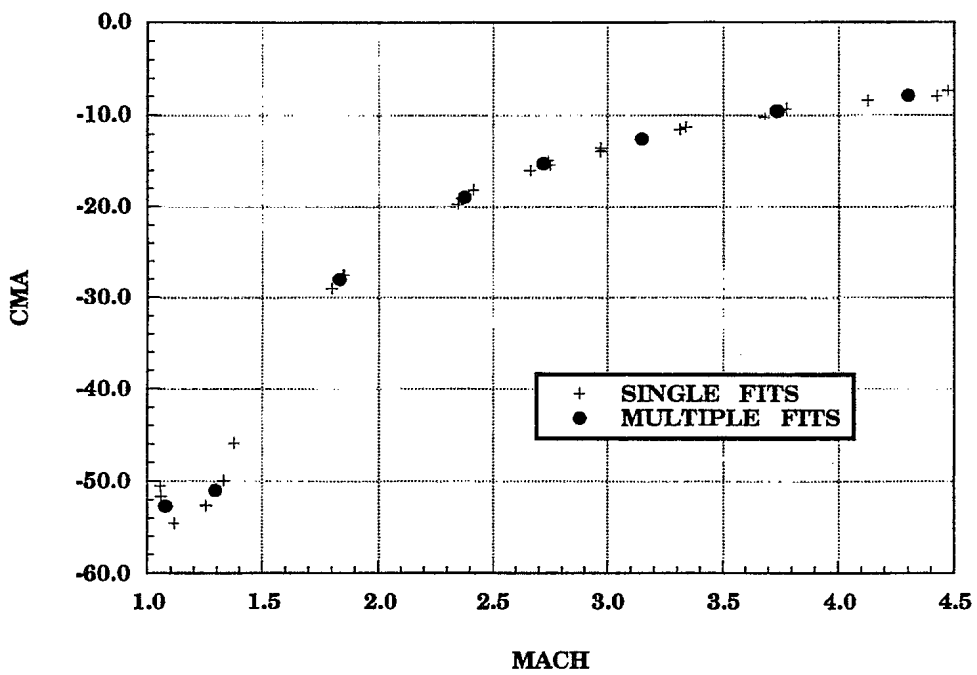
FIGURE 12 - Pitch moment coefficient slope versus Mach number
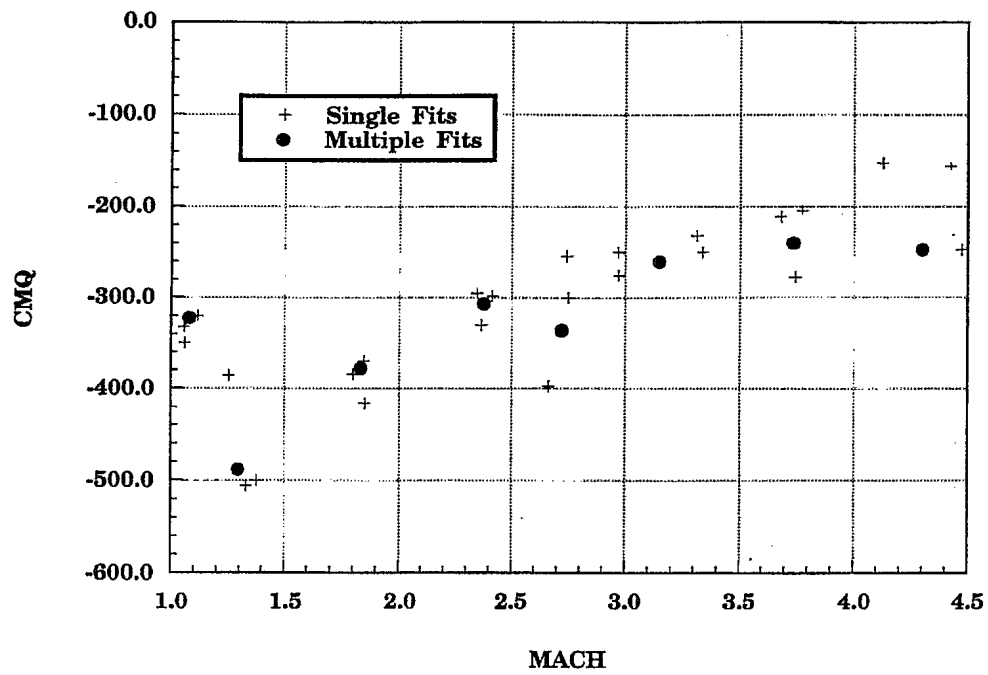
FIGURE 13 - Pitch damping coefficient versus Mach number
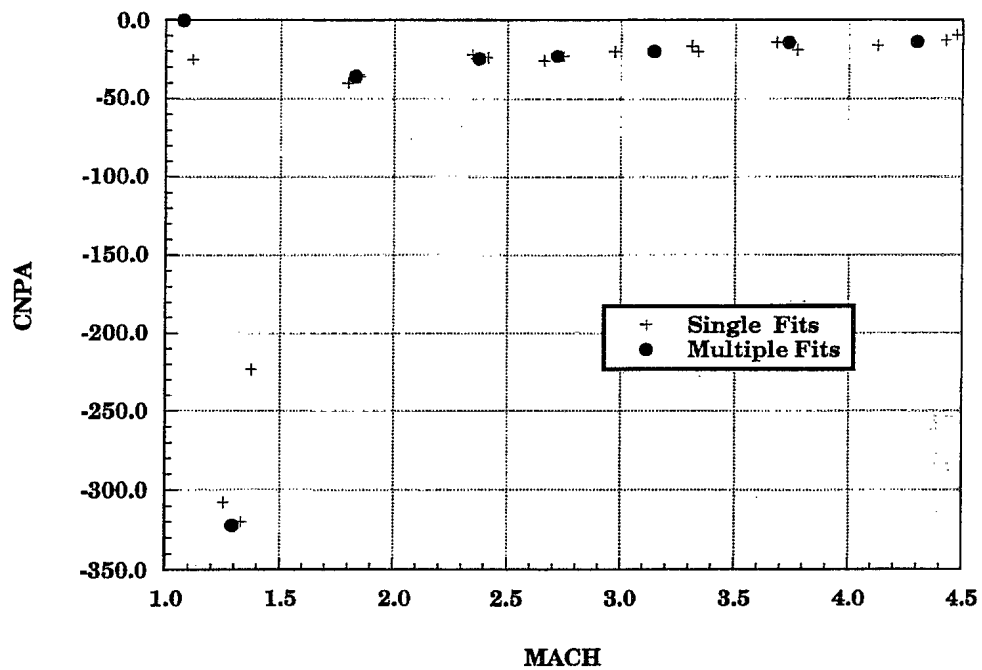
FIGURE 14 - Magnus moment coefficient slope versus Mach number
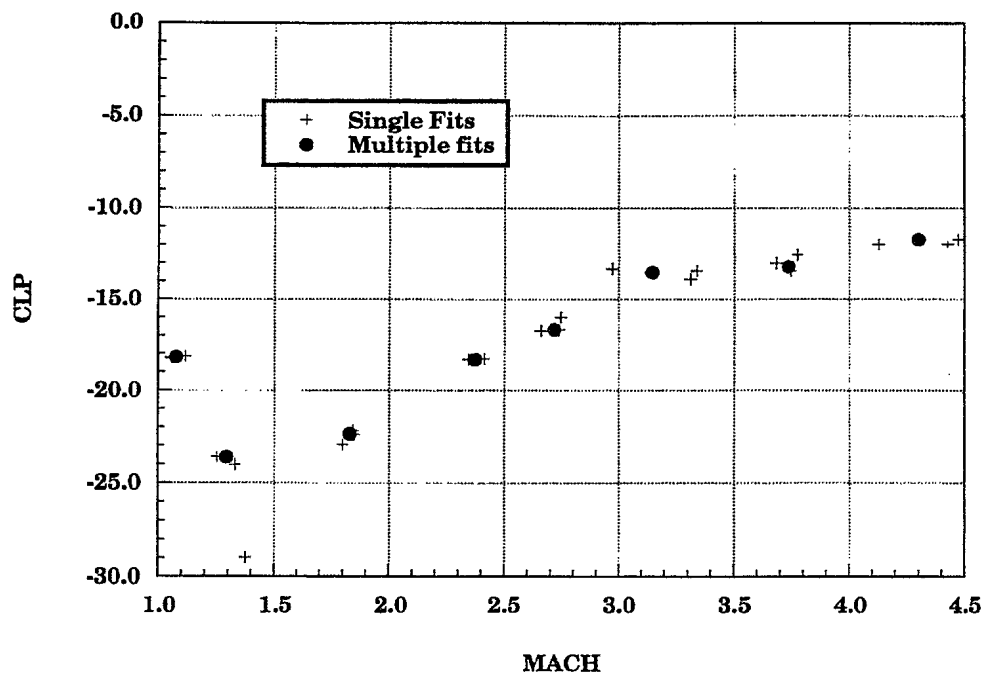
FIGURE 15 - Roll damping coefficient versus Mach number
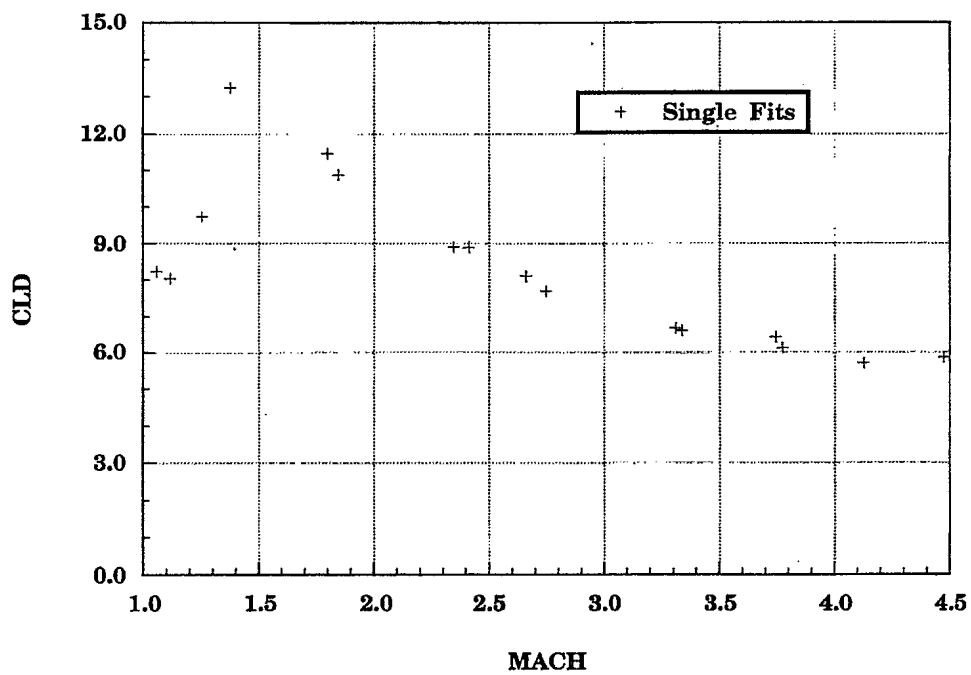
FIGURE 16 - Roll moment due to fin cant versus Mach number

Comparison of DREV results and published data
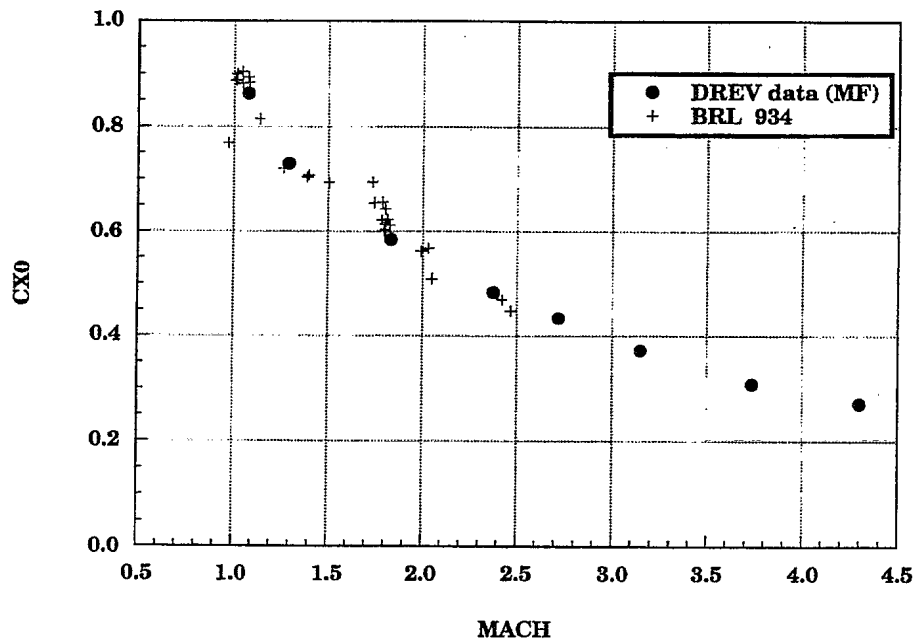
FIGURE 17- a)   Axial force
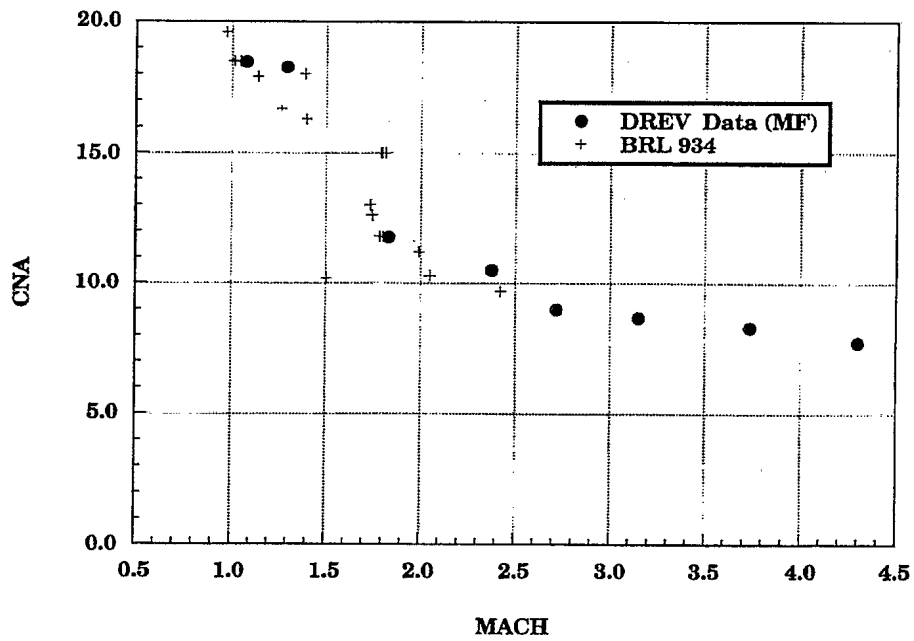
FIGURE 17- b)   Normal force coefficient slope
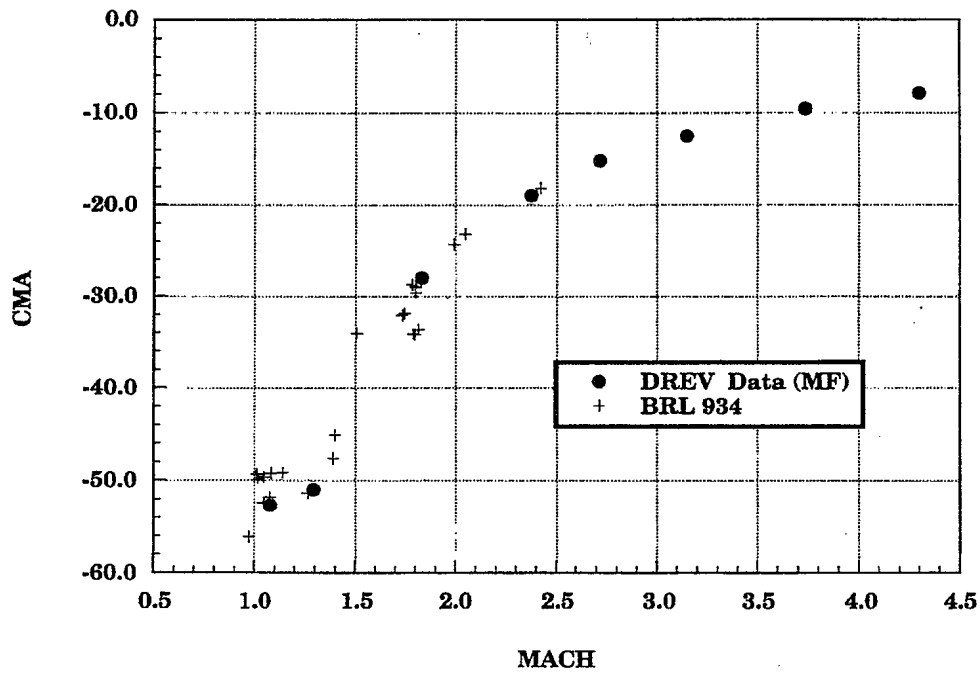
FIGURE 17- c)   Pitch moment coefficient slope
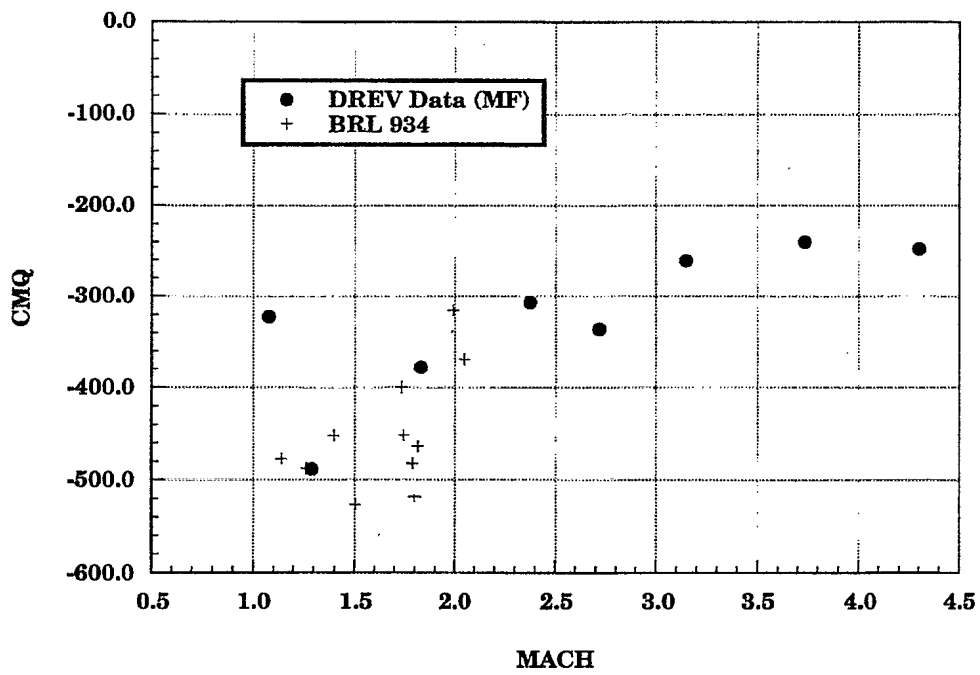
FIGURE 17- d)   Pitch damping coefficient
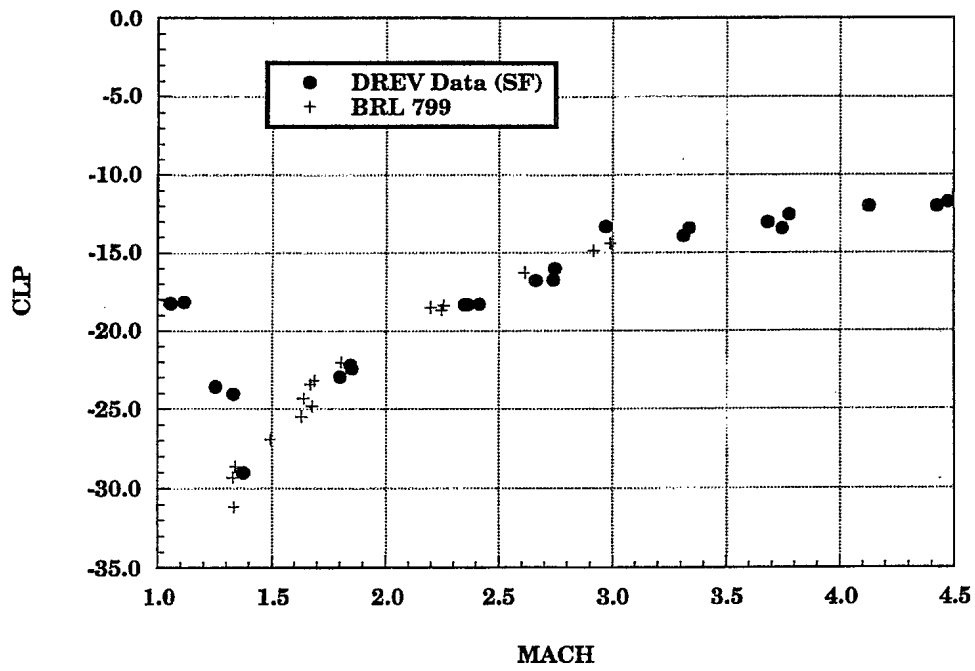
FIGURE 17- e)   Roll damping coefficient
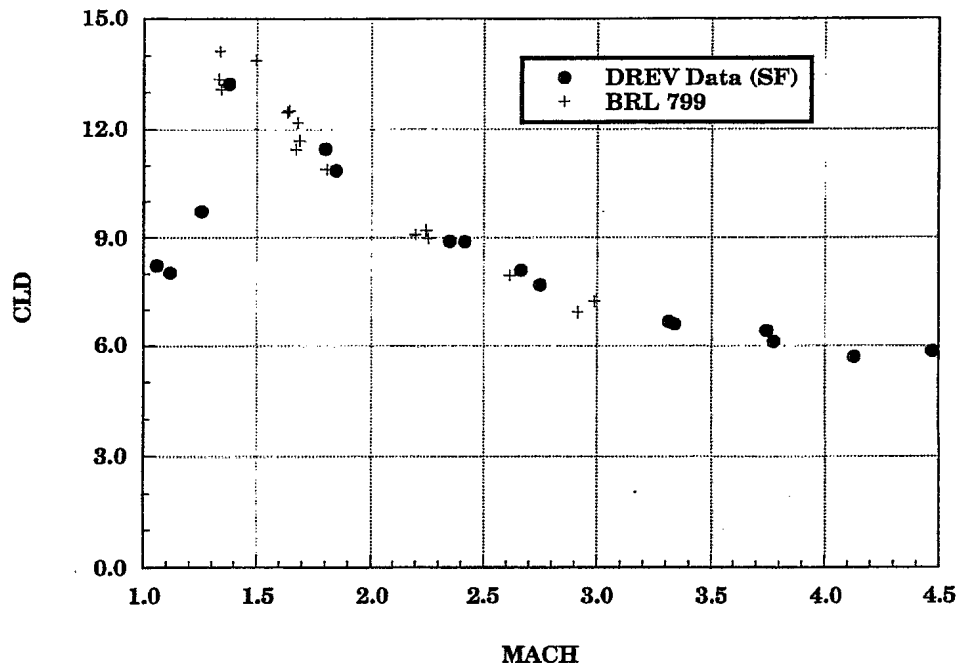
FIGURE 17- f)   Roll moment due to fin cant

Dynamic stability limits
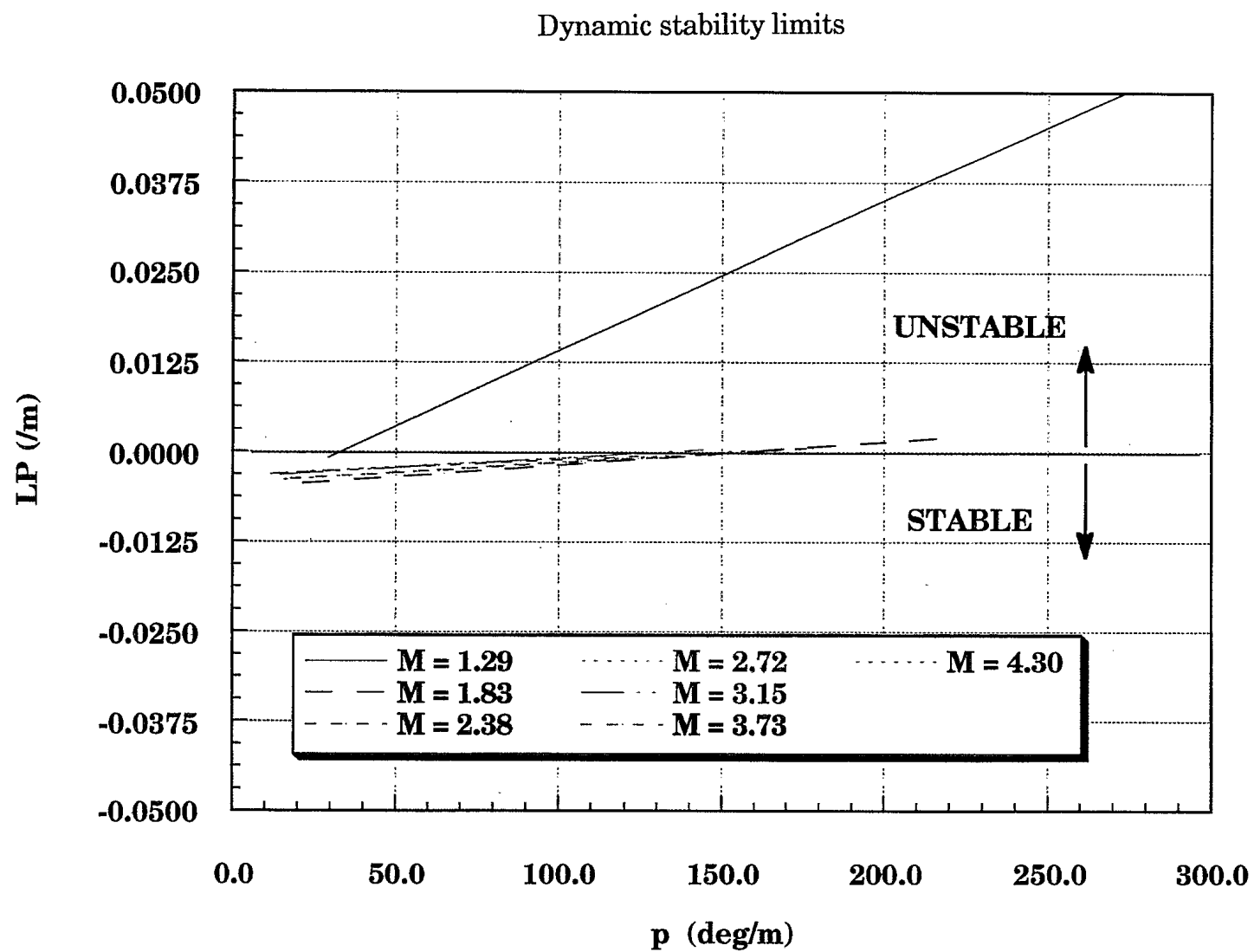
FIGURE 18 - a)   View 1
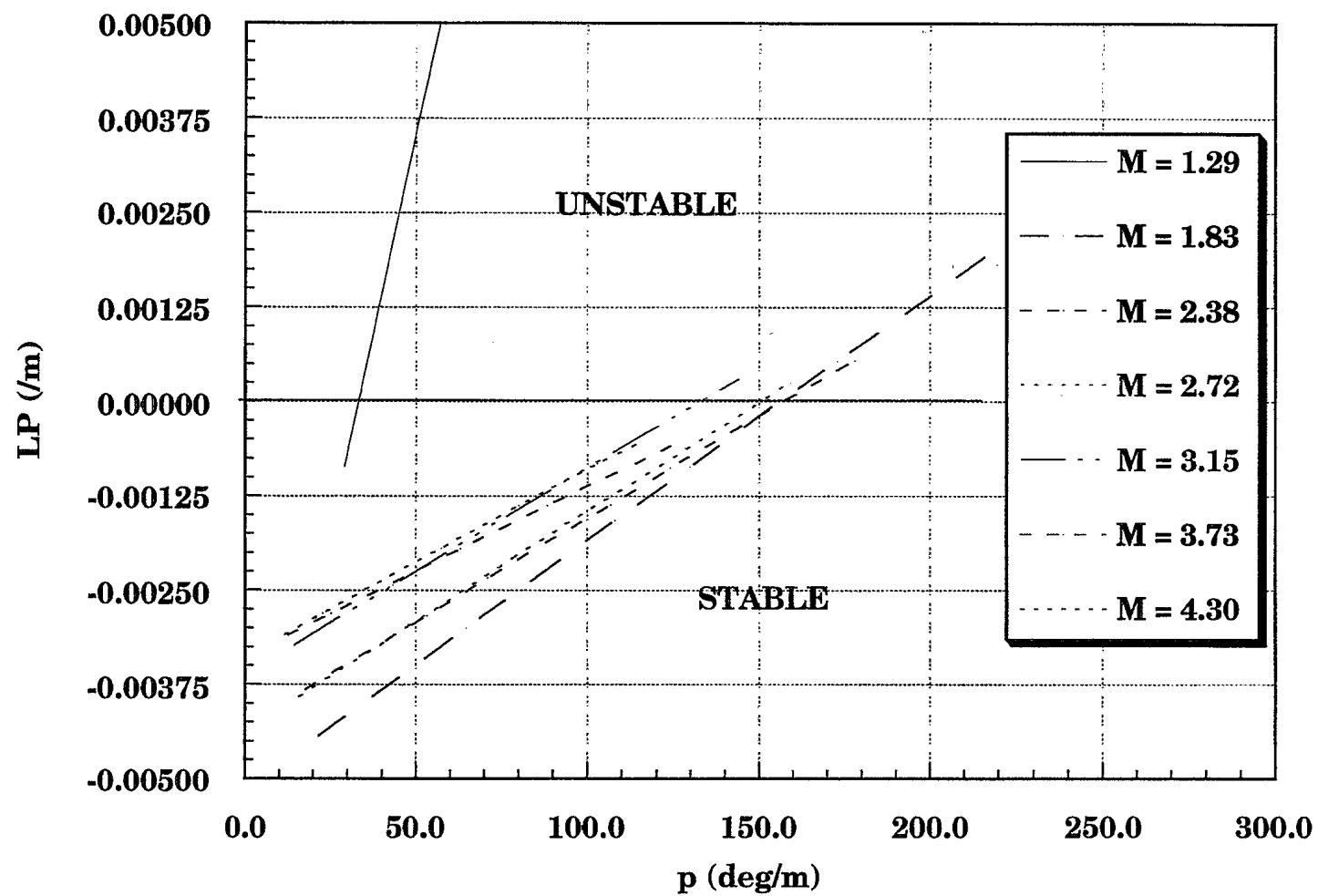
FIGURE 18 - b)   View 2 (expanded scale)

APPENDIX A

Drawings for Sabot Design of Basic Finner Model
(All dimension in inches)

Item	Numéro de dessin Drawing number	Description	Qté Qty
1	110 SB - 300	SEAL	1
2	110 SB - 305	SABOT	1
3	110 SB - 306	SOC. HD. CAP SCREW ⅜-24NF (REWORKED)	4
4	110 SB - 304	RIDER (BONDABLE TEFLON ¹⁄₁₆ × 1" × LENGTH TO SUIT	2
5	110 SB - 306	PIN	1
6	110 SB - 306	PAD	1
7	N.D.	#2 -36 × 1"LG . SOC. HD. CAP SCR	4
8	110 SB - 305	SABOT	1

DIA -A-

.06 SAWCUT

4.318 ⁻.002 DIA.
MACHINE AFTER BONDING
RIDER BANDS (SEE NOTE)

⁹⁄₁₆ DRILL
(SEE NOTE 1)

.50

SAWCUT DEPTH
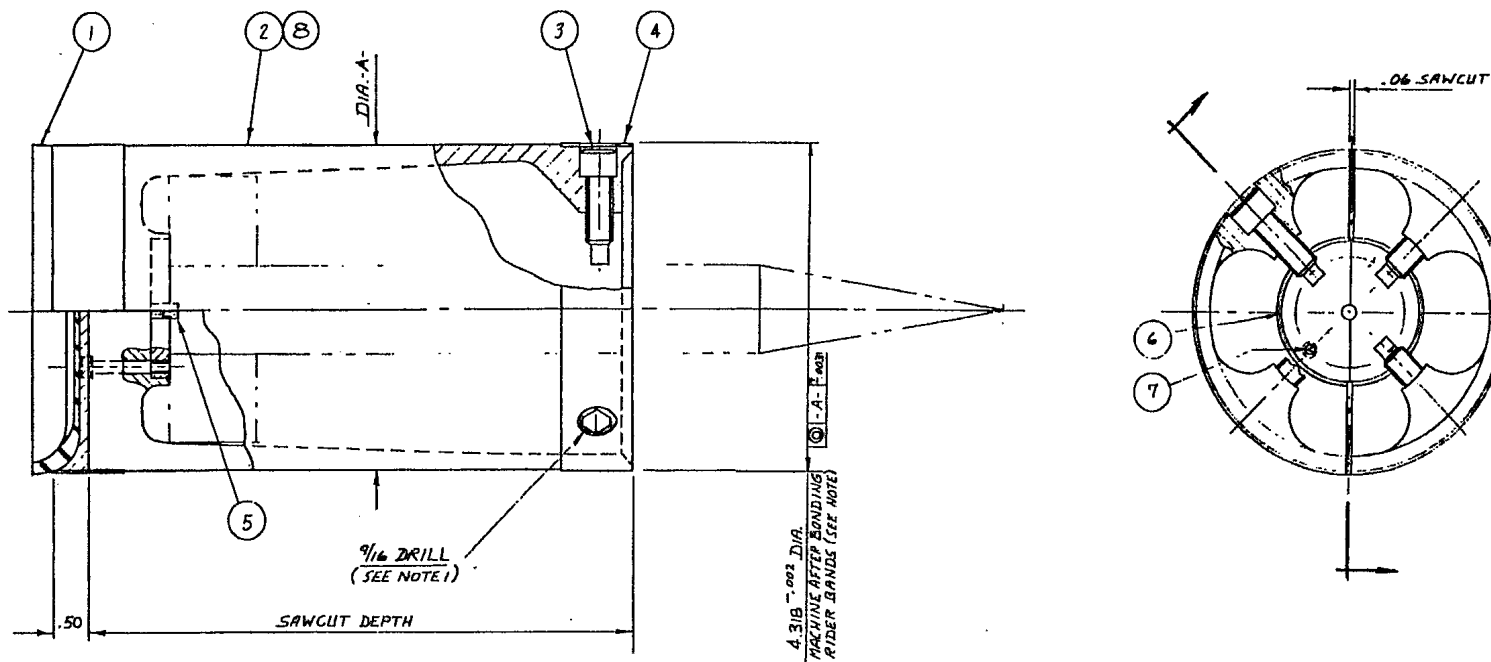
NOTE : 1.. BOND ITEM ④ TO ITEM ② WITH CONTACT CEMENT
MACHINE RIDER BANDS (EACH END) AS SHOWN.
DRILL 4 HOLES ⁹⁄₁₆ DIA. IN CONJUNCTION WITH DWG 110SB-
2.. BOND ITEM ① TO ITEM ② WITH CONTACT CEMENT
LINING UP MOULDED GROOVE IN RUBBER SEAL WITH SAWCUT

Sauf indications contraires
Unless otherwise specified

Symbole
Symbol

Modification
Amendment

Par
By

Date

Autorisé
Authorized

Dimensions sont en mm
Dimensions are in mm
Etat de surface
Surface roughness

TOLERANCES
Décimales, Decimals
1. 1 (X) ± .05
2. 2 (XX) ± .25
3. 3 (XXX) ± 0.100
Angles ± 0°-30'
Enlever arêtes et bavures vifs
Remove sharp edges & corners
Biseaux, Chanfrein 45°

Tracé Traced

Revisé Drawn
A. ?. 15/10/88
Verifié Verified

Approuvé Approved

Approuvé Approved

TITRE TITLE

BASIC FINNER SABOT

Demande de travail
Work order

Accepté Accepted

Projet Project

Feuille de
Sheet of

CENTRE DE RECHERCHES POUR LA DEFENSE, VALCARTIER.
DEFENCE RESEARCH ESTABLISHMENT VALCARTIER.
Case postale 880 P.O. Box. Courcelette, P.Q. Canada, G0A 1R0

Echelle
Scale

Numéro de dessin Drawing number
110 SB -304

Format
Size
A₂

11.81

3.350

1.180
±.003

.005 FLAT
MAX.
(TYP.)

1.180 DIA.
±.0015

.50

.047
DIA.

7/8-14 UNF
CLASS 2

1.57

.005 FLAT
MAX.

FINISH MACHINE
AFTER ASSY

-A-

3/4-16 UNF
CLASS 2

-A- TOOL

BODY

TAIL

1.57

.093
DIA.

NO BE ALL OVER

.25
(TYP.)

.37
(TYP.)

#0-80 THR.
(TYP.)

PIN
(DRILL ROD)
(TYP.)

NOSE
MAT: HEVIMET
(TELEDYNE DENSALOY)

90° ±15'
(TYP.)

3.540
DIA.

1/16 DRILL
1/4 DEEP

.02 RAD. (FIN ROOT)
PERMISSIBLE
(TYP.)

±15'
(4 FINS)

.59

∝ =	PART	MATERIAL	REQ
0°	BODY	AISI 4340	4
2°	TAIL	HT. TREAT-HRM	4
4°		ROC."C" 40-42	4
0°	BODY	STRESSPROOF	6
2°	TAIL	STEEL	6
4°		100,000 PSI YIELD	6

TITRE TITLE
BASIC FINNER

Numéro de dessin Drawing number
110 SB -.307

Format Size A2

MAT : 75 ST ALUM

3/16 DRILL
1/4 DEEP

SABOT (ITEM ②)
SAME AS ITEM ②
EXCEPT AS SHOWN

COARSE
SAND BLAST

1.0 +.01

4.300 +.005 DIA-A-

3.92 -.02 DIA.

1.50 ±.03

.46 +.01

.12 -.01

.375 +.002

45°

1/4 R.

45°

.71
(REF.)

4.230 ±.003 DIA.

4.230 ±.002 DIA.

1.800 +.005 DIA.
.25 R
2.0 DIA.

3.55 DIA.

1/4 R.

1 R
2

.37
1.25   .37

8.0

1.0 +.01

45°   45°

1/2 R

.50

1.50
P.C.

2.50
DIA.

3.92 -.02 DIA.

4 HOLES,
DRILL & C'BORE
FOR # 5 - 40 SOC. HD.
CAP SCR. IN CONJUNCTION
WITH PAD. ITEM ⑥

CENTRE DE RECHERCHES POUR LA DÉFENSE, VALCARTIER.
DEFENCE RESEARCH ESTABLISHMENT VALCARTIER.
Case postale 880 P.O. Box, Courcelette, P.Q. Canada, G0A 1R0

TITRE TITLE
SABOT

Numéro du dessin Drawing number
110 SB - 305

A2

Format
Size
A3

Numéro du dessin   Drawing number.

Item	Numéro du dessin Drawing number	Description	Qté Qty

BREAK CORNERS

±.001

PIN
(MAT: NYLON
OR EQUIV.)

.37   .187 DIA.

SCREW
(MAT: 3/8 -24 SOC. HD.
CAP SCR. REWORKED)

.25

25

2 PIECES
3/16 DRILL
.25   +.01

1.800 +.003 DIA.

PAD
MAT: AISI 4340
HEAT TREAT & HARDEN
TO ROC."C" 42 -45

#5-40 TAP
4 HOLES
IN CONJUNCTION
WITH ITEM ②

Sauf indications contraires.
Unless otherwise specified.

Dimensions sont en mm.
Dimensions are in mm.

Etat de surface
Surface roughness

TOLERANCES·
Décimales, Decimals
1.   1 (X)   ± 0.5
2.   2 (XX) ± 0.20
3.   3 (XXX) ± 0.100
Angles ± 0°-30'

Enlever arêtes et coins vifs.
Remove sharp edges & corners.
Biseaux, Chamfers 45°

Symbole Symbol	Modification Amendment	Par By	Date	Autorisé Authority

CENTRE DE RECHERCHES POUR LA DEFENSE, VALCARTIER.
DEFENCE RESEARCH ESTABLISHMENT VALCARTIER.
Case postale 880 P.O. Box. Courcelette, P.Q. Canada. G0A 1R0

Tracé Traced	Approuvé Approved	TITRE TITLE
Dessiné Drawn 2/10/84	Approuvé Approved	PIN, SCREW, PAD.
Vérifié Verified		
Accepté Accepted	Projet Project	
	Feuille de Sheet of	Echelle Scale

Numéro du dessin   Drawing number
110 SB - 306

Format Size
A3

Demande de travail
Work order

D   C   B   A

MAT: NEOPRENE
RUBBER

UNCLASSIFIED

Item	Numéro du dessin Drawing number	Description	Qté Qty

3/4 R.

.18

4.20

40°

.06

.18

½ R.

30°

½ R.

.87

4.40 +.01 DIA.

10°

Seuf Indications contraires Unless otherwise specified.	Symbole Symbol	Modification Amendment	Par By	Date	Autorisé Authority

Dimensions sont en mm.
Dimensions are in mm.

État de surface
Surface roughness

TOLERANCES·
Décimales, Decimals
1.   1 (X)   ± 0.5
2.   2 (XX) ± 0.20
3.   3 (XXX) ± 0.100
Angles ± 0°-30'

Enlever arêtes et coins vifs.
Remove sharp edges & corners
Biseaux, Chamfers 45°

Demande de travail
Work order

CENTRE DE RECHERCHES POUR LA DEFENSE, VALCARTIER.
DEFENCE RESEARCH ESTABLISHMENT VALCARTIER.
Case postale 880 P.O. Box. Courcelette, P.Q. Canada. G0A 1R0

Tracé Traced	Approuvé Approved	TITRE TITLE	
Dessiné Drawn 9/7/84	Approuvé Approved	SEAL	
Vérifié Verified	Projet Project		
Accepté Accepted		Echelle Scale	Numéro du dessin. Drawing number. 110 SB -300	Format Size A3
		Feuille de Sheet of		

D   C   B   A

APPENDIX B

Motion Plots

.

DA95030101

ALPHA - DEG

DOWN - RANGE TRAVEL [X] - METERS

PSI

THETA

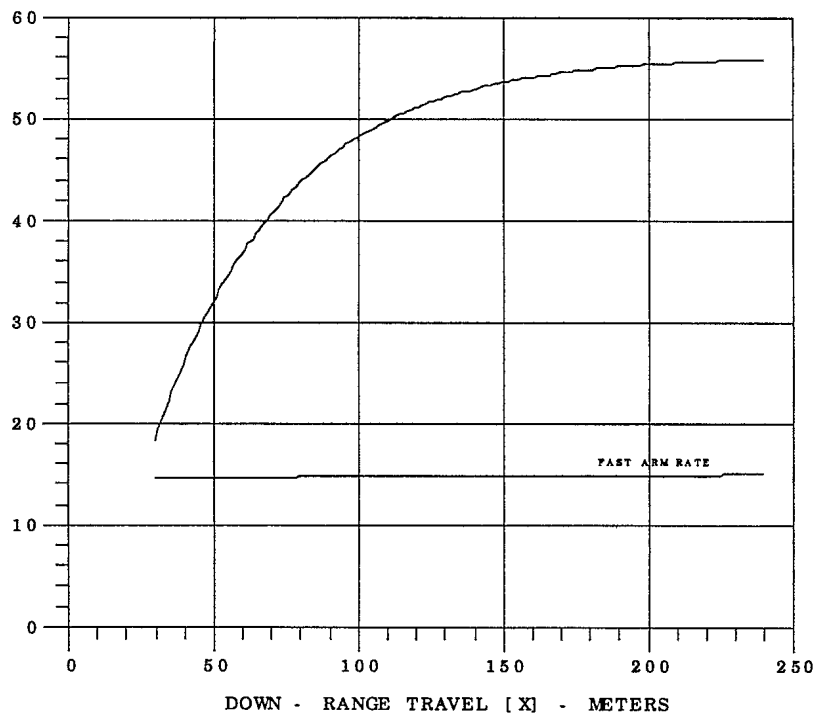DA95030101

PITCH - THETA - DEG

YAW [PSI] - DEG

ROLL RATE - DEG / M -

PACT ARM RATE

DOWN - RANGE TRAVEL [X] - METERS

DA95022702

ALPHA - DEG

DOWN - RANGE TRAVEL [X] - METERS

PSI

THETA

DA95022702

PITCH - THETA - DEG

- 5

5

- 5

5
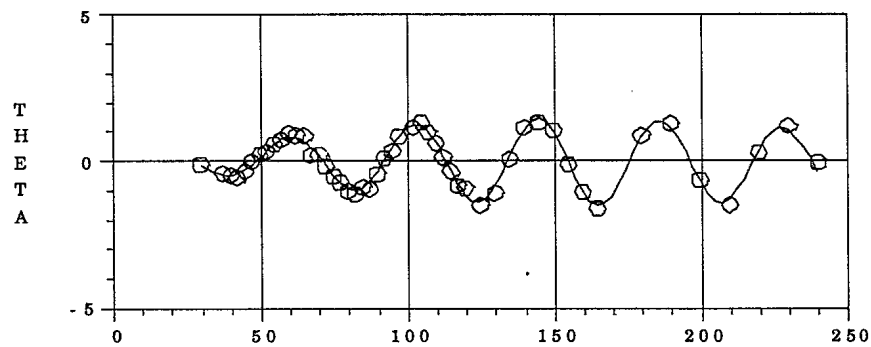
YAW [PSI] - DEG

ROLL RATE - DEG / M -

8

6

FAST ARM RATE

4

2

0

0   50   100   150   200   250

DOWN - RANGE TRAVEL [X] - METERS

DA95030603

DOWN - RANGE TRAVEL [X] - METERS

DA95030603

PITCH - THETA - DEG

- 5

5

- 5

5

YAW [PSI] - DEG

ROLL RATE - DEG / M -

8

FAST ARM RATE

6

4

2

0

- 2

0   50   100   150   200   250

. DOWN - RANGE TRAVEL [X] - METERS

DA95022205

DA95022205

PITCH - THETA - DEG

-5

5

-5

5

YAW [PSI] - DEG

ROLL RATE - DEG / M -

8

FAST ARM RATE

6

4

2

0

-2

0   50   100   150   200   250

DOWN - RANGE TRAVEL [X] - METERS

DA95020906

DOWN - RANGE TRAVEL [X] - METERS
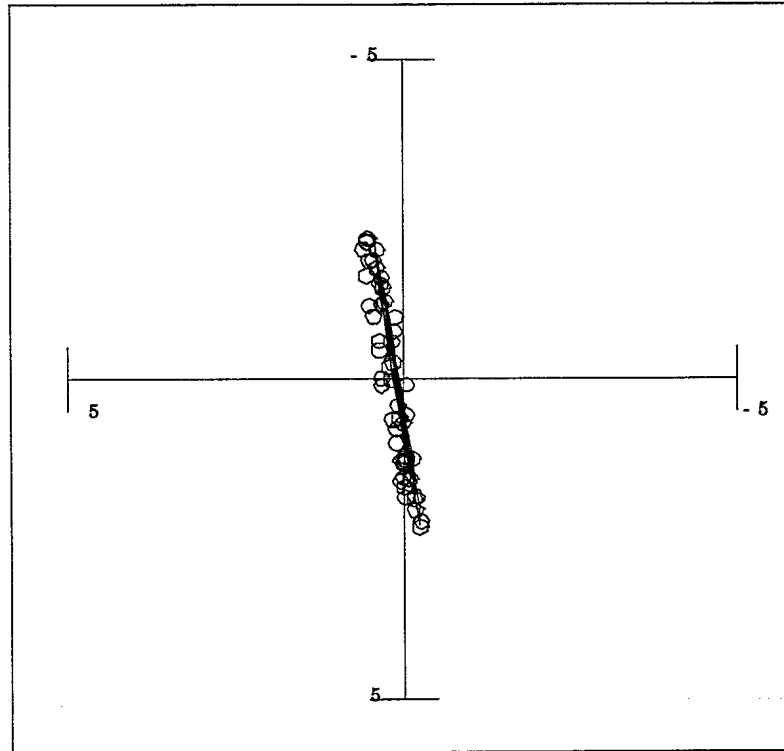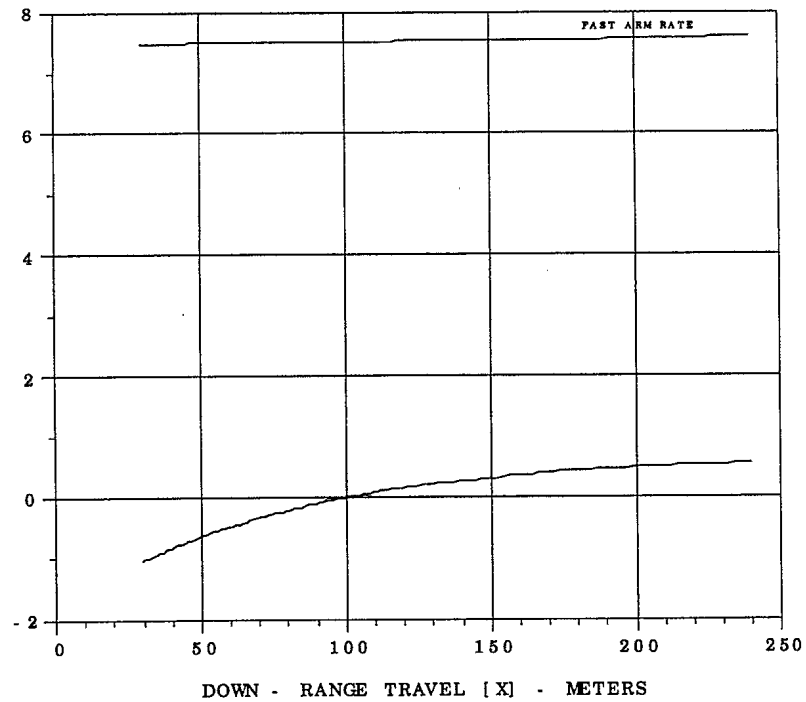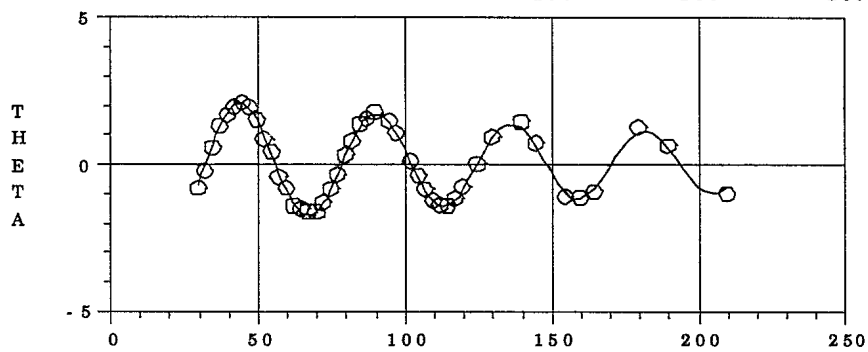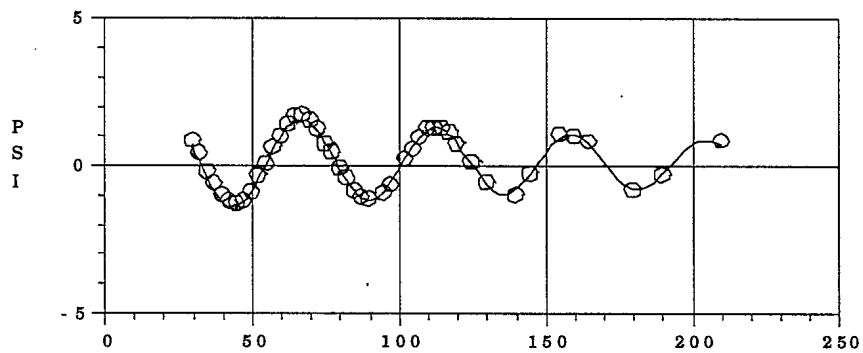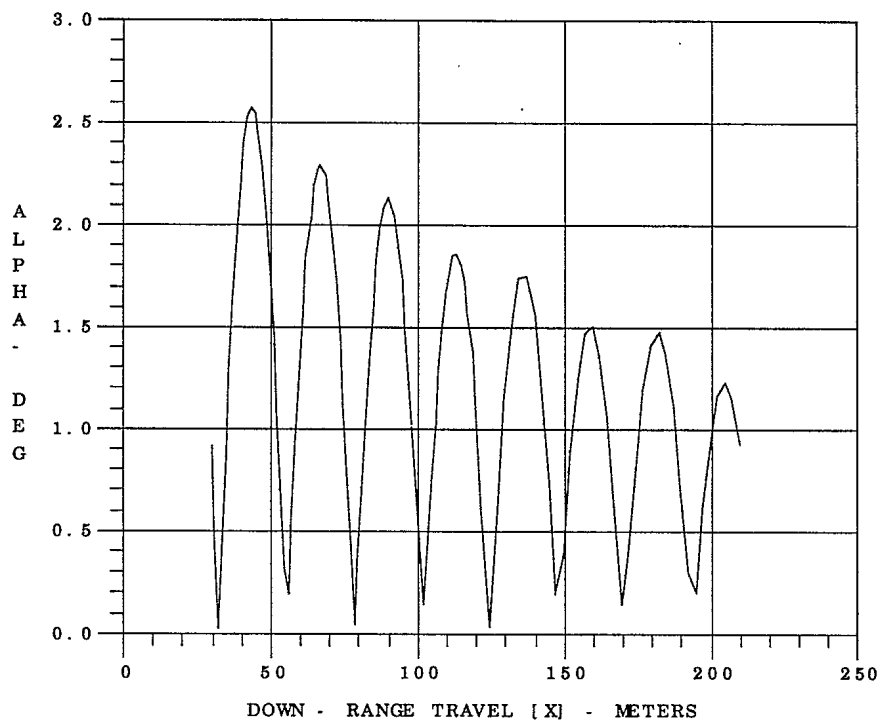
DA95020906

PITCH - THETA - DEG
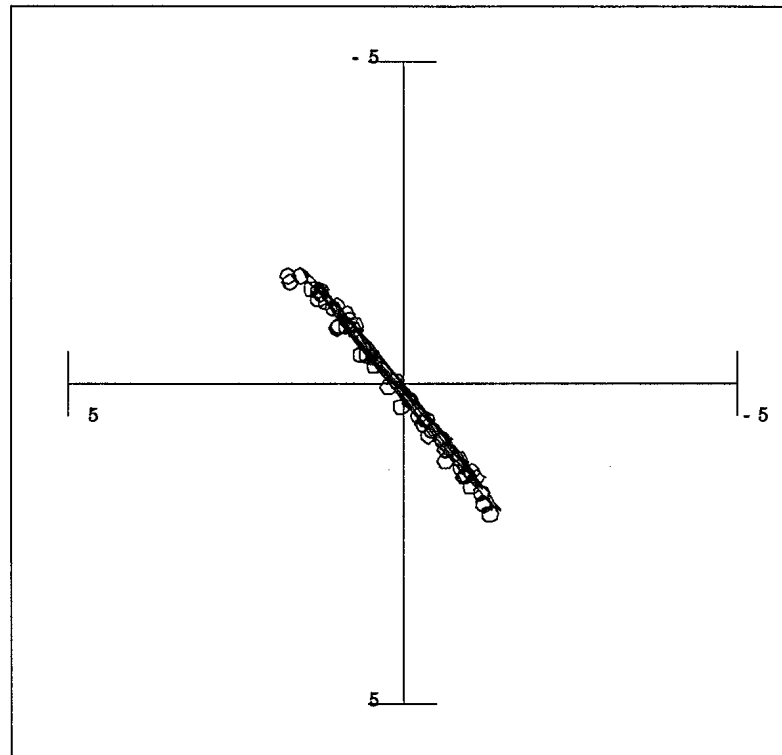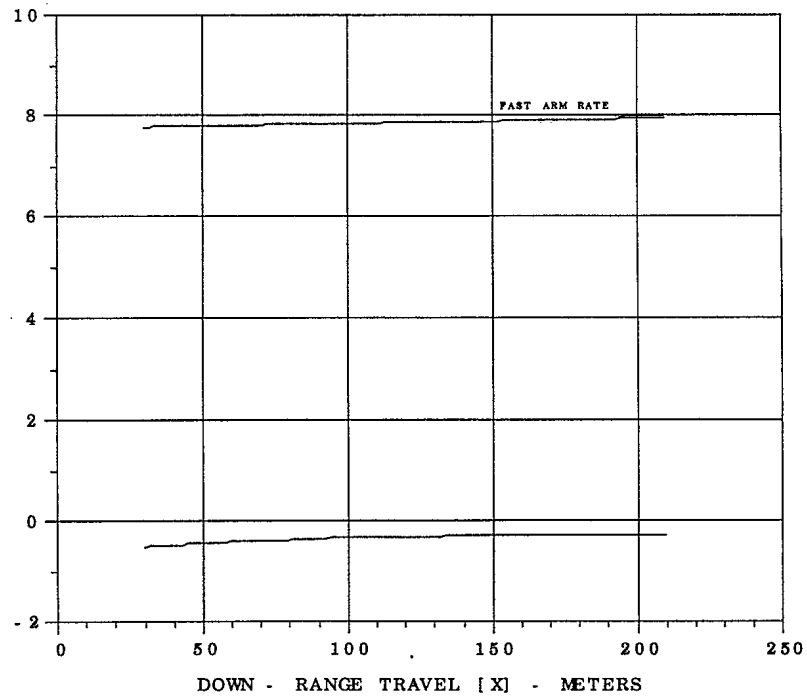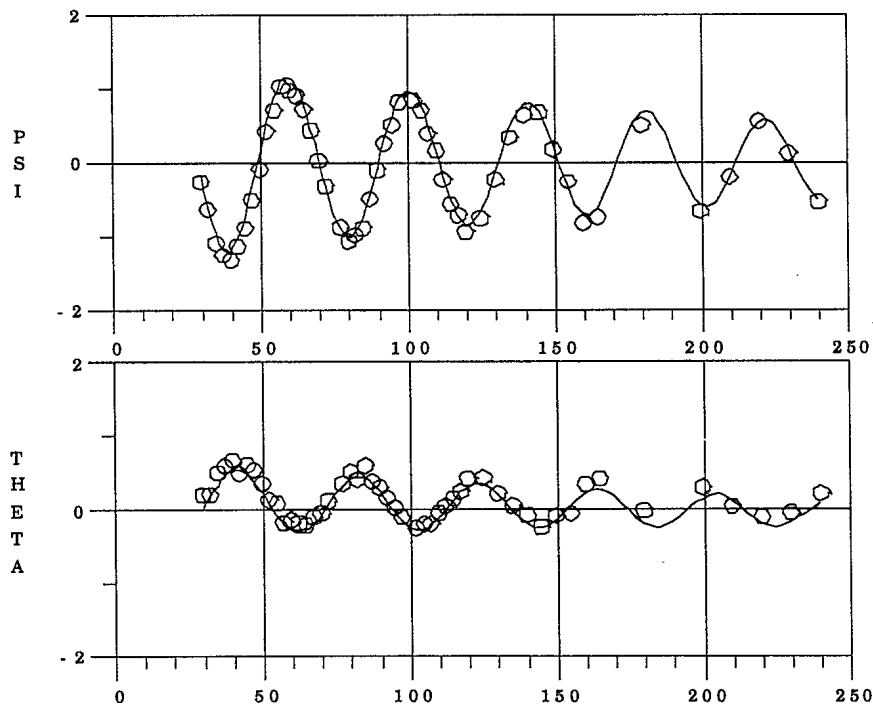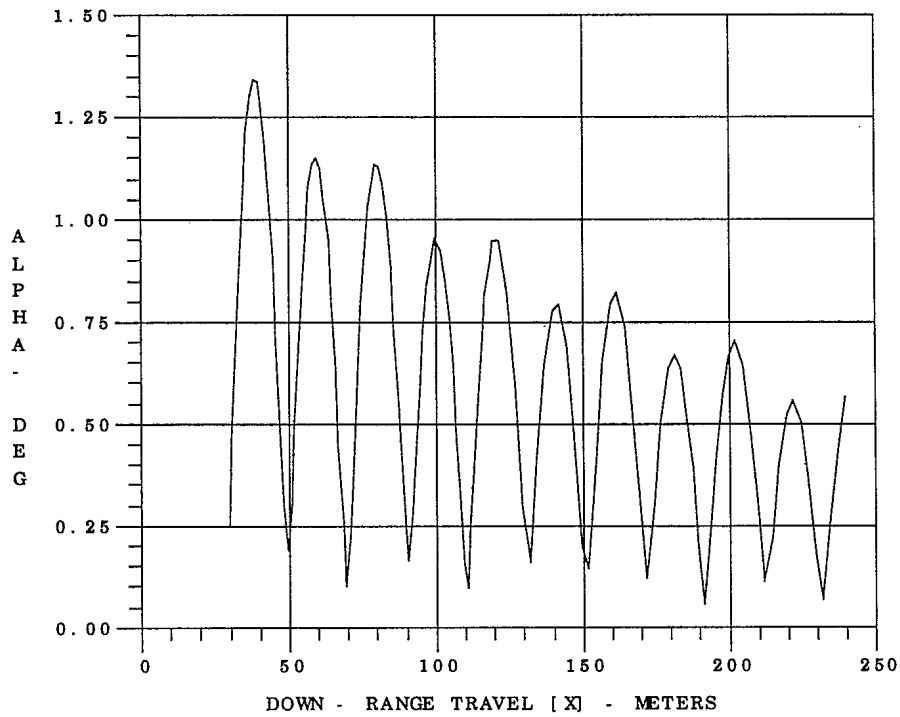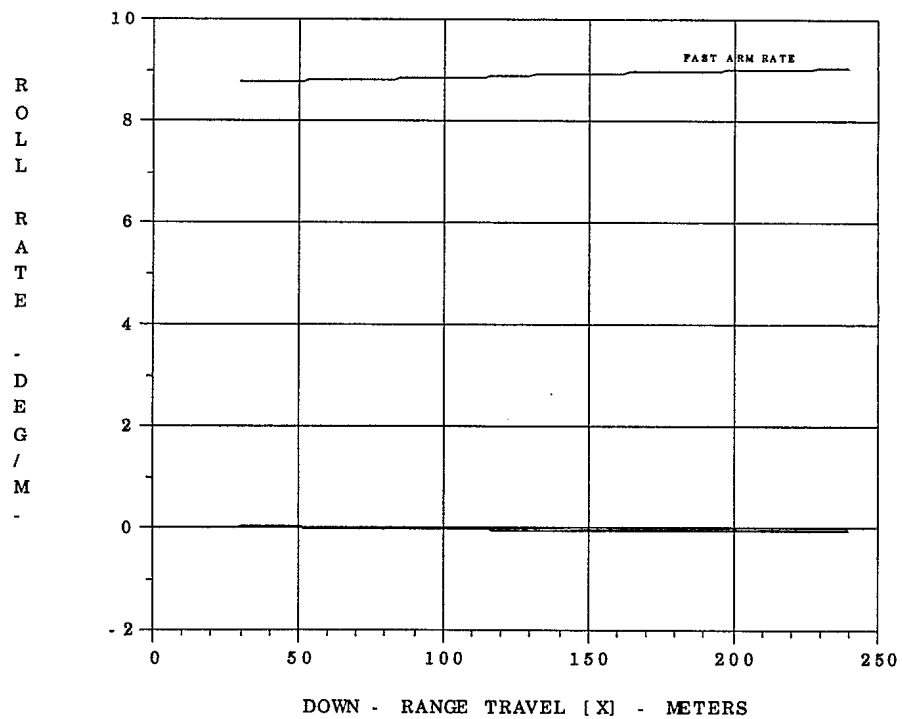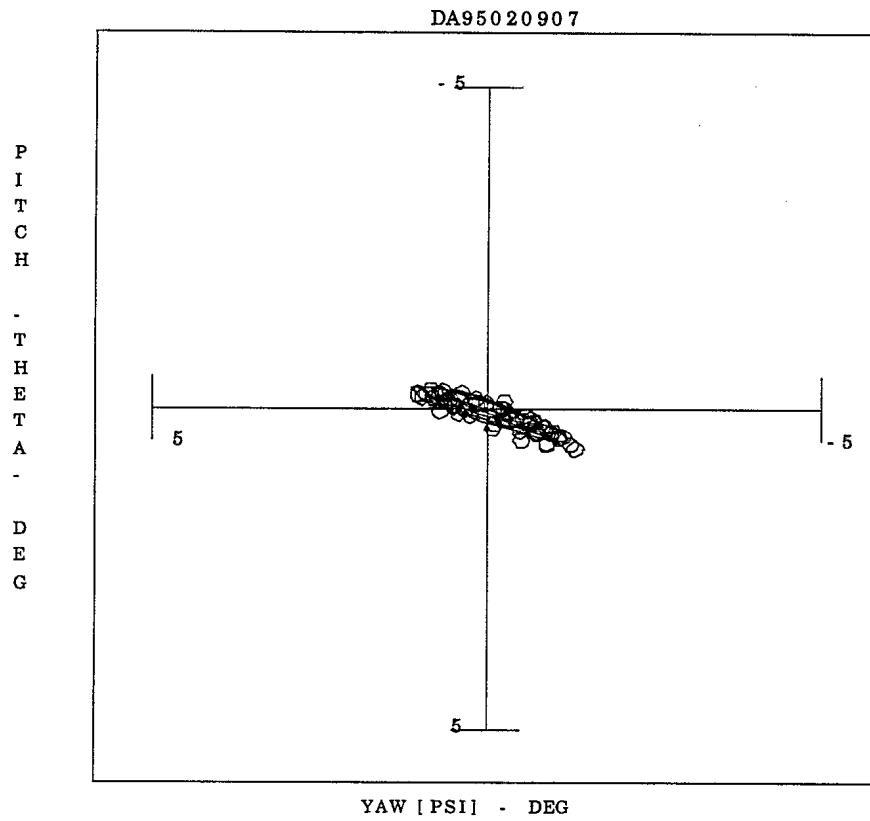
- 5

5

- 5

5

YAW [PSI] - DEG

ROLL RATE - DEG / M -

10

8

6

4

2

0

- 2

FAST ARM RATE

0   50   100   150   200   250

DOWN - RANGE TRAVEL [X] - METERS

DA95020907

DOWN - RANGE TRAVEL [X] - METERS

DA95020907

PITCH - THETA - DEG

-5

5

-5

5

YAW [PSI] - DEG

ROLL RATE - DEG/M -

FAST ARM RATE

10

8

6

4

2

0

-2

0   50   100   150   200   250

DOWN - RANGE TRAVEL [X] - METERS

DA95021308

ALPHA-DEG

DOWN - RANGE TRAVEL [X] - METERS

PSI

THETA

DA95021308

YAW [PSI] - DEG

DOWN - RANGE TRAVEL [X] - METERS

DA95022009

DOWN - RANGE TRAVEL [X] - METERS

DA95022009

YAW [PSI] - DEG

DOWN - RANGE TRAVEL [X] - METERS

DA95022010

DOWN - RANGE TRAVEL [X] - METERS

DA95022010

PITCH - THETA - DEG

-5

5 .... -5

5

YAW [PSI] - DEG

ROLL RATE - DEG / M -

20

15   FAST ARM RATE

10

5

0

-5

0   50   100   150   200   250

DOWN - RANGE TRAVEL [X] - METERS

DA95030111

DOWN - RANGE TRAVEL [X] - METERS

DA95030111

PITCH - THETA - DEG

YAW [PSI] - DEG

ROLL RATE - DEG / M -

FAST ARM RATE

DOWN - RANGE TRAVEL [X] - METERS

DA95022712

DOWN - RANGE TRAVEL [X] - METERS

DA95022712

PITCH - THETA - DEG

- 5

5

- 5

5

YAW [PSI] - DEG

ROLL RATE - DEG / M -

80

60

40

20

0

FAST ARM RATE

0   50   100   150   200   250

DOWN - RANGE TRAVEL [X] - METERS

DA95030613

DOWN - RANGE TRAVEL [X] - METERS
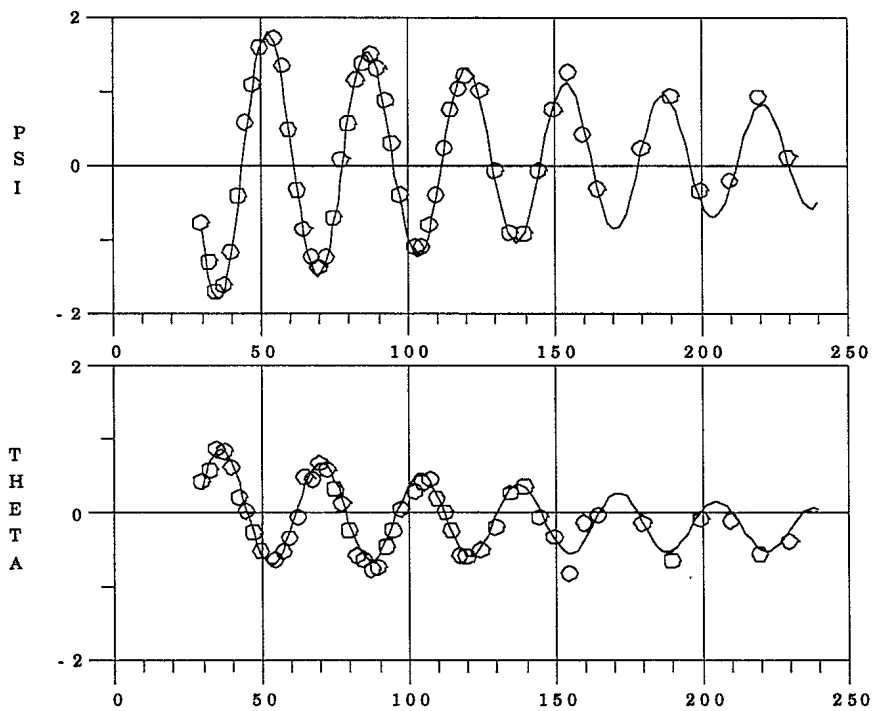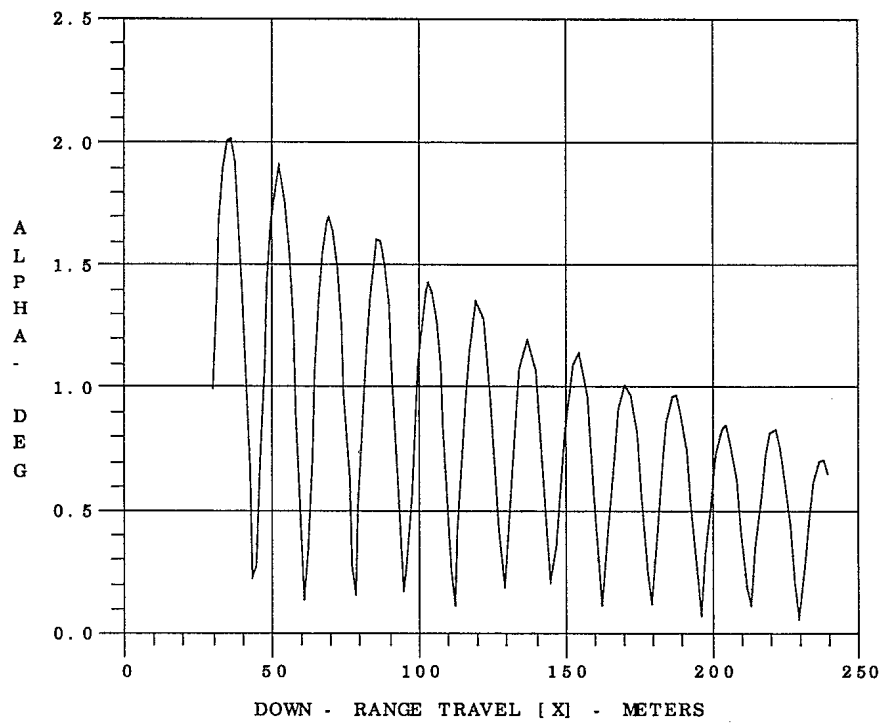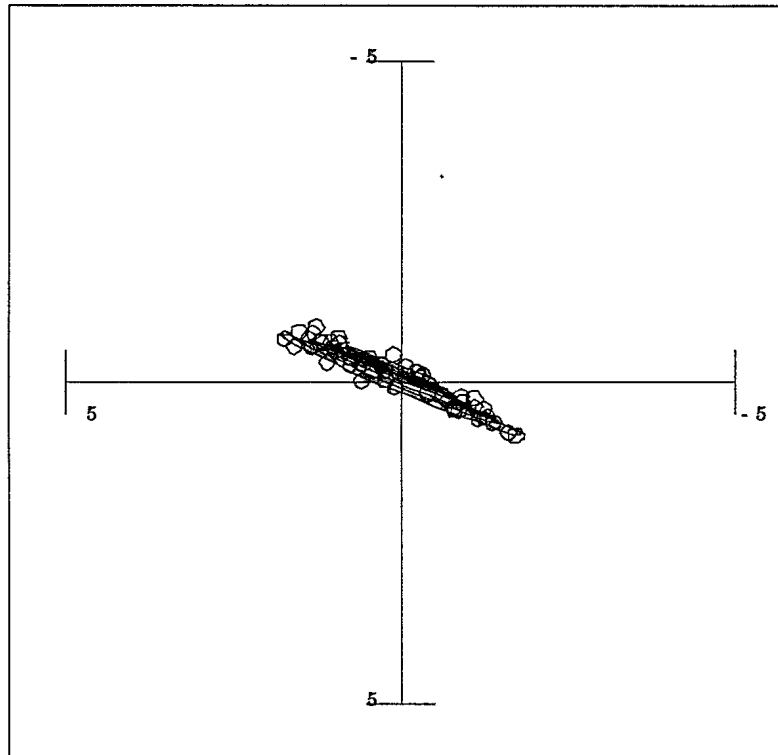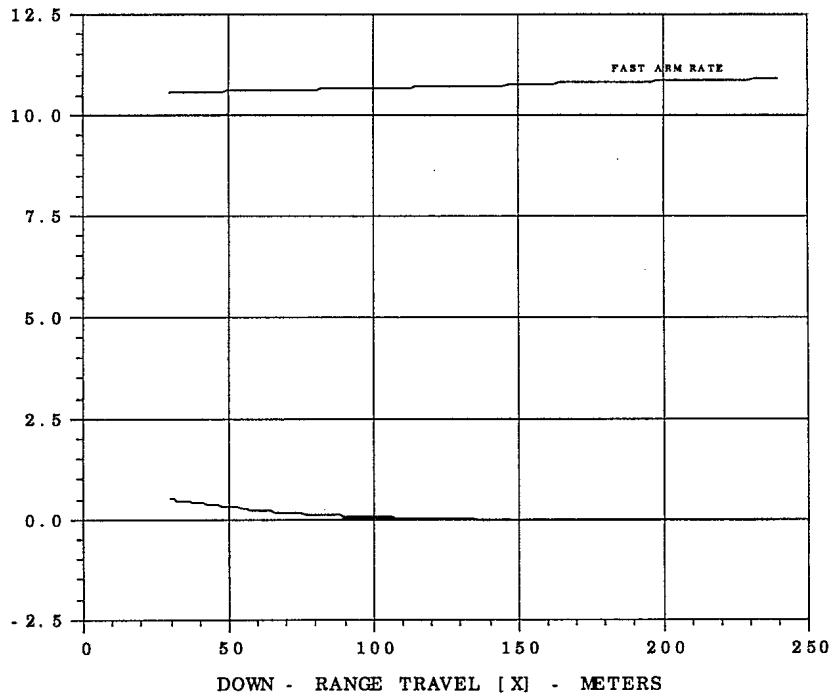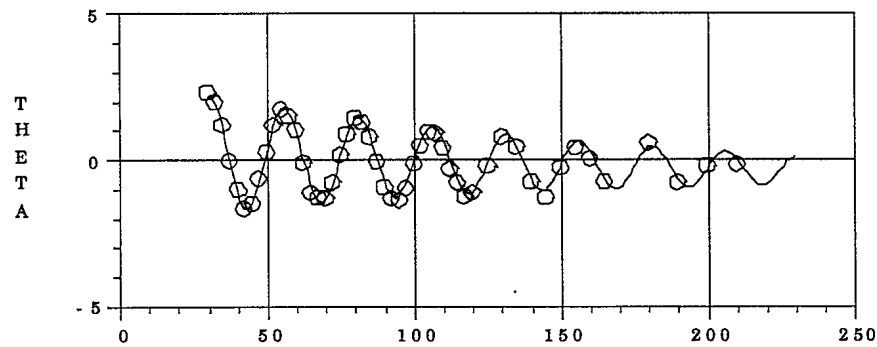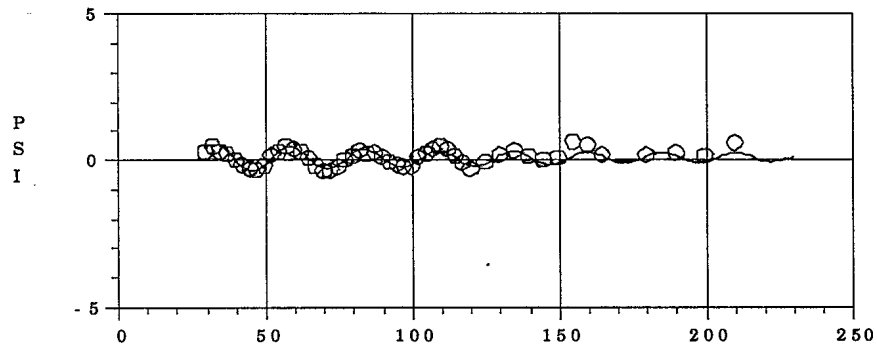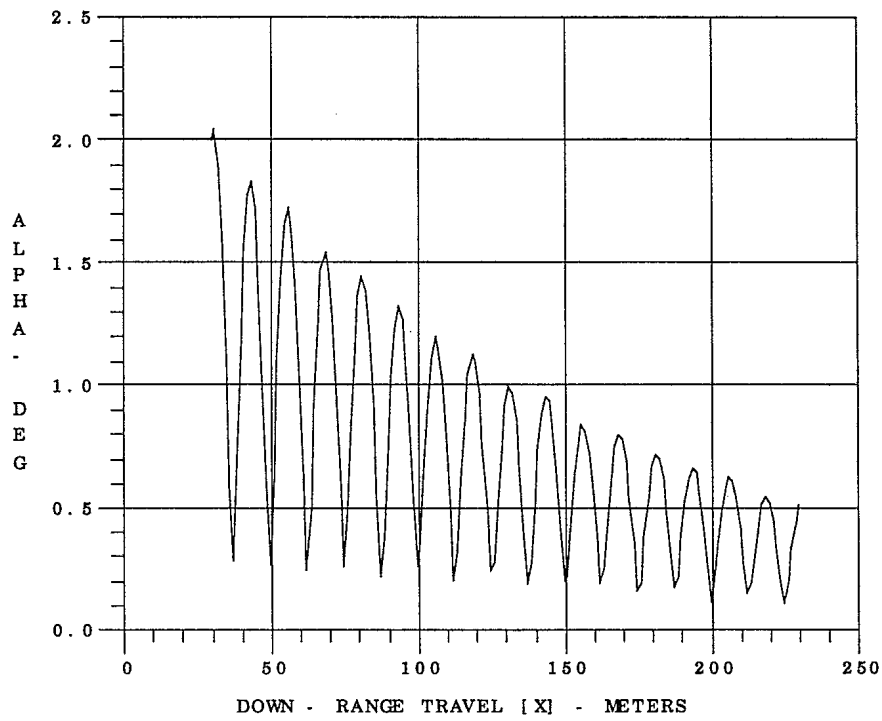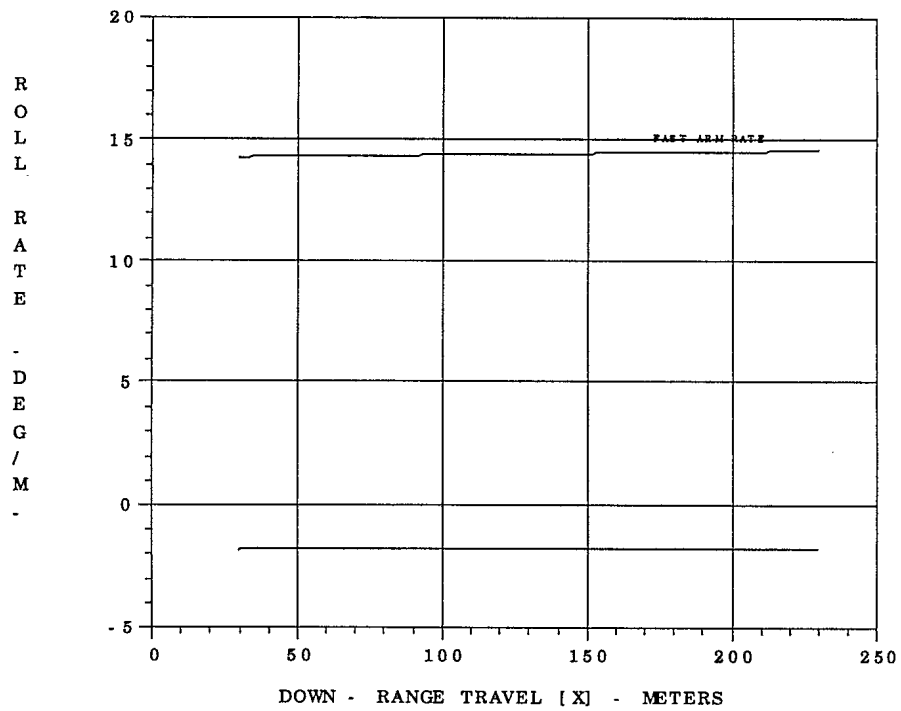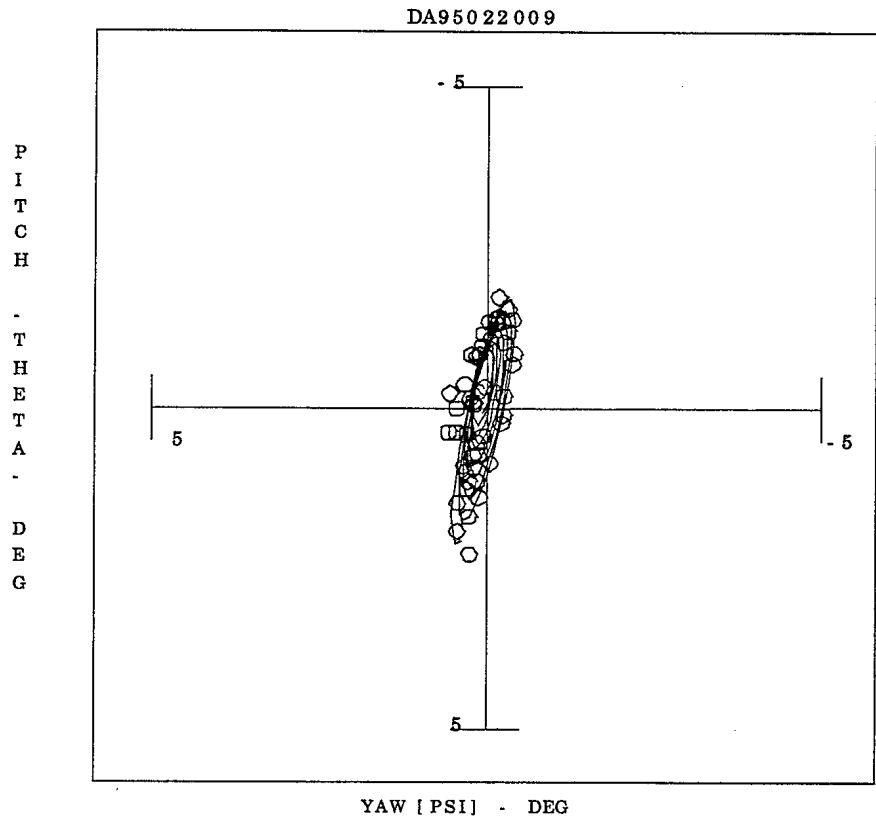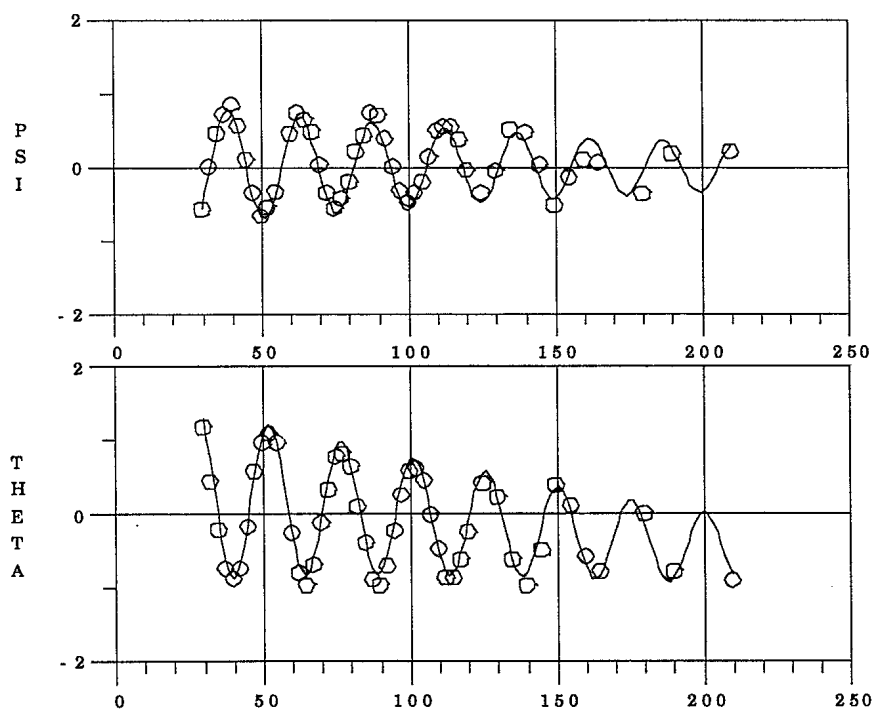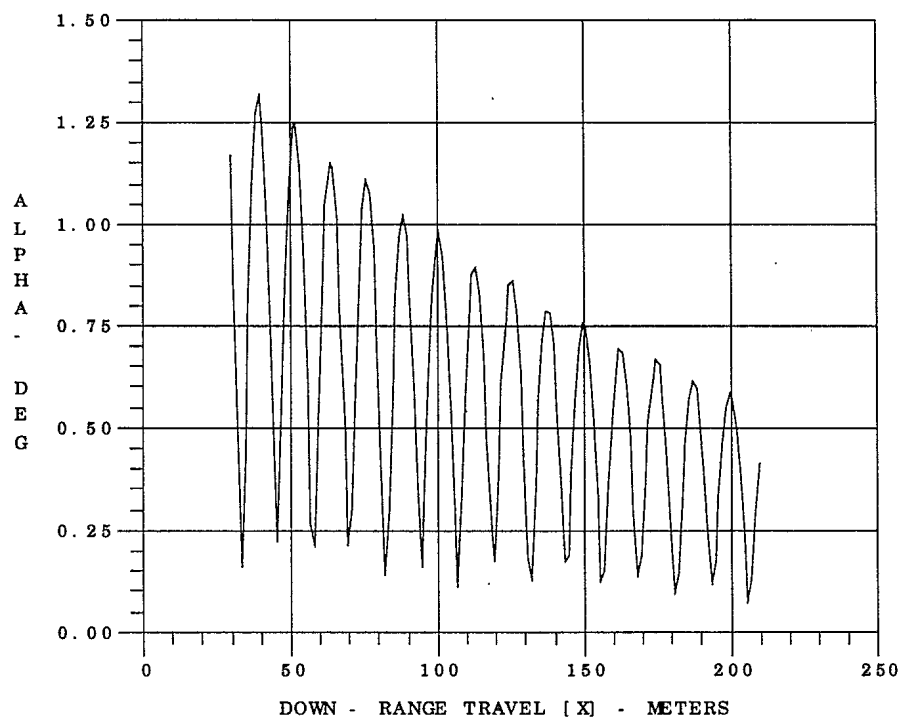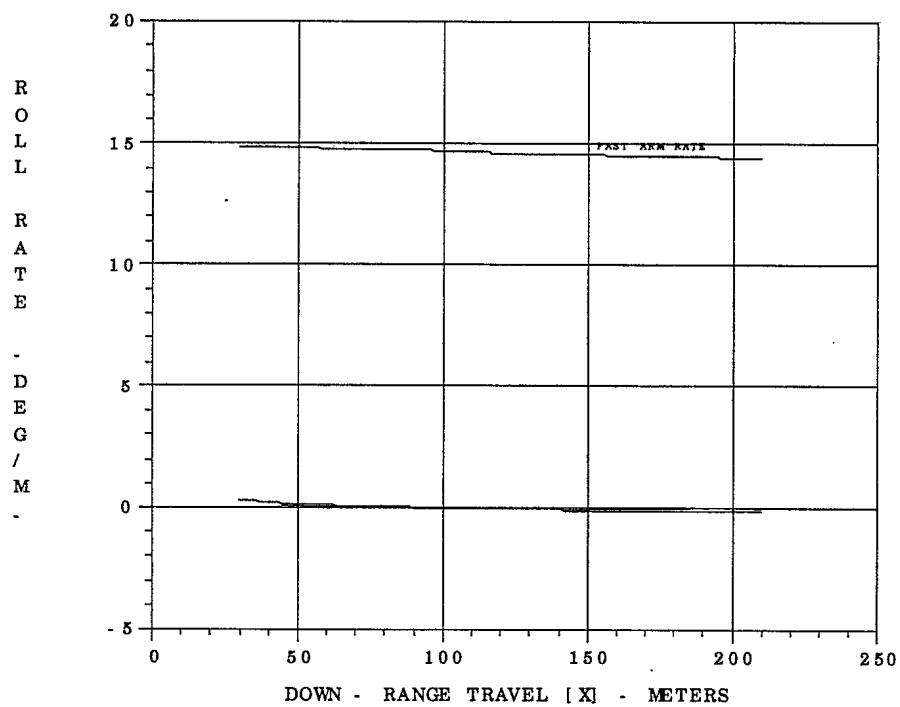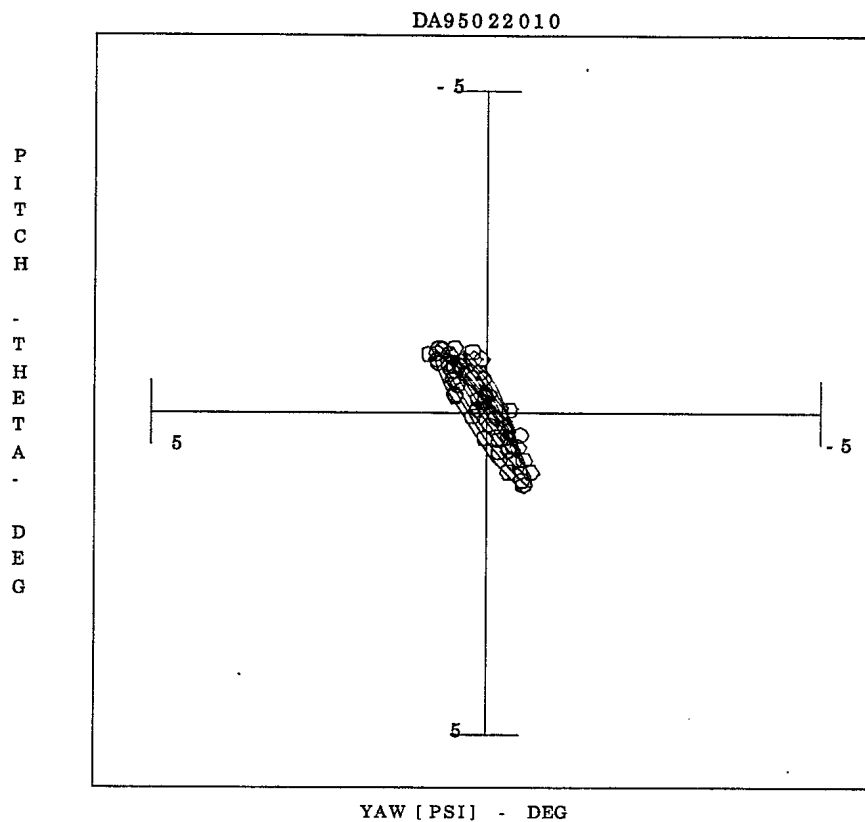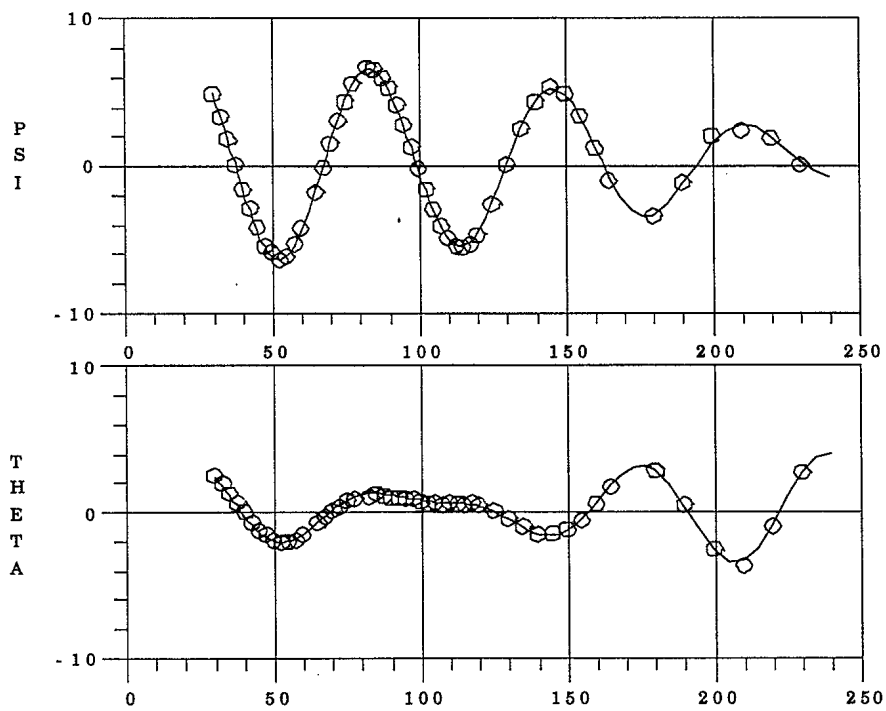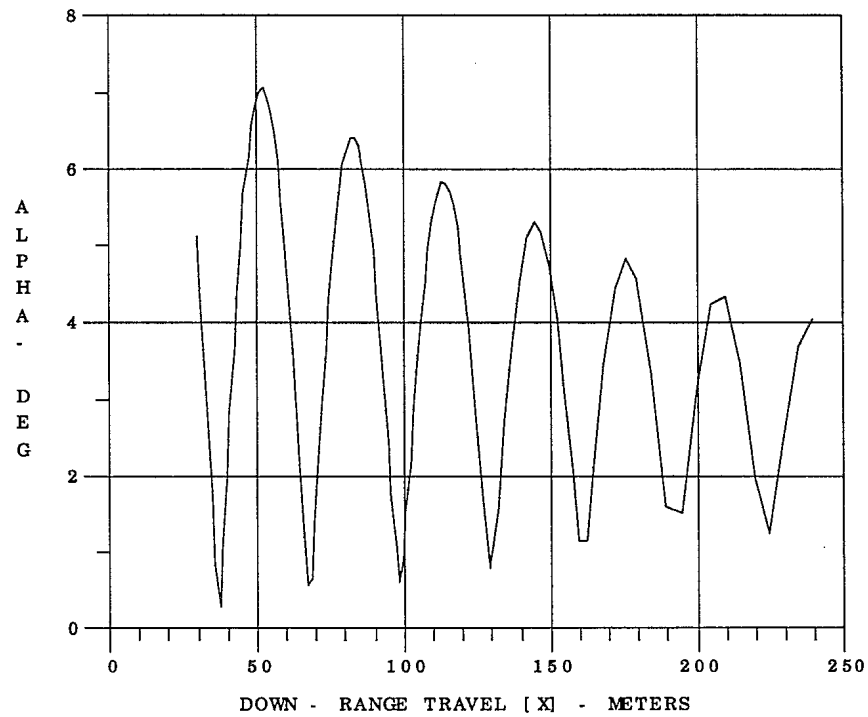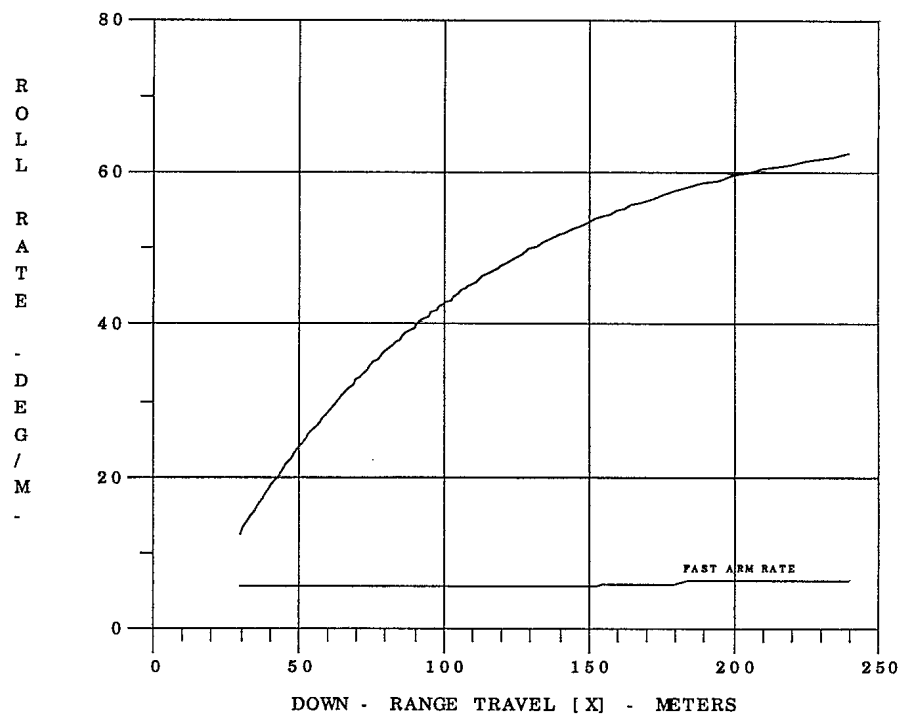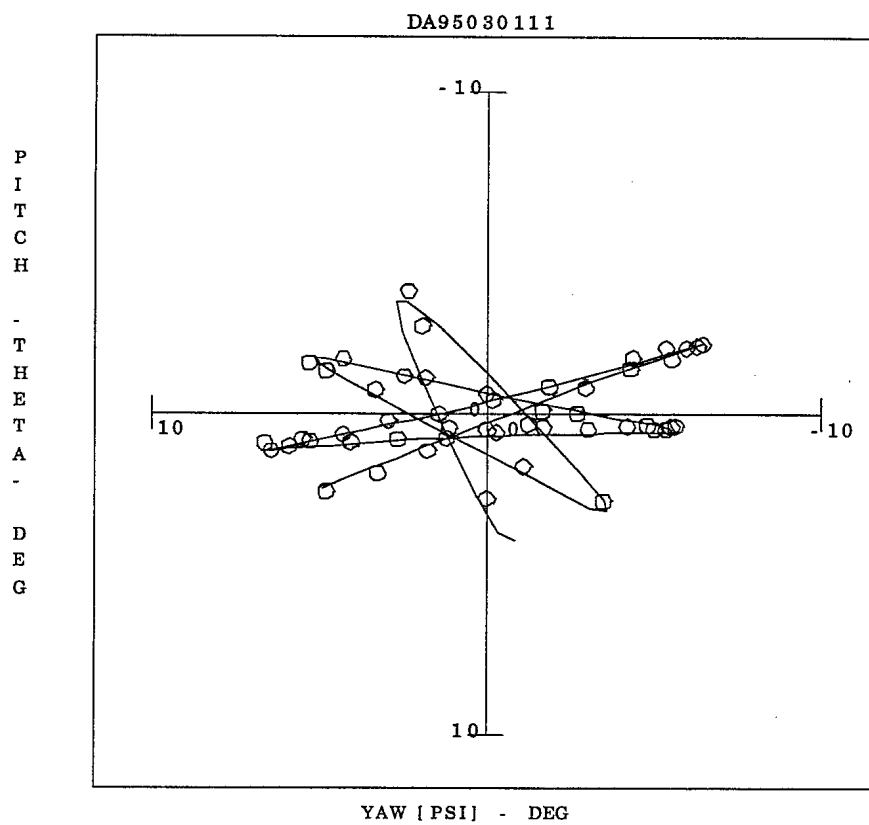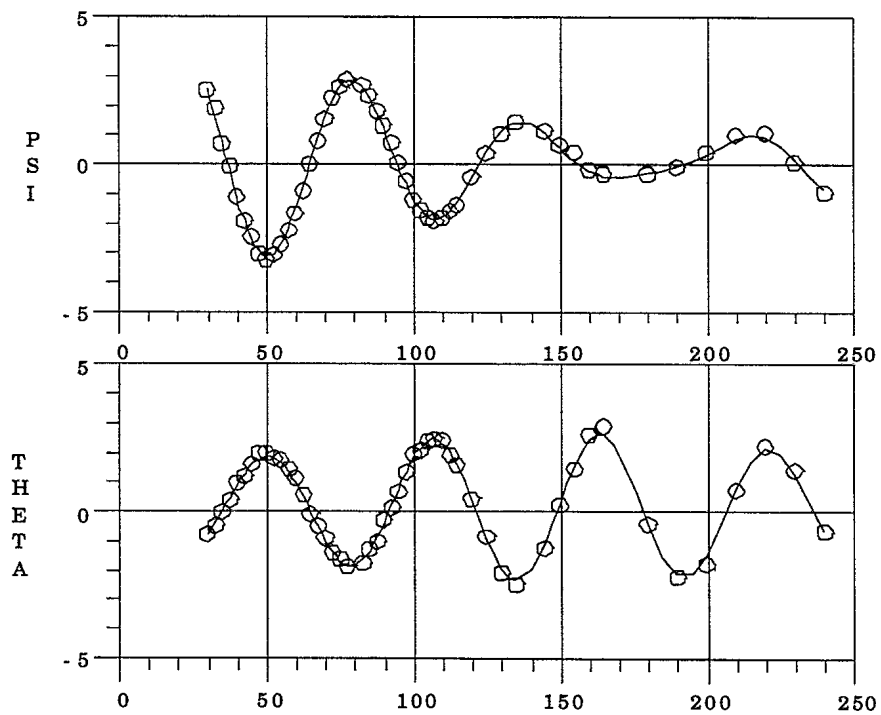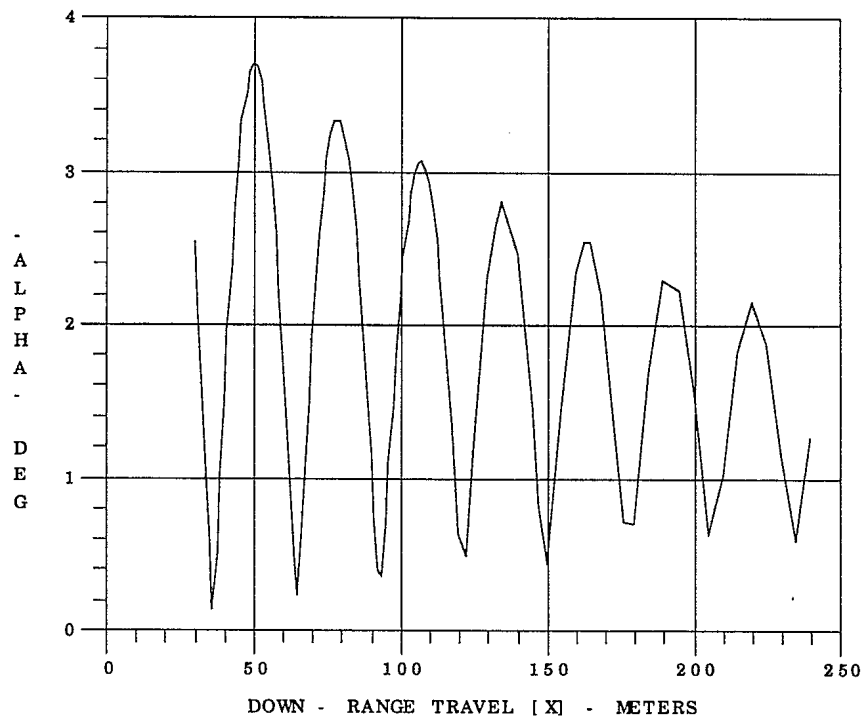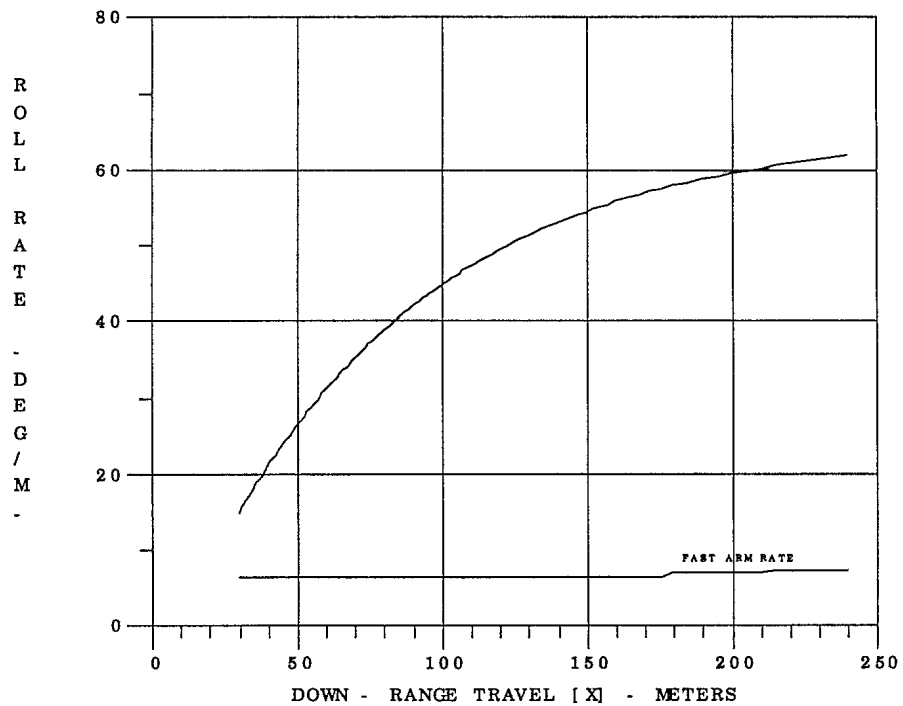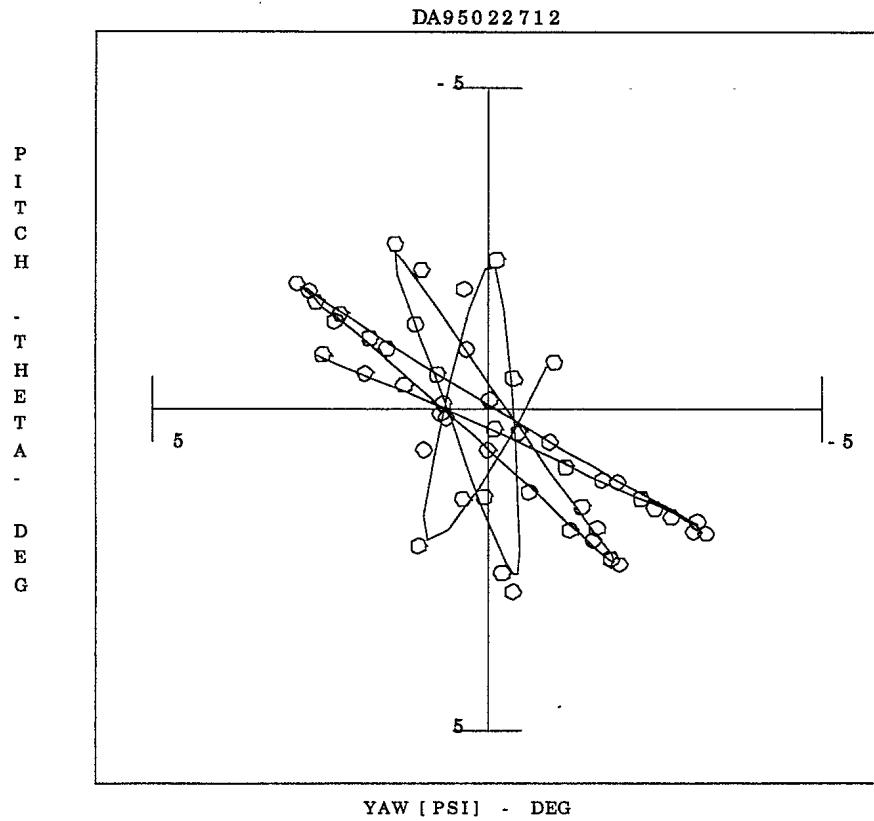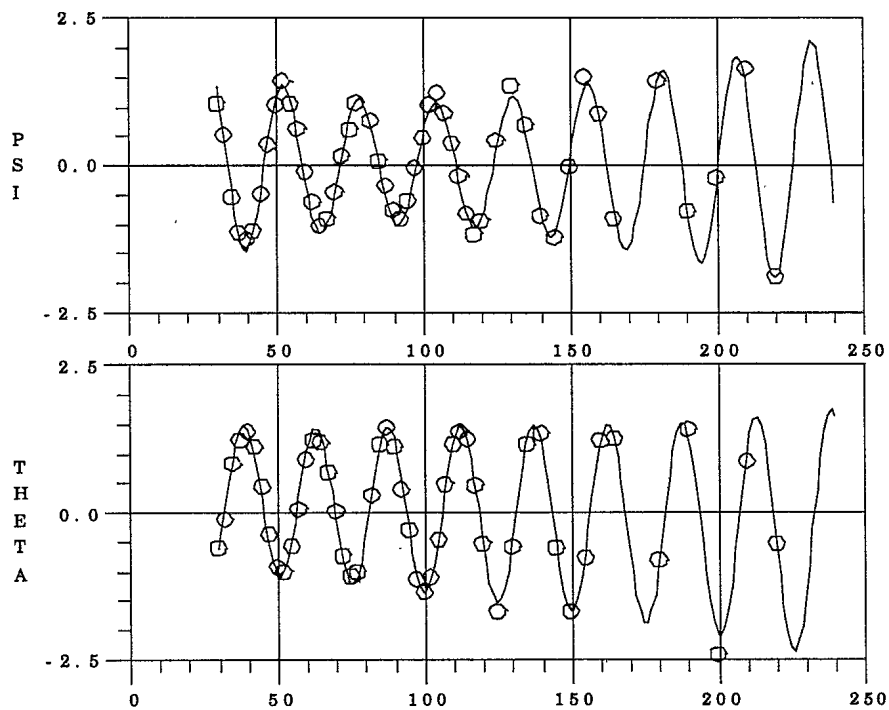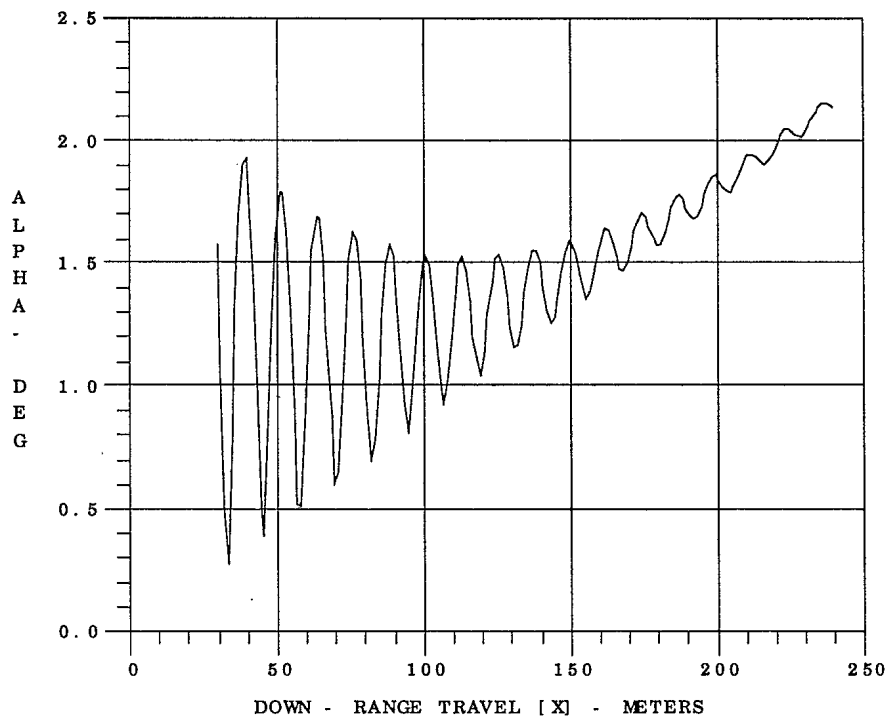
DA95030613

PITCH - THETA - DEG
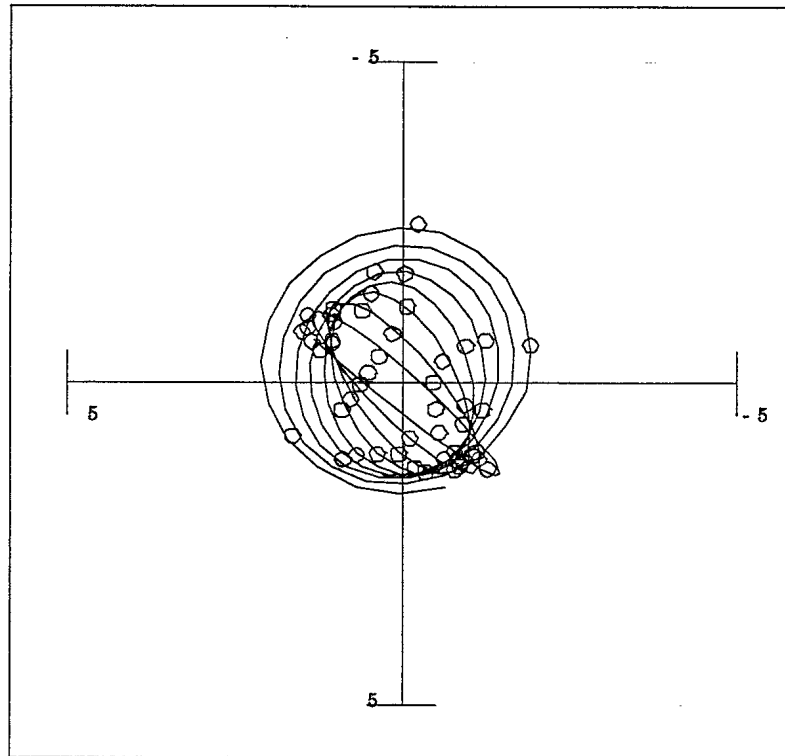
- 5

5

- 5

5

YAW [PSI] - DEG

ROLL RATE - DEG / M -

60

50

40

30

20

10

0

FAST ARM RATE

0   50   100   150   200   250

DOWN - RANGE TRAVEL [X] - METERS

DA95022215

ALPHA - DEG

DOWN - RANGE TRAVEL [X] - METERS

PSI

THETA

DA95022215

PITCH - THETA - DEG

YAW [PSI] - DEG

ROLL RATE - DEG / M -

FAST ARM RATE

DOWN - RANGE TRAVEL [X] - METERS
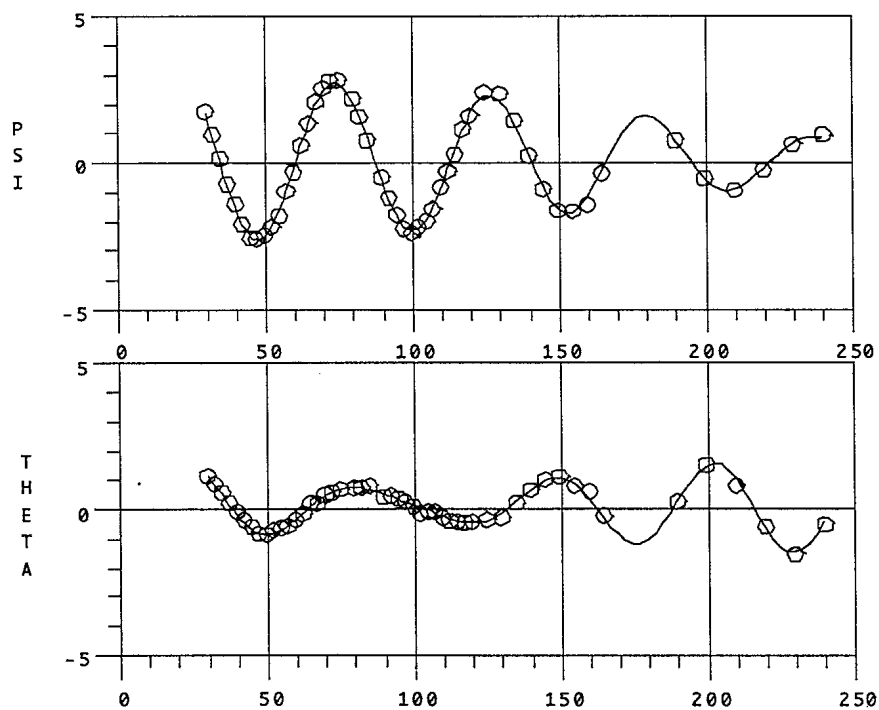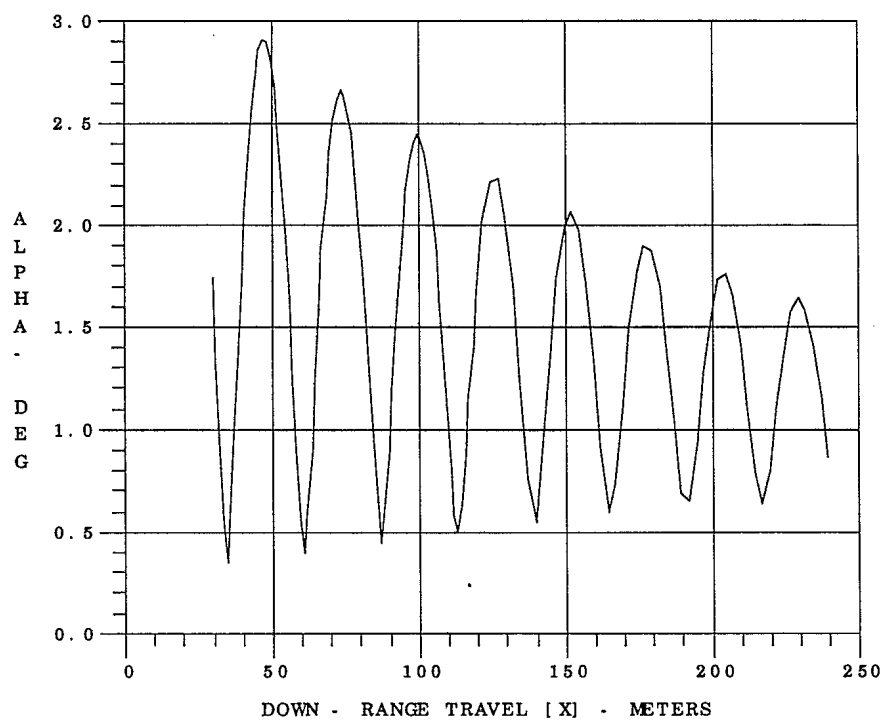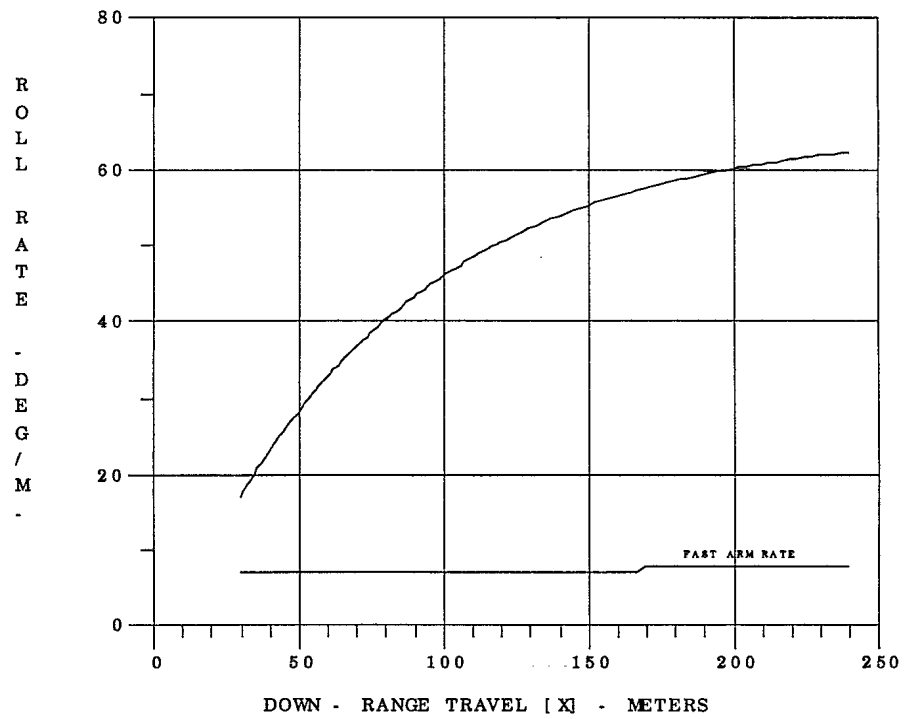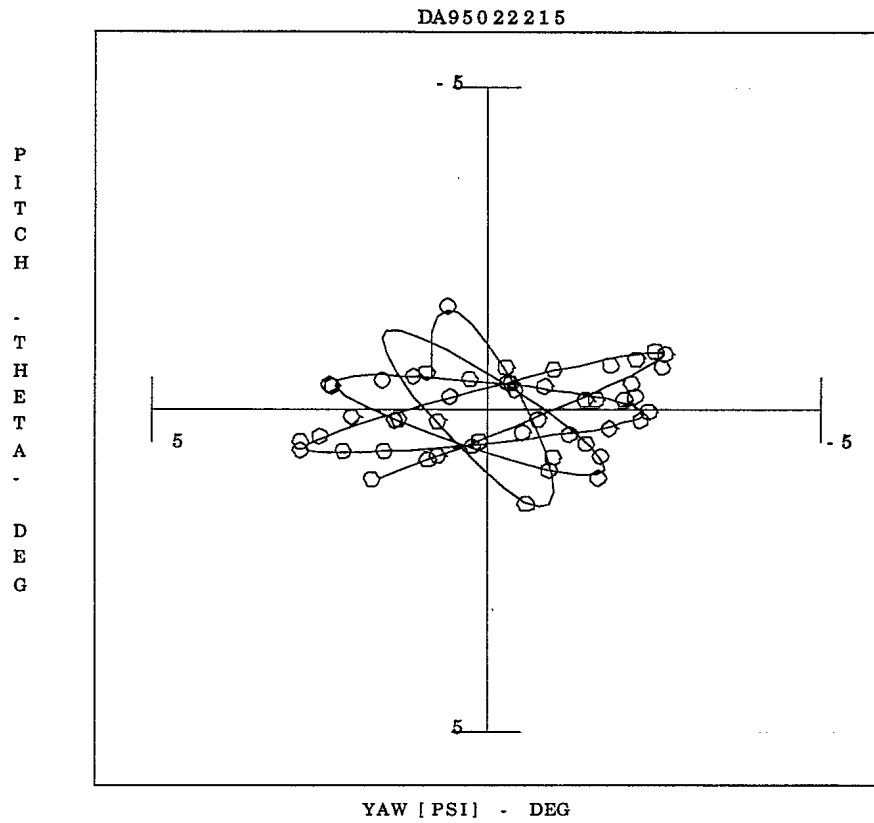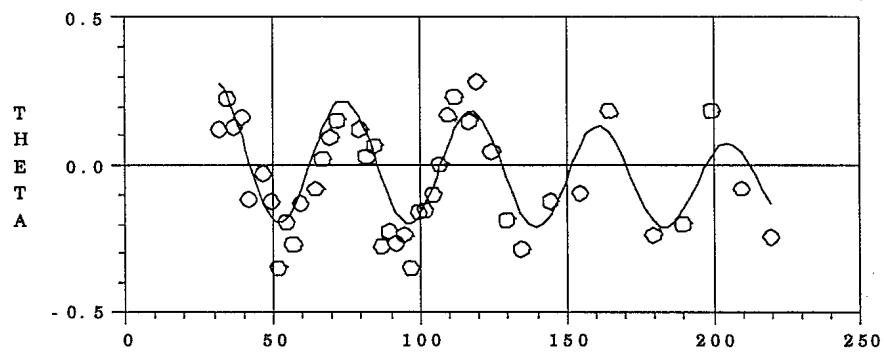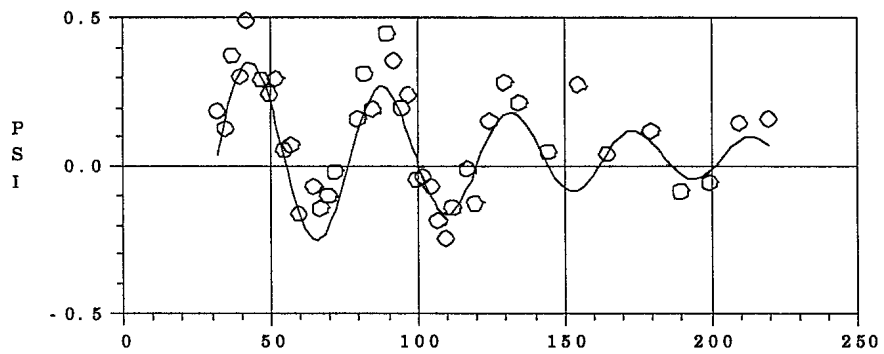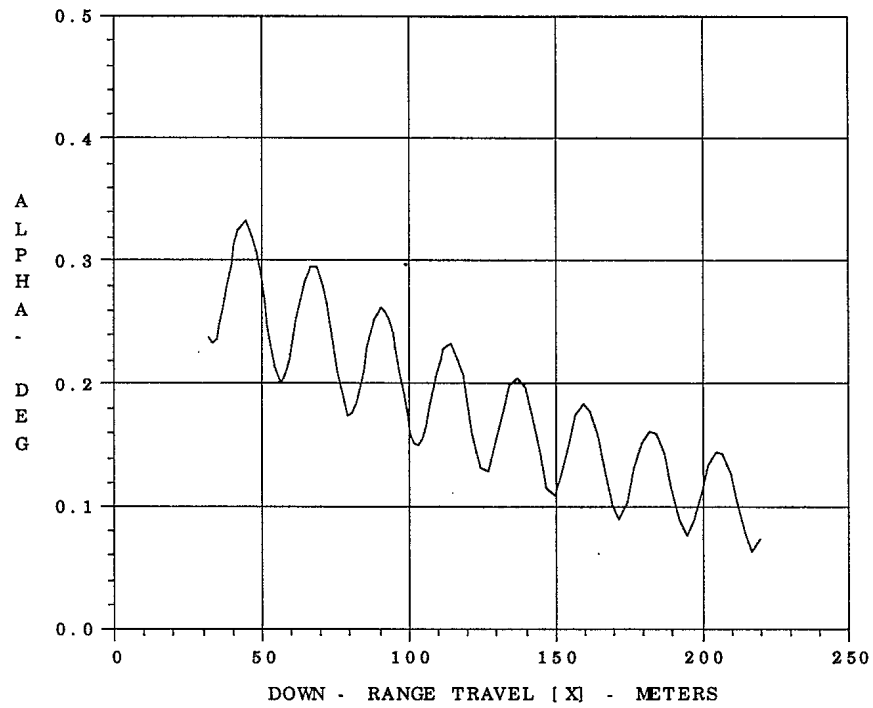
DA95020916

DA95020916

PITCH - THETA - DEG

- 5

5

- 5

5

YAW [PSI] - DEG

ROLL RATE - DEG / M -

80

60

40

20

0

FAST ARM RATE

0   50   100   150   200   250

DOWN - RANGE TRAVEL [X] - METERS

DA95021317

DOWN - RANGE TRAVEL [X] - METERS

DA95021317

PITCH - THETA - DEG

- 5

5

- 5

5

YAW [PSI] - DEG

ROLL RATE - DEG / M -

80

60

40

20

0

FAST ARM RATE

0   50   100   150   200   250

DOWN - RANGE TRAVEL [X] - METERS

DA95021318

ALPHA - DEG

DOWN - RANGE TRAVEL [X] - METERS

PSI

THETA

DA95021318

PITCH - THETA - DEG

- 5

5

- 5

5

YAW [PSI] - DEG

ROLL RATE - DEG / M -

80

60

40

20

0

FAST ARM RATE

0   50   100   150   200   250

DOWN - RANGE TRAVEL [X] - METERS

DA95022219

DOWN - RANGE TRAVEL [X] - METERS

DA95022219

PITCH - THETA - DEG

YAW [PSI] - DEG

ROLL RATE - DEG / M -

FAST ARM RATE

DOWN - RANGE TRAVEL [X] - METERS

DA95030121

DOWN - RANGE TRAVEL [X] - METERS

DA95030121

YAW [PSI] - DEG

DOWN - RANGE TRAVEL [X] - METERS

DA95030622

DOWN - RANGE TRAVEL [X] - METERS

DA95030622

PITCH - THETA - DEG

-10

10

-10

0

10

YAW [PSI] - DEG

ROLL RATE - DEG / M -

120

100

80

60

40

20

0

FAST ARM RATE

0   50   100   150   200   250

DOWN - RANGE TRAVEL [X] - METERS

DA95031523

DOWN - RANGE TRAVEL [X] - METERS

DA95031523

PITCH - THETA - DEG

YAW [PSI] - DEG

ROLL RATE - DEG/M -

FAST ARM RATE

DOWN - RANGE TRAVEL [X] - METERS

DA95022726

ALPHA - DEG

DOWN - RANGE TRAVEL [X] - METERS

PSI

THETA

DA95022726

PITCH - THETA - DEG

- 5

5

- 5

5

YAW [PSI] - DEG

ROLL RATE - DEG / M -

150

125

100

75

50

25

0

FAST ARM RATE

0   50   100   150   200   250

DOWN - RANGE TRAVEL [X] - METERS

DA95020927

DOWN - RANGE TRAVEL [X] - METERS

DA95020927

PITCH - THETA - DEG

YAW [PSI] - DEG

ROLL RATE - DEG / M -

FAST ARM RATE

DOWN - RANGE TRAVEL [X] - METERS

DA95021328

ALPHA - DEG

DOWN - RANGE TRAVEL [X] - METERS

PSI

THETA

DA95021328

PITCH - THETA - DEG

YAW [PSI] - DEG

ROLL RATE - DEG / M .

FAST ARM RATE

DOWN - RANGE TRAVEL [X] - METERS

DA95021529

DA95021529

P
I
T
C
H

.
T
H
E
T
A
.

D
E
G

- 5

5   - 5

5

YAW [PSI] - DEG

R
O
L
L

R
A
T
E

.
D
E
G
/
M
.

150

125

100

75

50

25

0

FAST ARM RATE

0   50   .100   150   200   250

DOWN - RANGE TRAVEL [X] - METERS

DA95022230

DOWN - RANGE TRAVEL [X] - METERS

DA95022230

PITCH - THETA - DEG

5

- 5

5

- 5

5

YAW [PSI] - DEG

120

100

80

60

40

20

0

ROLL RATE - DEG / M -

FAST ARM RATE

0   50   100   150   200   250

DOWN - RANGE TRAVEL [X] - METERS

INTERNAL DISTRIBUTION

DREV- TM- 9703

1 - Deputy Director General
6 - Document Library
1 - A. Dupuis (author)
1 - F. Lesage
1 - B. Girard
1 - E. Fournier
1 - A. Jeffrey
1 - G. Dumas
1 - P. Twardawa
1 - R. Delagrave
1 - G. Bérubé
1 - M. Lauzon
1 - C. Bradette
1 - L. Audet
1 - C. Julien
1 - Maj. Côté

EXTERNAL DISTRIBUTION

DREV- TM - 9703

2 - DRDIM
1 - DRDB
1 - DSAL
1 - DLR
1 - DAR
1 - DARFT
1 - DNR
1 - DSAA
1 - DSAM
1 - DAEPM (FT)
1 - DTA
1 - DAMM
1 - DAES
1 - DRES
1 - PETE
1 - PMO LAV

1 - Mr. W. Hathaway (author)
   Arrow Tech Associates, Inc.
   1233 Shelbourne Road
   S. Burlington, VT 050403
   USA

1 - Dr. B. J. Walker
   AMSMI-RD-SS-AT
   Commander
   U. S. Army Missile Command
   Redstone Arsenal, AL
   35898-5252
   USA

1 - Mr. G. L. Winchenbach
    Weapon Flight Mechanics Division
    Wright Laboratory Armament Directorate
    Eglin AFB, FLA 32542-5434 (USA)

1 - Dr. P. Plostins
    SLCBR-LF-F
    Army Research Laboratory
    Aberdeen Prooving Ground
    Maryland 21005-5066
    USA

3 - Dr. C. Berner
    Dr. M. Giraud
    Dr. V. Fleck
    Institut Franco-Allemand de Recherches
    5, rue du Général Cassagnou
    B.P. 34
    68301 - Saint-Louis (France)

1 - Mr. A. Bernier
    Les Technologies Industrielles SNC Inc.
    Usine Le Gardeur
    5, montée des Arsenaux
    Le Gardeur, Québec
    J5Z 2P4

2 - Bristol Aerospace Limited
    P. O. Box 874
    Winnipeg, Manitoba
    R3C 2S4

1 - Dr. L. Chan
High Speed Aerodynamic Laboratory
Institute for Aerospace Research
National Research Council Canada
Montreal Road
Ottawa, Ontario
K1A 0R6

1 - Mr. M. Normand
MAETEC
6161 Boulv. Fossambault
Fossambault, QC
G0A 3M0

1 - Dr. J. Edwards
WX7 Division, Weapons Sector
DRA - Fort Halstead
Sevenoaks
Kent TN14 7BP
England

1 - Mr. A. J. Sadler
Weapons Aerodynamics Division
DRA
Bedford MK41 6AE
England

1 - Dr. A. R. Rye
DSTO
Surveillance Research Laboratory
P. O. Box 1500
Salisbury, SA 5108
Australia

DOCUMENT CONTROL DATA

1. ORIGINATOR (name and address) Defence Research Establishment Valcartier 2459 Blvd. Pie XI Nord Val-Bélair QC G3J 1X5	2. SECURITY CLASSIFICATION (Including special warning terms if applicable) UNCLASSIFIED

3. TITLE (Its classification should be indicated by the appropriate abbreviation (S,C,R or U) AEROBALLISTIC RANGE TESTS OF THE BASIC FINNER REFERENCE PROJECTILE AT SUPERSONIC VELOCITIES

4. AUTHORS (Last name, first name, middle initial. If military, show rank, e.g. Doe, Maj. John E.) DUPUIS, A.D., HATHAWAY, W.

5. DATE OF PUBLICATION (month and year)	6a. NO. OF PAGES	6b. NO. OF REFERENCES 11

7. DESCRIPTIVE NOTES (the category of the document, e.g. technical report, technical note or memorandum. Give the inclusive dates when a specific reporting period is covered.) TM

8. SPONSORING ACTIVITY (name and address) DREV

9a. PROJECT OR GRANT NO. (Please specify whether project or grant) 2EA14	9b. CONTRACT NO.

10a. ORIGINATOR'S DOCUMENT NUMBER	10b. OTHER DOCUMENT NOS. N/A

11. DOCUMENT AVAILABILITY (any limitations on further dissemination of the document, other than those imposed by security classification) [X] Unlimited distribution [ ] Contractors in appoved countries (specify) [ ] Canadian contractors (with need-to-know) [ ] Government (with need-to-know) [ ] Defence departments [ ] Other (please specify) :

12. DOCUMENT ANNOUNCEMENT (any limitation to the bibliographic announcement of this document. This will normally correspond to the Document Availability (11). However, where further distribution (beyond the audience specified in 11) is possible, a wider announcement audience may be selected.) UNLIMITED ANNOUNCEMENT

13. ABSTRACT (a brief and factual summary of the document. It may also appear elsewhere in the body of the document itself. It is highly desirable that the abstract of classified documents be unclassified. Each paragraph of the abstract shall begin with an indication of the security classification of the information in the paragraph (unless the document itself is unclassified) represented as (S), (C), (R), or (U). It is not necessary to include here abstracts in both official languages unless the text is bilingual).

Free-flight tests were conducted in the Defence Research Establishment Valcartier (DREV) Aeroballistic Range on the Basic Finner reference projectile from transonic to high supersonic velocities. The projectile consisted of four rectangular fins on a cone-cylinder body with a total length-to-diameter ratio of 10.0. Fin cants of $0°$, $2°$ and $4°$ were imposed. The Mach number range tested was between 1.0 and 4.5. All the main aerodynamic coefficients and stability derivatives were well determined using linear theory, six-degree-of-freedom single- and multiple-fit reductions techniques. The results were also compared with results from other aeroballistic ranges. The fins on the models fired at Mach 4.5 ablated during flight. A dynamic stability analysis showed a Magnus instability at certain Mach numbers and spin rates.

14. KEYWORDS, DESCRIPTORS or IDENTIFIERS (technically meaningful terms or short phrases that characterize a document and could be helpful in cataloguing the document. They should be selected so that no security classification is required. Identifiers, such as equipment model designation, trade name, military project code name, geographic location may also be included. If possible keywords should be selected from a published thesaurus. e.g. Thesaurus of Engineering and Scientific Terms (TEST) and that thesaurus-identified. If it is not possible to select indexing terms which are Unclassified, the classification of each sould be indicated as with the title.)

FREE-FLIGHT TESTS
FIN STABILIZED PROJECTILES
BASIC FINNER
AERODYNAMIC COEFFICIENTS
SUPERSONIC
TRANSONIC
FLIGHT DYNAMICS
MAGNUS INSTABILITY
AEROBALLISTIC RANGE TESTS
SIX DEGREE OF FREEDOM
MAXIMUM LIKELIHOOD
SCHLIEREN
SHADOWGRAPH
STABILITY ANALYSIS
DYNAMIC INSTABILITY
6 DEGREES OF FREEDOM
LINEAR THEORY
ABLATION

(DCD03E.IFD - 95.02.22)

UNCLASSIFIED

Requests for documents
should be sent to:

DIRECTORATE RESEARCH AND DEVELOPMENT
INFORMATION MANAGEMENT

Dept. of National Defence
Ottawa, Ontario
K1A 0K2

Tel.: (613) 995-2971
Fax: (613) 996-0392

505377

Toute demande de document
doit être adressée à:

DIRECTEUR-GESTION DE L'INFORMATION DE RECHERCHE
ET DE DÉVELOPPEMENT

Ministère de la Défense nationale
Ottawa, Ontario
K1A 0K2

Téléphone: (613) 995-2971
Télécopieur: (613) 996-0392

SANS CLASSIFICATION